

2013

## **A Neurophysiologic Study Of Visual Fatigue In Stereoscopic Related Displays**

Hanniebey Dolphyne Nutung-Wiyor  
*North Carolina Agricultural and Technical State University*

Follow this and additional works at: <https://digital.library.ncat.edu/dissertations>



Part of the [Other Operations Research, Systems Engineering and Industrial Engineering Commons](#)

---

### **Recommended Citation**

Nutung-Wiyor, Hanniebey Dolphyne, "A Neurophysiologic Study Of Visual Fatigue In Stereoscopic Related Displays" (2013). *Dissertations*. 127.

<https://digital.library.ncat.edu/dissertations/127>

This Dissertation is brought to you for free and open access by the Electronic Theses and Dissertations at Aggie Digital Collections and Scholarship. It has been accepted for inclusion in Dissertations by an authorized administrator of Aggie Digital Collections and Scholarship. For more information, please contact [iyanna@ncat.edu](mailto:iyanna@ncat.edu).

A Neurophysiologic Study of Visual Fatigue in Stereoscopic Related Displays

Hanniebey Dolphyne Nutung-Wiyor

North Carolina A&T State University

A dissertation submitted to the graduate faculty  
in partial fulfillment of the requirements for the degree of

DOCTOR OF PHILOSOPHY

Department: Industrial & Systems Engineering

Major: Industrial & Systems Engineering

Major Professor: Dr. Celestine A. Ntuen

Greensboro, North Carolina

2013

School of Graduate Studies  
North Carolina Agricultural and Technical State University  
This is to certify that the Doctoral Dissertation of

Hanniebey Dolphyne Nutung-Wiyor

has met the dissertation requirements of  
North Carolina Agricultural and Technical State University

Greensboro, North Carolina  
2013

Approved by:

---

Dr. Celestine A. Ntuen  
Major Professor

---

Dr. Joseph D. W. Stephens  
Committee Member

---

Dr. Steven Jiang  
Committee Member

---

Dr. Zongliang Jiang  
Committee Member

---

Dr. Tonya Smith-Jackson  
Department Chair

---

Dr. Sanjiv Sarin  
Dean, The Graduate School

© Copyright by  
Hanniebey Dolphyne Nutung-Wiyor  
2013

## Biographical Sketch

Hanniebey Dolphyne Nutung Wiyor was born on August 16, 1975, in Kumasi, Ghana. He received the Bachelor of Science degree in Building Technology from Kwame Nkrumah University of Science and Technology in Kumasi, Ghana in 2003. He received his Master of Science degree in Industrial Engineering in 2009 from the North Carolina Agricultural & Technical State University at Greensboro, North Carolina. In 2010, he joined the doctoral program.

Before pursuing graduate studies, Mr. Wiyor worked as a quantity surveyor with Balfour Beatty Construction Company in London, United Kingdom. He also worked as a process engineer at Sherwin Williams Company in Greensboro, North Carolina. While pursuing his degree, Mr. Wiyor worked as a Research and Teaching Assistant for the Department of Industrial & Systems Engineering.

Mr. Wiyor has presented his research at 59<sup>th</sup>, 60<sup>th</sup>, 61<sup>st</sup>, 62<sup>nd</sup> and 63<sup>rd</sup> Annual Industrial and Systems Engineering Research Conference (ISERC) in 2009, 2010, 2011, 2012, 2013, respectively; 4<sup>th</sup> International Conference on Applied Human Factors and Ergonomics (AHFE) in 2011; 8<sup>th</sup> and 9<sup>th</sup> Annual Symposium of the Human Interaction with Complex Systems (HICS) in 2008 and 2009, respectively; 2<sup>nd</sup> Annual Workshop for Human Research Engineering Directorate of the Army Research Laboratory (ARL) in 2008.

Mr. Wiyor's dissertation is entitled, "A Neurophysiologic Study of Visual Fatigue in Stereoscopic Related Displays," which is supervised by Dr. Celestine Ntuen. He is a candidate for the Doctor of Philosophy in Industrial Engineering.

## Dedication

I dedicate my dissertation work to my family, especially to my wonderful daughters, Hayoun Nutung Hanniebey-Wiyor and Harweseh Nutung Hanniebey-Wiyor, for being there for me throughout the entire doctorate program. Both of you have been my best cheerleaders. To Lucy Abaka Wiyor, for her patience, understanding and encouragement, a very special thanks. This is also dedicated to my loving parents, Abudu Nutung Wiyor and Yaa Adjei for instilling the importance of hard work and higher education. A special feeling of gratitude to Uncle Seywiah Nutung Wiyor, who supported me during my educational formative years. To my siblings Ralph, Barbineh, Lardi, Karim, Barto-Hense, Asuma, and Adams, may you all be motivated and encouraged to reach your dreams. Lastly, to my late grandparents Hayoun and Nutung Wiyor for their continual blessing.

## Acknowledgements

I would never have been able to finish my dissertation without the giver of life, Almighty GOD, the guidance of my committee members, support from my wife, and help from friends.

I would like to gratefully and sincerely thank Dr. Celestine A. Ntuen for his guidance, understanding, patience, and most importantly, his friendship during my graduate studies at North Carolina A & T State University. His mentorship was vital in providing an informed experience consistent with my long-term career goals. He encouraged me to not only grow as an engineer but also as an instructor and an independent thinker. For everything you've done for me, Dr. Ntuen, I thank you.

I would also like to thank the Department of Industrial & Systems Engineering and Psychology Department at North Carolina A & T State University, especially my doctoral committee members, Dr. Steven Jiang, Dr. Zongliang S. Jiang, and Dr. Joseph D.W. Stephens for their input, valuable discussions, and accessibility. Special thanks go to Dr. George Robinson, Jr. for teaching me the basics of neuropsychology and electrophysiology.

I would like to express my deepest gratitude to Mr. Abdul Abubakar for helping me on October 16, 2003 through to September 20, 2004. You gave me a place to sleep in the middle of the nights against all odds. I always have serious reflections of those days. I owe you a great debt of thankfulness Mr. Abubakar, I thank you.

I would like to thank my wife, Lucy Abaka Wiyor. She always stood by me through the good and bad times.

Finally, I would like to thank all my friends especially Dr. Osei Agyemang, Ernest Gyimah-Danquah, and IRC 222 Human-Machine lab students for some much needed humor and entertainment in what could have otherwise been a somewhat stressful laboratory environment.

## Table of Contents

List of Tables .....	xiv
List of Abbreviations .....	xvii
Abstract.....	2
CHAPTER 1 Introduction.....	3
1.1 Asthenopia and Stereoscopic Display.....	5
1.2 Study Objectives .....	7
1.3 Tasks to be Accomplished .....	8
1.4 Application and Intellectual Contributions.....	9
1.4.1 Health and etiology.....	9
1.4.2 Vision and neuroscience advancement.....	9
1.4.3 Aviation industry.....	9
1.4.4 Anthropometry.....	10
1.4.5 Fraud prevention and reduction of lawsuits.....	10
1.5 Taxonomy of Visual Fatigue and Related Studies.....	12
1.5.1 Psychophysical factors of visual fatigue.....	12
1.5.2 Information factors.....	15
1.5.3 Operational factors.....	15
1.5.4 Stereoscopic and autostereoscopic display .....	17
1.5.5 Cognitive factors.....	18

1.6 A Summary of Visual Fatigue Studies from Medical, Human Factors and Neurophysiology Perspectives.....	19
1.7 Chapter Summary .....	19
CHAPTER 2 Equipment Used for the Study.....	21
2.1 Functional Near-Infrared Spectroscopy (fNIRS).....	21
2.2 Biopac MP-150 .....	22
2.3 Head Mounted Display (HMD) with ViewPoint Eye Tracker Device .....	24
2.4 Simulator Sickness Questionnaire (SSQ) .....	26
2.5 Task Simulation Testbed.....	27
CHAPTER 3 Experiment I: The Impact of Alignment Errors on Visual Fatigue .....	30
3.1 Experimental Design.....	31
3.2 Apparatus .....	32
3.3 Participants.....	33
3.3.1 Estimating number of subjects.....	33
3.3.2 Visual acuity test and interpupillary distance (IPD) measurements. ....	34
3.3.3 Participants' preparation. ....	35
3.4 Procedure .....	36
3.5 Task.....	39
3.6 Data Acquisition .....	40

CHAPTER 4 Data Analyses and Results for Study Experiment I.....	42
4.1 Data Pre-Processing.....	42
4.1.1 Simulator sickness questionnaire (SSQ) ratings.....	42
4.1.2 Electroencephalogram (EEG).....	45
4.1.3 Hemodynamic responses.....	49
4.1.4 NASA task load index (NASA- TLX).....	50
4.2 Experimental Hypotheses Testing.....	51
4.3 Prediction Equations for Visual Fatigue.....	67
4.4 Analysis on Magnification Differences Error.....	69
CHAPTER 5 Experiment II: Cognitive Neuroscience for Visual Fatigue.....	73
5.1 Experimental Design.....	74
5.2 Apparatus and Experimental Set up.....	75
5.3 Participant Preparation and Procedure.....	75
5.4 Tasks.....	76
5.5 Analysis, Results and Discussion.....	78
5.5.1 Experimental hypotheses testing.....	78
5.6 Relationship between Visual Fatigue and other Physiological Signals.....	86
CHAPTER 6 Visual Fatigue Classification with a Neural Network Algorithm.....	99
6.1 Neurophysiological Basis of Visual Fatigue.....	99

6.2 A Neural Network Approach .....	101
6.3 Selection of the Classification Neural Network Model .....	102
6.3.1 Preparing data for analysis. ....	106
6.4 Results and Discussions for Model-Based Visual Fatigue Classification .....	108
6.4.1 Sensitivity and specificity. ....	112
CHAPTER 7 Summary, Discussions, And Suggestions for Future Research.....	117
7.1. Summary .....	117
7.2. Discussions and Observations.....	123
7.3. Suggestions for Future Research .....	125
References.....	126
<i>Appendix A</i> .....	150
<i>Appendix B</i> .....	152
<i>Appendix C</i> .....	155
<i>Appendix D</i> .....	157
<i>Appendix E</i> .....	158
<i>Appendix F</i> .....	159
<i>Appendix G</i> .....	160
<i>Appendix H</i> .....	161
<i>Appendix I</i> .....	162

## List of Figures

Figure 1. Taxonomy of visual fatigue and their corresponding symptoms. ....	4
Figure 2. The relation graph between visual fatigue and depth [Source Liu et al. 2001]. ....	13
Figure 3. Configuration of the Viewpoint Eye Tracker [ViewPoint EyeTracker® by Arrington Research, 2010]. ....	25
Figure 4. ATCM interface design for the study 1. The Interface is designed with LabView 9.1® software provided National Instrument. ....	28
Figure 5. ATCM interface design for the study 2. The Interface is designed with E-Prime® software provided psychological software tools incorporated. ....	29
Figure 6. Interpupillary Distance (IPD) measurements using the Limbus method. ....	35
Figure 7. Experimental procedure with three ATC task sessions, four sets of SSQ questionnaires, and three sets of NASA-TLX questionnaires. ....	37
Figure 8. Participant performing experimental tasks with various alignment error conditions. ....	39
Figure 9. Sample 4s-12s raw EEG plot for participant 12 during magnification difference treatment 1 and 2 on channels O <sub>1</sub> , Oz, and O <sub>2</sub> . ....	46
Figure 10. Sample 4s-12s raw EEG plot for participant 12 rotational error for treatment 1 and 2 on channels O <sub>1</sub> , Oz, and O <sub>2</sub> . ....	47
Figure 11. Sample 4s-12s raw EEG plot for participant 12 vertical shifts for treatment 1 and 2 on channels O <sub>1</sub> , Oz, and O <sub>2</sub> . ....	48
Figure 12. Graphical composition of workloads for subjects ID 6 and 22. The sources of workload were Mental Demand (MD), Physical Demand (PD), Temporal Demand (TD), Performance (PF), Effort (EF) and Frustration (FR). The weight was scaled between 0-5, and ratings are scaled between 0-100. ....	50

Figure 13. Side-by-side box plot of SSQ ratings for BATC and ATC 3. ....	53
Figure 14. A radial plot of SSQ rated symptoms on ATC task sessions. ....	54
Figure 15. Mean SSQ ratings for Air Traffic Control (ACT) tasks. The SSQ ratings are from 0 to 3 for 34 symptoms, and N = 24 subjects. ....	55
Figure 16. A radial plot of SSQ rated symptoms on ATC task session during magnification difference. ....	56
Figure 17. A radial plot of SSQ rated symptoms on ATC task session during rotational error. ..	57
Figure 18. A Radial plot of SSQ rated symptoms on ATC task session during vertical shift. ....	57
Figure 19. Side-by-side box plots for the alignment errors based on NASA workload. ....	58
Figure 20. Profile plot of EEG band relative at the three alignment display error type. ....	64
Figure 21. Temporal patterns for hemodynamic responses for the dorsolateral prefrontal cortex for all the alignment errors in the ATCIM display. ....	65
Figure 22. Subject performing ATC task. ....	76
Figure 23. Experimental protocol for simulated air traffic control (ATC) tasks. ....	77
Figure 24. Side-by-side box plot of participants' SSQ ratings for BATC and ATC 3. ....	79
Figure 25. A radial plot of SSQ rated symptoms on ATC task session during BATC and ATC 3. The SSQ ratings are from 0 to 3 for 34 symptoms, and N = 8 subjects. ....	80
Figure 26. Side-by-side box plot of response time for ATC1 and ATC 3. ....	81
Figure 27. Line graph of the interactive effect plot for cognitive response variables and task difficulty on response time. ....	84
Figure 28. Change of mean psychological rating score of visual fatigue with time. The SSQ ratings are from 0 to 3 for 34 symptoms, and N = 8 subjects. SSQ ratings are 0 (None), 1 (Slight), 2 (Moderate), and 3 (Severe). ....	87

Figure 29. A radial plot of SSQ symptoms ratings on ATC task sessions. ....	88
Figure 30. Bar plot of mean changes in oxygenated hemoglobin and deoxygenated hemoglobin. .....	89
Figure 31. Mean hemodynamic changes with response time for an individual.....	90
Figure 32. Change of mean maximum and minimum pupil diameters with ATC task sessions..	91
Figure 33. Change of mean saccade with ATC task sessions.....	92
Figure 34. Mean fixation changes with ATC task sessions.....	93
Figure 35. Sample eye movements at ATC task sessions.....	94
Figure 36. Effects of hidden neuron counts on mean square error with testing and training sets of size 108. ....	104
Figure 37. Mean square error verse number of epoch plot for feed forward neural network with piecewise linear function. ....	104
Figure 38. Feed forward neural network with piecewise linear function. ....	105
Figure 39. ROC curve for all data combined.....	113
Figure 40. ROC curve for electroencephalogram (EEG) signals. ....	113
Figure 41. ROC curve for eye movement (saccade and fixation).....	114
Figure 42. ROC curve for oxygenated and deoxygenated hemoglobin from the dorsolateral prefrontal cortex.....	114
Figure 43. ROC curve for oxygenated and deoxygenated hemoglobin from the dorsolateral prefrontal cortex and electroencephalogram (EEG) signals. ....	115
Figure 44. ROC curve for eye movement (saccade and fixation) and electroencephalogram (EEG) signals.....	115

Figure 45. ROC curve for eye movement (saccade and fixation) and oxygenated and deoxygenated hemoglobin from the dorsolateral prefrontal cortex..... 116

## List of Tables

Table 1 Ophthalmological Classification of Visual Fatigue (Asthenopia) with Their Respective Symptoms .....	3
Table 2 Varying Estimates of the Prevalence of Eye Problems Based on Source and Reporting Year(s).....	11
Table 3 EEG Frequency Band .....	24
Table 4 Experimental Independent Variables, their Levels, and Measurement Units.....	32
Table 5 Relationship between Gender and Corresponding Visual Acuity Composition.....	34
Table 6 Pre-Experimental SSQ Rating Data Before Air Traffic Control Task (BATC).....	43
Table 7 Sample SSQ Ratings After Air Traffic Control Task Session 1 (ATC1).....	43
Table 8 Sample SSQ Ratings After Air Traffic Control Task Session 2 (ATC2).....	44
Table 9 Sample SSQ Ratings After Air Traffic Control Task Session 3 (ATC3).....	45
Table 10 Descriptive Statistics for Hemodynamic Responses .....	49
Table 11 Subjective Responses for Overall Workload (WL <sup>1</sup> ) Using NASA-TLX and Perceptual Ratings of Visual Fatigue Symptoms Using SSQ <sup>2</sup> .....	59
Table 12 ANOVA Summary of Significant Effect of Hemodynamic Responses for the Alignment Errors .....	60
Table 13 ANOVA Results Based on Alignment Error Using EEG Data .....	61
Table 14 Tukey Post Ad Hoc Analyses of EEG Data for Alignment Errors on the Midline Cerebral Cortex Hemisphere.....	62
Table 15 Tukey Post Ad Hoc Analyses of EEG data for Alignment Errors on the Right Cerebral Cortex Hemisphere .....	62

Table 16 ANOVA Results for Hemodynamics Data on the Dorsolateral Prefrontal Cortex	
Location during ATC Tasks.....	70
Table 17 Summary of Major Findings from Hypotheses in Study I.....	71
Table 18 List of Factors and Their Levels for Experiment II.....	74
Table 19 Summary of Descriptive Statistics of Response Time for All ATC Task Sessions .....	82
Table 20 Descriptive Statistics for the Visual Responses.....	89
Table 21 Physiological Response Characteristics Related to Onset Visual Fatigue .....	94
Table 22 Summary of Correlation Analyses of Visual Fatigue (SSQ) with Visual Responses and Hemodynamic Responses .....	96
Table 23 Summary of Major Findings from Hypotheses in Study II .....	97
Table 24 Dataset Descriptions for the Model .....	106
Table 25 Variables in the Model Formulation for the Neural Network. Note IV Means Input Variable and OV is the Output Variable for the Network .....	107
Table 26 Data Sources and FF-ANN Model Classification Accuracy for Visual Fatigue Ratings .....	109
Table 27 Classification of Visual Fatigue Ratings Using All Data Combined.....	110
Table 28 Classification of Visual Fatigue Ratings Using Electroencephalogram (EEG) Data .	110
Table 29 Classification of Visual Fatigue Ratings Using Saccade and Fixation Data .....	110
Table 30 Classification of Visual Fatigue Ratings Using Hemodynamic Response Variables..	111
Table 31 Classification of Visual Fatigue Ratings Using Hemodynamic Response Variables and EEG Data .....	111
Table 32 Classification of Visual Fatigue Ratings Using EEG Data and Eye Movements (Saccade and Fixation).....	111

Table 33 Classification of Visual Fatigue Ratings Using Hemodynamic Response Variables and Eye Movements (Saccade and Fixation).....	112
Table 34 Post Ad Hoc Analyses of EEG Data for Alignment Errors on Cerebral Cortex Hemisphere .....	120
Table 35 Predictions of Onset of Visual Fatigue .....	122
Table 36 Classification Accuracies.....	122

## List of Abbreviations

A	Absorbance
AAO	America Association of Ophthalmologist
AD	Aircraft Display
Ag-Gal	Silver-Silver Chloride
AHR	Average Heart Rate
Alsace	Average Saccade
AOA	America Optometric Association
ATC	Air Traffic Control
ATCIM	Air Traffic Control Interface Model
B	path length
BA	Blink Amplitude
BD	Blink Duration
BldVol	Blood Volume
BR	Blink Rate
c	concentration of the compound
CNS	Central Nervous System
COBI	Cognitive Optical Brain Imaging
EEG	Electroencephalograph
EM	Electromagnetic
EOG	Electrooculograph
fMRI	functional Magnetic Resonance Imaging
FMT	Flight Maneuvered Task
fNIRS	Functional Near-Infrared spectroscopy
HbO <sub>2</sub> , oxy-Hb	Oxyhemoglobin
HbR, deoxy-Hb	De-ox hemoglobin
HMD	Head Mounted Display
I	Transmitted Intensity
I <sub>0</sub>	Incident Intensity
ICD	International Classification of Diseases
IPD	Interpupillary Distance

LCR	Long Closure Rate
/DLPFC	left Dorsolateral Prefrontal Cortex
LGN	Lateral Geniculation Nucleus
MEG	Magneto encephalography
MSLT	Multiple Sleep Latency Tests
NI	National Instruments
Nm	nanometers
Od	Optical density
OXY	Oxygenation
PALT	Pupillometric Alertness Level Test
Pd	max maximum Pupil diameter
PD	Pupil Diameter
Pdmin	minimum Pupil diameter
PET	Positron Emission Tomography
PMSD	Perceived Minimum Separation Distance
PSV	Peak Saccadic Velocity
R	Pearson Correlation Coefficient
rCBF	regional Cerebral Blood Flow
rDLPFC	right Dorsolateral Prefrontal Cortex
ReT (Fix)	Residence Time (Fixation)
ROI	Region of Interest
RPE	Retinal Pigment Epithelium
RPLH	Random Position Linear Heading
RPNLH	Random Position Non-Linear Heading
RT	Response Time
SAS	Statistical Analytical Software
SDHR	Standard Deviation Heart Rate
SDK	Software Development Kit
SLT	Straight Flying Task
SPECT	Single Positron Emission Computed Tomography
SR	Saccade Rate

SSQ	Simulator Sickness Questionnaires
SV	Saccade Velocity
VDT	Visual Display Task
VEP	Visual Evoked Potential
VOR	Vestibule-Ocular Reflexes
WHO	World Health Organization
$\epsilon_\lambda$	molar absorptivity or extinction coefficient
$\lambda$	wavelength
$\mu\text{mol g}^{-1} \text{min}^{-1}$	micro moles per gram per minute
$\mu\text{mol g}^{-1}$	micro moles per gram

## Abstract

Two tasks were investigated in this study. The first study investigated the effects of alignment display errors on visual fatigue. The experiment revealed the following conclusive results: First, EEG data suggested the possibility of cognitively-induced time compensation changes due to a corresponding effect in real-time brain activity by the eyes trying to compensate for the alignment. The magnification difference error showed more significant effects on all EEG band waves, which were indications of likely visual fatigue as shown by the prevalence of simulator sickness questionnaire (SSQ) increases across all task levels. Vertical shift errors were observed to be prevalent in theta and beta bands of EEG which probably induced alertness (in theta band) as a result of possible stress. Rotation errors were significant in the gamma band, implying the likelihood of cognitive decline because of theta band influence. Second, the hemodynamic responses revealed that significant differences exist between the left and right dorsolateral prefrontal due to alignment errors. There was also a significant difference between the main effect for power band hemisphere and the ATC task sessions. The analyses revealed that there were significant differences between the dorsal frontal lobes in task processing and interaction effects between the processing lobes and tasks processing. The second study investigated the effects of cognitive response variables on visual fatigue. Third, the physiologic indicator of pupil dilation was 0.95mm that occurred at a mean time of 38.1min, after which the pupil dilation begins to decrease. After the average saccade rest time of 33.71min, saccade speeds leaned toward a decrease as a possible result of fatigue on-set. Fourth, the neural network classifier showed visual response data from eye movement were identified as the best predictor of visual fatigue with a classification accuracy of 90.42%. Experimental data confirmed that 11.43% of the participants actually experienced visual fatigue symptoms after the prolonged task.

## CHAPTER 1

### Introduction

The terms visual fatigue (asthenia) and visual discomfort are often used interchangeably but in fact, they have different meanings. Visual fatigue is the decrement in performance in relation to any visual dysfunction of the human visual system and can only be objectively measured by optometry equipment. However, visual discomfort is the subjective counterpart. American Optometric Association (AOA), (1999) defined visual fatigue or asthenopia as the inability of the human visual system to continuously provide efficient visual processing functions. Lack of visual skills can be caused by one or more combinations of the visual disorders. These disorders are accommodative disorders, binocular disorders, and ocular mobility disorders.

Asthenopia occurs on a daily cycle. Visual performance usually decreases naturally from morning until night. This problem is exacerbated when daily Visual Display Task (VDT) lasts between 4 to 7 hours (Sallamander, 2010). The medical code for asthenopia is ICD-9, 368.13. ICD, and the America Association of Ophthalmologist (AAO) sub classifies asthenopia as ophthalmological disease as shown in the Table 1. The last two digits of the medical code indicate the seriousness of the ophthalmological disease. The larger the last two digits, the more severe are the symptoms of the disease. Astheponia is the worst form of eye disease.

Table 1

*Ophthalmological Classification of Visual Fatigue (Asthenopia) with Their Respective Symptoms*

Ophthalmological Medical Code	Ophthalmological Symptoms
ICD-9, 368.1	Subjective Visual Disturbances
ICD-9, 368.10	Subjective Visual Disturbance, Unspecified
ICD-9, 368.13	Asthenopia, Eye strain, Photophobia.

Sheedy and Hayes (2003) classified asthenopia symptoms that manifest itself as nonspecific and specific. The nonspecific sensation of asthenopia are eyestrain, discomfort, burning, irritation, pain, ache, sore eyes, and headache, and the specific sensations are photophobia, blur vision, double vision, itching, tearing, dryness, and foreign-body vision. The aforementioned symptoms are most often identified in subjective reports, which are easily flawed with individual perception, as well as unreliable reports associated with certain particular visual activities. For example, although neck pain may be reported as a symptom of visual fatigue, it may be more closely related to characteristics of an individual's seating posture during performance of a visual task, workplace orientation, or type of equipment being used. It is also likely that general fatigue is often reported as visual fatigue when observers have difficulty keeping their eyes open. Therefore, factors of visual fatigue or asthenopia are varied. It can be caused by physical, environmental, and organizational factors. As shown in Figure 1, asthenopia symptoms can be caused by uncorrected refractive errors (hypermetropia, myopia, astigmatism, and anisometropia). These conditions are termed as refractive asthenopia.

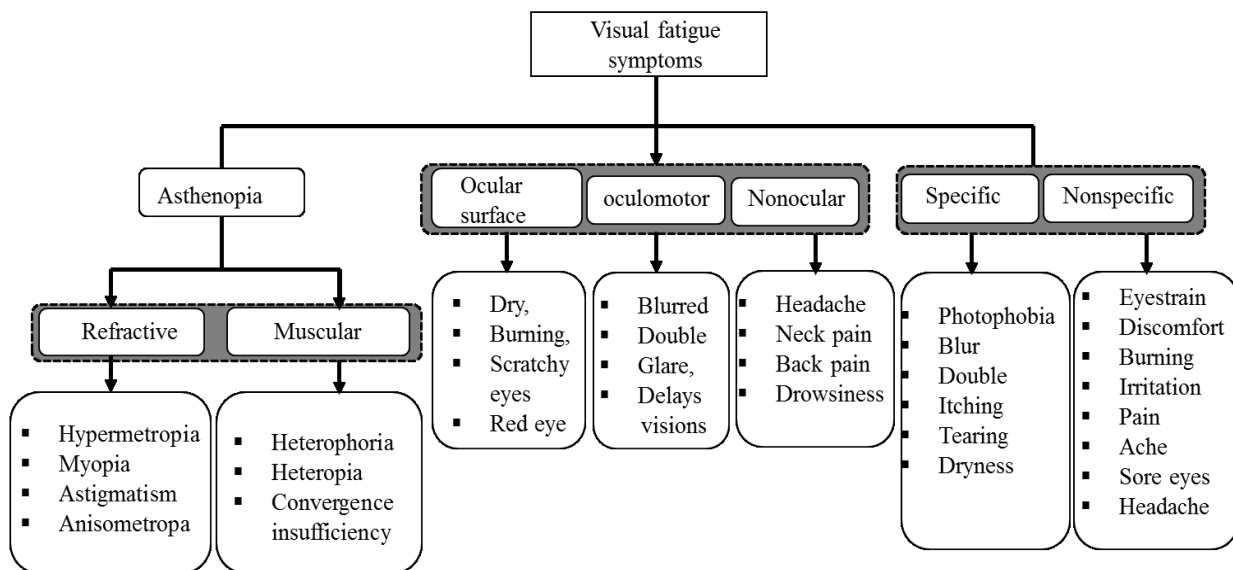


Figure 1. Taxonomy of visual fatigue and their corresponding symptoms.

Asthenopia symptoms can also be caused by neuromuscular anomalies and this is termed muscular asthenopia. These types of conditions include heterophoria, heterotopia, and convergence insufficiency (Abdi, 2007). Visual fatigue symptoms are also categorized into three kinds of discomfort, namely, ocular-surface, oculomotor, and nonocular (Sullivan, 2008). Ocular-surface symptoms include complaints about dry, burning, or scratchy eyes, and are for the most part associated with both environmental irritants and insufficient lubrication of the eye. Improving measures of visual fatigue in the use of Head Mounted Displays (HMDs) will help improve their designs as well as to help provide for greater responsiveness of devices to the state of the user. The conventional methods of detecting visual fatigue, which typically involve subjective responses to questionnaires and/or physiological measurements of the eyes taken before and after some visual task, do not provide real-time data about the progression of visual fatigue as it develops. This research incorporates cognitive neuroscience techniques that include Head Mounted Display (HMD) eye-tracking, Electroencephalograph (EEG), Electrooculograph (EOG), and Functional Near-Infrared Spectroscopy (fNIRS). These devices have not been used extensively in the study of stereoscopic HMD displays and visual fatigue.

### **1.1 Asthenopia and Stereoscopic Display**

Visual fatigue commonly arises when people view stereoscopic motion images (Ukai & Howarth, 2008). In a stereoscopic image, the viewer watches two images corresponding to the right and left eyes with convergence eye movement. Based on individual characteristics and instrumentation issues, conflicts can occur between convergence or divergence eye movement and the accommodation function thus causing visual fatigue (Pastoor & Wöpking, 1997). A number of recent studies have evaluated visual fatigues resulting from the use of stereoscopic displays, including stereoscopic television (TV) viewing as well as use of HMDs.

In general, these studies have found greater fatigue resulting from stereoscopic viewing than from monoscopic viewing. For example, in one of their experiments, Kuze and Ukai (2008) had participants play a video game using a stereoscopic HMD or monoscopic TV display, and found significantly greater increases in subjective ratings of general discomfort, nausea, and headache after using the HMD compared to the increases observed with the conventional TV display.

Chi and Lin (1998) found that among several physiological measures of fatigue, only pupil dilation and eye-movement velocity reliably differentiated between task conditions. These measures involve additional challenges. For example, pupil dilation is related to a variety of psychological states (Granholm & Steinhauer, 2004), and eye-movement velocity may be difficult to evaluate in situations involving complex visual scenes that may demand a variety of saccadic movements.

The existing past studies have not explicitly addressed the issues of image alignment errors between the two eyes and whether visual fatigue is increased by alignment errors that may occur inadvertently with HMDs. A further consideration is the interaction between stereoscopic alignment error and information load in causing visual fatigue. Although alignment errors or conflicts between accommodation and convergence may play a role in the visual fatigue induced by stereoscopic displays, other factors related to visual stimuli can also contribute to visual fatigue. For example, Wilkens (1995) states that visual fatigue can be a consequence of processing “strong sensory stimuli.” A strong stimulus has three criteria: 1) it is easy to detect at its threshold. For example, when a pattern offers intense contrast at a high spatial frequency, the threshold for that pattern will be easier to detect. 2) Even when perceiving another object, the “strong stimulus” is hard to ignore. 3) Due to its characteristics such as spatial frequency, contrast, or luminance, it elicits large electrical and vascular responses in the brain. This makes

the sensory system to respond differently to a stimulus depending on its characteristics. Going and Ntuen (2008) suggest that information load contributes to visual fatigue because of the overloading of the iconic memory. It is possible that these stimulus-related causes of fatigue may be exacerbated by problems of stereoscopic HMDs, thus making the user even less capable of dealing with high information load. If this is the case, it could have important consequences for the use of HMDs in battlefield scenarios and other situation awareness tasks. In light of these previous studies and their limitations, it is important to study the effects of alignment errors and information load on visual fatigue caused by stereoscopic displays, and to incorporate more reliable physiological methods to assess visual fatigue during task performance.

## **1.2 Study Objectives**

The objectives are organized into types of experimental investigations.

Experiment I: Study the impact of vertical and rotational stereo pair alignment as well as stereo pair magnification differences on visual fatigue.

Five hypotheses are investigated for Experiment I:

1. A prolonged use of stereoscopic display does not cause visual fatigue.
2. Alignment errors in stereoscopic displays do not increase the prevalence of visual fatigue
3. Alignment errors in stereoscopic displays have no effect on workload during visual display tasks.
4. Alignment errors in stereoscopic displays have no effect on dorsolateral prefrontal cortex hemodynamic responses during visual display tasks.
5. Alignment errors in stereoscopic displays have no effect on cerebral cortex relative power bands during visual display tasks.

Experiment II: Use cognitive neuroscience techniques to predict the on-sets of visual fatigue during situation awareness tasks.

Three hypotheses will be studied in this Experiment II:

1. A prolonged use of stereoscopic display does not cause visual fatigue.
2. A prolonged use of stereoscopic display has no effect on response time.
3. Cognitive loadings have no effects on response time.
4. Task difficulty (i.e., aircraft separation types) has no effects on response time.
5. There is no effect of interaction between cognitive workload response variables and task difficulty on response time.

### **1.3 Tasks to be Accomplished**

The following tasks will be performed.

1. An existing SA interface simulation model in the aviation domain will be used for the experimental testbed. The simulation model is a prototype of Air Traffic Controller (ATC) tasks involving separation, information load, and response time task (Wiyor, 2009).
2. Use functional Near Infrared (fNIRS) spectroscopy to obtain measurements of oxygenated Hemoglobin (HbO<sub>2</sub>) and deo- oxygenated hemoglobin (Hb) as one of the evaluation parameters of visual fatigue.
3. Complement fNIRS with electrophysiological measures using Biopac MP 150 for the measurement of brain neuron synaptic potentials and resting potentials of the eye retina, respectively.
4. Use a Head Mounted Display (HMD) equipped with eye-tracking device to measure pupil dilation, fixation, and saccades of the eye.

5. Use subject questionnaires to collect data on perception of visual fatigue.

## **1.4 Application and Intellectual Contributions**

**1.4.1 Health and etiology.** One of the established diagnoses for asthenopia is based on subjective questionnaires. This method is limited in its precision due to the unscientific nature of the diagnosis. This widely accepted methodology has been characterized by varied ethical flaws, and it is questionable among oculists (ophthalmologists and optometrists) because it lacks scientific and/or clinical diagnosis credibility, substance, integrity, or empirical support. Hence, the need for standardized and pragmatic clinical diagnosis is paramount. Using EEG and EOG measures will provide robust physiological information. The use of fNIRS for neuroimaging of the brain can yield an unquestionable rich neurophysiologic data to objectively and clinically classify and diagnose onsets of visual fatigue.

**1.4.2 Vision and neuroscience advancement.** Vision is a complex interaction between the brain and the eye, and it is controlled by the conscious and unconscious judgments with varying degrees. It involves parallel and distributed processing multiple areas through pathways of the brain, especially the cerebral cortex (Xu, Bosking, Sary, Stefansic, Shima, & Casagrande, 2004). This research outcome should provide further understanding of visual fatigue on the basis of neurophysiologic and neuropsychology of visual data.

**1.4.3 Aviation industry.** In the aviation industry, specialists such as pilots, aerospace transportation schedulers, and air traffic controllers' tasks are usually characterized by longer working hours and demand of visual resources. For example, air traffic controllers' daily routine tasks may take twelve to fifteen hours schedules, about 16 or longer flight durations for pilots. In addition to the longer working periods, the task demands are also cognitive dependent. Examples are vigilance, tracking estimation, decision making, and etcetera. These conditions

often lead to excess use of the visual resources, leading to visual fatigue and consequently accidents and hazards. This research is to provide an objective method for assessing the stages of visual fatigue on-sets for visual related tasks that will eventually help identify and prevent visual fatigue; in the long run it should prevent aviation accidents and/or hazards.

**1.4.4 Anthropometry.** It is well documented that the introduction of three-dimensional displays such 3D TV, High-Definition Multimedia Interface (HDMI) desktop, Head-Mounted Display, Helmet-Mounted Display, and 3D-glass into consumer markets have resulted in the increase of oculist visits for visual complaints (Martínez, de la O Escápita, de la Riva, & Rodriguez, 2009; Svensson, 2011). Regrettably, the designers of the 3D display have been successful on developing energy efficient, profitable and affordable 3D technologies without consideration to the users. 3D displays lack the fundamentals of the user-centered designs in terms of depth perception. People differ in human visual system particularly in terms of the eye physiology, which directly reflects the variability of perception of 3D or stereoscopic depth. A typical oculomotor characteristic of the eye is the Interpupillary Distance (IPD). Lambooij, IJsselsteijn, Fortuin, and Heynderickx (2009) noted that people with small IPD perceive more stereoscopic depth than people with large IPD. The outcome of this research can be used to establish some statistical quality standards for introduction of depth anthropometry based on gender and age, and in 3D displays.

**1.4.5 Fraud prevention and reduction of lawsuits.** It is projected that the use of Visual Display Terminal (VDT) at workplaces in advanced countries should reach 300 million units. This is over a 500% increase from 1978 with 600,000 VDT units (Martínez et al., 2009). It is also estimated that reports of visual fatigue symptoms should affect about 75% of computer users worldwide (American Optometric Association, 1999; Anshel, 2006; Leavitt, 1995 ; Tamez,

Ortiz, & Martínez, 2003). Further, Juliussen and Petska-Juliussen (1994) estimated that by the end of 1994, 74 million computers were being used in the United States, making up 43% of the world-wide computer market. Additionally, in 1995 reports were expected to increase to 100 million units (Juliussen & Petska-Juliussen, 1994; Sommerich, Starr, Smith, & Shivers, 2002). As a result, there has been a spike in the ophthalmologist and optometrist visits for Computer Visual Syndrome (CVS). This trend has resulted in an increase in insurance claims for visual syndrome disability. Thomson (1998) observed that determining the prevalence of eye problems among VDT users is problematic due to the vague nature of the complaints, symptoms definitions across different disciplines, and the presence of numerous confounding factors such as the user's eye physiology, device effects, and working conditions. This is reflected by the wide range of figures cited in the literature as shown in Table 2.

Table 2

*Varying Estimates of the Prevalence of Eye Problems Based on Source and Reporting Year(s)*

Authors	Years	% of Complaints
Hultgren and Knave (1974)	1974	47
Laubli and Hunting (1980)	1980	65
Dainoff (1980)	1980	45
Smith, Stammerjohn, Cohen, and Lalich	1980	67-93
Rey and Meyer (1980)	1980	75
Turner (1982)	1982	37-59
Starr, Thompson, and Shute (1982)	1982	76
Dain, McCarthy, and Chan-Ling (1985)	1982	25
Pickett and Lees (1991)	1991	85
Thomson (1994)	1993	40
Leavitt (1995)	1995	75

## 1.5 Taxonomy of Visual Fatigue and Related Studies

Research conducted by Yano, Emoto, and Mitsuhashi (2004); Emoto, Niida, and Okano (2005); Seuntiëns, Meesters, and IJsselsteijn (2005); Hušák et al. (2006); Woods, Docherty, and Koch (1999) revealed that the causes of asthenopia could be attributed to two major interacting factors :

1) Instrument designs that include anomalies of binocular vision due to dichoptic errors such as geometrical distortion between the left and right eye (i.e., binocular rivalry, depth-plane curvature, crosstalk). These errors can compromise the quality of viewing image by affecting contrast or legibility and less than optimal gaze angles (Sheedy, Kang, & Ota, 2002 ) and flickering stimuli in Cathode Ray Tube (CRT).

2) Eye physiology attributed to a conflict between accommodation and convergence; excessive binocular parallax; esophoria (inward deviation of the eye) (Hennessey, Iosue, & Rouse, 1984; Jaschinski-Kruza & Schweflinghaus, 1992); and uncorrected refractive error including presbyopia (Tarutta et al., 2011; Wiggins & Daum, 1991; Wiggins, Daum, & Snyder, 1992). Other contributing factors are related to performing visual tasks that may lead to reduced blinking which increases the symptomology of dry eye (Ousler, Wilcox, Gupta, Abelson, & Fink, 2004; Ousler III, Hagberg, Schindelar, Welch, & Abelson, 2008). Broadly, the attributing factors of asthenopia include only psychophysical, information, operation settings, device effects, and cognitive factors.

**1.5.1 Psychophysical factors of visual fatigue.** The physiological factors of visual fatigue are premised on the function of the ocular motor of the visual system. These ocular motor functions are accommodation (focusing), vergence (convergence and divergence of the eyes), eye movements (pursuit and saccadic movements), blink rate (frequency and amplitude), and

pupillary response (constriction and dilation). Accommodation is the functional changes in the eyes' ciliary muscles to increase or decrease the optical power of the eyes' lens to form sharp images on the retina. Convergence is a phenomenon which involves horizontal ocular muscles to converge at the axes of the eyes to fuse the two retinal images in order for the brain to process the images as a binocular vision, making it possible to see one single image (Chi & Lin, 1998). To see near objects, two eyeballs must rotate inwardly to increase the convergence power. To see far objects, two eyeballs must rotate outwardly and the function of the convergence decreases (Liu, Wang, & Wang, 2009). The discrepancy between accommodation and convergence occurs when objects come out of the screen causing out of the depth limit set by the depth of focus of the human visual system (ranges from about -0.2D to 0.2D). Yano, Ide, Mitsuhashi, and Thwaites (2002) investigated this problem by measuring subjective degrees of visual fatigue from the change of accommodation response before and after viewing stereo images. They found that the change of accommodation response waveform corresponds to the estimation of visual fatigue and that our visual functions return to normal in about 30 minutes after an exposure to such unnatural condition. As shown in Figure 2, visual fatigue ( $G$ ) increases with an increase in depth ( $T$ ).

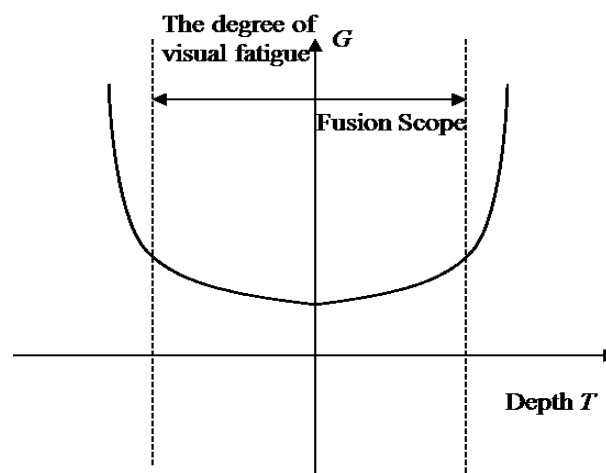


Figure 2. The relation graph between visual fatigue and depth [Source Liu et al. 2001].

When  $T$  is not in the fusion scope, the diplopia (double vision) phenomenon occurs and  $G$  increases greatly. When  $T$  is in the fusion scope, the fatigue degree is less. Double vision may occur as a result of the simultaneous perception of two images of a single object that may be displaced horizontally, vertically, or diagonally (i.e. both vertically and horizontally) in relation to each other (O'Sullivan & Schmitz, 2007).

Eyelid movements are one of the visual behaviors that reflect a person's level of fatigue (Zhu & Ji, 2004b). Increased eye blink rates have long been reported as evidence of visual fatigue (Mourant, Lakshmanan, & Chantadisai, 1981) and increased visual workload has been associated with reduction in eye blink rate (Hancock, Meshkati, & Robertson, 1985; Hancock, Wulf, Thom, & Fassnacht, 1990; Veltman, 1996). Costanza (1994) stated that a reduced blink rate leads to drying of the eye surface with a corresponding decrease in oxygen supply to the cornea epithelium. Electroculogram (EOG) provides a measure for blink rate (BR), blink duration, long closure rate (LCR), and blink amplitude (BA).

The eye pupils play a leading role in the optical system of the eye because its size determines the amount of light falling on the retina and controls the aberrations and the depth of focus of the eye (Rabbetts, 2000). Pupillometric methods are used to measure variations in the diameter of the pupillary aperture of the eye in response to psychophysical and/or psychological stimuli (Granholm & Steinhauer, 2004).

Eye gaze has the potential to indicate a person's level of vigilance. A fatigued individual tends to have a narrow gaze. Gaze may also reveal one's needs and direction of visual attention. The direction of a person's gaze is determined by two factors: the orientation of the face (face pose), and the orientation of eye (eye gaze). Face pose determines the global direction of the gaze, while eye gaze determines the local direction of the gaze. Global gaze and local gaze

together determine the gaze of a person. So far, the most common approach for ocular-based gaze estimation is by eye tracker. Eye fixation in contrast to saccade is the relatively stable eye-in-head position characterized by threshold of dispersion (approximately  $2^\circ$ ), minimum duration of the range of 100ms to 200ms, and velocity of  $15^\circ$  to  $100^\circ$  per second (Jacob & Karn, 2003; Pavlas, Lum, & Salas, 2012). McGregor and Stern (1996) and Van Orden, Jung, and Makeig (2000) found that eye fixation covary with changes in performance due to drowsiness, loss of vigilance, increasing time-on-task, and visual discomfort. Saccadic eye movements are rapid conjugate shifts of gaze to track environmental stimuli, such as targets. They are the intermittent eye movements that occur when the eye fixate on one point after another in the field of view (Pavlas et al., 2012). They are high-velocity movements that quickly direct the eyes toward the target (Kornyllo, Dill, Saenz, & Krauzlis, 2003).

**1.5.2 Information factors.** The effectiveness of information visualization largely depends on the ease and accuracy with which the users can easily access the information. This, however, depends on the visualization constraints, such as information cluster, information dynamics, iconic memory aids, and information refresh rate. Information cluster can distract the user's attention to properly visualize and read information, thereby increasing workload via eye strain. Refresh rates present perceptual distortions and interference with eye movements (Wilkins & Neary, 1991). Refresh rate is the number of times per minute the screens repainted to produce an image (measured in Hz). If the rate is too slow, characters will start to flicker. It causes annoyance fatigue and headache.

**1.5.3 Operational factors.** Workstation variables such as glare, lighting conditions, image and character legibility have shown a relationship with the reporting of subjective visual fatigue symptoms (Collins, Brown, Bowman, & Carkeet, 1990). Sauter, Schleifer, and Knutson

(1991) found a significant effect when relating glare to subjective reports of visual fatigue resulting when Visual Display Unit (VDU) is used. Inability to see the characters displayed on a VDU prompts the user to increase visual attention which may lead to an increase in reports of visual fatigue.

Visual fatigue can result from operational setting factors relating to visual inefficiencies or from eye-related symptoms caused by a combination of individual visual abnormalities and poor visual ergonomics. Usually, problems occur whenever the visual demands of the task exceed the abilities of the individual, and symptoms of visual fatigue usually resolve with a combination of changes in the environment and an appropriate visual care (Blehm, Vishnu, Khattak, Mitra, & Yee, 2005). As noted by Turville, Psihogios, Ulmer, and Mirka (1998), visual fatigue during VDT use is often caused by prolonged visual activity performed during near-work. Near sighted work distance often caused the extraocular and ciliary muscles of the eye to contract and maintain contraction in order for the eye lens to converge and accommodate for the proper focus. The extraocular and ciliary muscle work effort and exertion lead to eye strain and visual fatigue (Jaschinski-Kruza, 1984, 1991; Jaschinski-Kruza & Schweflinghaus, 1992; Jaschinski-Kruza, 1993; Wimalasundera, 2009). Aarås, Horgen, Bjørset, Ro, and Thoresen (1998) showed that visual fatigue with use of a Cathode Ray Tube (CRT) monitor was significantly decreased by enhancing the level from 300Lux to 600Lux. Further, the contrast ratio decreases with an increase in ambient illumination due to surface reflection which makes the screen brighter, and display brightness has been a factor of visual fatigue (Wang et al., 2011).

Prolonged visual engagement can cause visual fatigue. Mutti and Zadnik (1996) noted that visual complaints were reported by 75% of VDT operators working 6-9 hours in front of their screens compared to 50% of other workers. Also, surveys of optometrists in the United

State and the United Kingdom indicate that 12.4% and 9.0%, respectively, of their patients are examined primarily because of symptomatic visual or ocular problems associated with using a computer (Mutti & Zadnik, 1996). Similarly, about 50% -75% of full-time VDU operators in Sweden have complained of visual fatigue symptoms (Knave, Wibom, Vos, Hedstrom, & DBerquist, 1985; Koh, Ong, & Jeyaratnam, 1994; TCO Work Environment Committee, 1986). The more intense and prolonged the VDU is, the more likely an operator is likely to experience the symptoms of visual fatigue such as reduced blinks, blurred vision, or irritated eyes (Koh et al., 1994). For example, in Singapore where the average office worker spends about 10-16 hours performing tasks with VDUs, about 94% of the VDU operators reported suffering from visual fatigue symptoms (Ong, 1984). The prevalence of symptoms of visual fatigue is slightly greater in females than males (Salibello & Nilsen, 1995; Shimmura, Shimazaki, & Tsubota, 1999). The literature has shown that after age 40, most people experience ocular-motor problems such as accommodations and convergence spasm (Millodot & Newton, 1981; Stein & Stein, 1994).

Devices may also cause visual fatigue. For example, a head mounted display (HMD) gives rise to certain health and performance problems even when they are used in a non-stereoscopic (bi-ocular) mode. These problems are axes, magnification factor, and image distortion. Stereoscopic HMDs require strict alignment of axes; otherwise, viewers have to put up with alignment errors in addition to binocular disparity. Apart from visual fatigue, HMDs have other characteristics that are different from other displays. Images on HMDs are not fixed to actual space coordinates, but to the head. Thus, when the head moves, reflex eye movements that are known as vestibulo-ocular reflexes (VOR) are evoked (Ukai & Kibe, 2003).

**1.5.4 Stereoscopic and autostereoscopic display.** Stereoscopic displays require that the viewer converges and accommodates at different depth planes, thus creating a conflict between

the two visual mechanisms (Jin, 2011). One of the major problems with stereoscopic 3-D displays is that a stereoscopic display produces a mismatch between the focus (accommodation distance) and the fixation (convergence distance) of human eyes. With this, stereoscopic 3-D images may give different depth information to the accommodation function and to the convergence function. This problem is common in 3-D display systems such as HMDs and displays that make use of a lenticular lens. The imbalance visual information may be one of the reasons for the visual load and the visual fatigue associated with 3-D images (Inoue & Ohzu, 1997).

Inoue and Ohzu (1997) noted that the common causes of visual fatigue in a stereoscopic display is mainly due to the fact that 3D spaces that are generated by stereoscopic image are artificial spaces which are different from real spaces. As a result, the perceived images through 3D glasses do not really exist. Okada et al. (2006) and Fukushima, Torii, Ukai, Wolffsohn, and Gilmartin (2009) showed that the improvements of image quality, when a stereoscopic system is used, increase the discrepancy of accommodation and convergence and may cause increased visual fatigue. Complaints and symptoms of visual fatigue have been reported with 3D stereoscopic displays (Emoto, Nojiri, & Okano, 2004; Hoffman et al., 2008; Svensson, 2011; Ukai & Howarth, 2008; Yano et al., 2002).

**1.5.5 Cognitive factors.** Costanza (1994) asserted that vision is comprised of two types of activities. The first activity involves the physical adjustment such as changes of the pupil, changes in the curvature of the crystalline of the eye in order to obtain high quality, and compatible retinal images. The second activity involves the perceptual and mental aspects which require cognitive resources. Different cognitive tasks seem to involve different information processing systems, and the resources and the limits of these systems determine the cognitive

capability to perform a given set of tasks (Francis, Rash, & Russo, 2009). Some of the cognitive resources affected by human visual systems are visual perception, attention, and memory. Visual tasks require perceptual and mental efforts. For example, deciphering an unfamiliar handwriting, or reading complicated instructions from a manual may produce eyestrain (Sauter, 1985).

The most basic requirement for stereoscopic related display with regard to visual perception is that the stereoscopic unit needs to be able to generate light patterns that can be easily detected by the earliest stages of the human visual system (Francis et al., 2009). The effect of alignment errors in the light patterns of stereoscopic displays are low or high intensity, loss of spatial frequency and spatial resolution, and temporal response (Anderson, 1993; Baddeley, 2003).

Simons and Levin (1997) observed that attentional effect is one of the major causes of 3D visual fatigue. Visual fatigue studies conducted by Van Orden et al. (2000), Pavlas et al. (2012), Kornylow et al. (2003), and Baloh et al. (1975) concluded that fixation frequency and fixation duration are lower in viewing 3D stereo content and saccade velocity higher when viewing 3D stereo content. These conclusions are strongly attributed to visual fatigue.

## **1.6 A Summary of Visual Fatigue Studies from Medical, Human Factors and Neurophysiology Perspectives**

Appendix A, Appendix B, and Appendix C provide the reviewed summaries of visual fatigue from medical, human factors, and neurophysiology points of view, respectively.

## **1.7 Chapter Summary**

This research is organized as follows: Chapter 2 summarizes all the equipment and resources used for the experiments and the type of data to be collected by this equipment.

Chapter 3 presents the experimental methodology, protocols, and experimental design and results

for Experiment 1 which investigates the impact of misalignments errors on visual fatigue. Chapter 4 discusses the data analyses and results for Experiment 1. Chapter 5 presents the experimental methodology, protocols, experimental design, results and discussion for Experiment 2, which uses cognitive neuroscience techniques to evaluate onset of visual fatigues during situation awareness tasks. Chapter 6 uses a feed forward neural network (FF-ANN) to combine the objective by classifying visual fatigue using objective and subjective data. Chapter 7 provides the summary, discussions, and suggestions for future research.

## CHAPTER 2

### Equipment Used for the Study

#### 2.1 Functional Near-Infrared Spectroscopy (fNIRS)

Functional near Infrared Spectroscopy (fNIRS), developed by Jobsis in 1977, is the most recent brain imaging device for exploring brain responses to a variety of stimulated cognitive and physical tasks in the field of cognitive neuroscience. Prior to the advent of fNIRS, similar equipment such as Positron Emission Tomography (PET), Functional Magnetic Resonance Imaging (fMRI), Magnetoencephalography (MEG), and Single Positron Emission Computed Tomography (SPECT) had been used to collect data associated with the human brain function (Akgül, 2004; M. Izzetoglu, Bunce, Izzetoglu, Onaral, & Pourrezaei, 2007). The fNIRS has numerous advantages over other brain imaging instruments. The device is a noninvasive, safe, portable and minimally intrusive monitoring system. These qualities make fNIRS versatile for cognitive studies in any working and educational environment, as well as field studies (M. Izzetoglu et al., 2007; Strangman, Boas, & Sutton, 2002; Villringer & Chance, 1997).

The device consists of an infra-red light source with a wavelength range of 650-850 nm into the head and detector that receives light after it has interacted with the tissue (Izzetoglu, 2004). The emitted photons after interacting with head tissues undergo two types of interaction; namely absorption (loss of energy to the medium) and scattering (Chance, Nioka, & Luo, 1998; Rolfe, 2000; Strangman et al., 2002). The photo-detector arrangement placed at a certain distance away from the light source can collect the photons that are not absorbed and those that traveled along the “banana shaped path” between the source and detector due to scattering (Gratton, Maier, Fabiani, Mantulin, & Gratton, 1994; Villringer & Chance, 1997). The light that passes through brain tissues are sufficiently low to allow tissue imaging at depths up to 2-3

centimeters. Deoxygenated (Hb) and oxygenated (HbO<sub>2</sub>) hemoglobin are the main absorbers of near infrared light in tissues, and they provide relevant markers of hemodynamic and metabolic changes associated with neural activity in the brain (Izzetoglu, Bunce, Onaral, Pourrezaei, & Chance, 2004).

The spatial resolution in fNIRS is limited to approximately 5 mm. Researchers have shown that by placing the probes on a subject's forehead, fNIRS provides accurate measures of activities within the frontal lobe of the brain, which are responsible for many high order cognitive functions, such as memory and problem solving that make up cognitive activities (Izzetoglu et al., 2004). The light passes through tissues are sufficiently low to allow for tissue imaging at depths up to 2-3 centimeters. Deoxygenated (Hb) and oxygenated (HbO<sub>2</sub>) hemoglobin are the main absorbers of near infrared light in tissues, and they provide relevant markers of hemodynamic and metabolic changes associated with neural activity in the brain. The levels of Hb and HbO<sub>2</sub> measured are relative to the baseline only. It is not possible to arrive at absolute values of concentration using fNIRS imaging on living samples. Once the Hb and HbO<sub>2</sub> levels are computed, they are used to calculate the levels of oxygenation (in  $\mu\text{M}$ ), and values that may be approximately treated as percent changes in blood volume.

## **2.2 Biopac MP-150**

The Biopac MP150 comprises of Electrooculogram amplifier (EOG100C), Electroenceelogram amplifier (EEG100C), Galvanic Skin Response amplifier (GSR100C), Respiratory Rate amplifier (RSP100C), and Electromyogram (EMG100C). The 100C series biopotential amplifier modules are single channel, differential input, linear amplifiers with adjustable offset and gain. These modules are used to amplify smaller voltage signals coming from raw electrodes and transducers (typically less than  $\pm 0.01$  volt). In addition to amplifying

signals, most of the 100C series modules include selectable signal conditioning ability so that data may be filtered or transformed as it is being collected.

The Biopac MP 150 device is operated by AcqKnowledge software (BIOPAC Systems Inc., 2011) that plots continuous temporal graphical distribution of brain as functions of voltage and time. The *AcqKnowledge* software is the integrated platform for acquiring, storing, and plotting data from the MP 150 for further analysis. As indicated earlier, the potential difference and the rotation of the eye are the basis for signal measurement of electrooculogram, electronystagmogram, and electroretinogram.

The Electroencephalography (EEG) signals indicate the electrical activity of the brain as continuous graphical distribution of spatiotemporal of voltage over time. Electrical activity of the brain is produced by billions of brain cells called neurons (Andreassi, 2009). As pointed by Barlow (1993), EEG is the measurement of the electrical potential current flow summation of excitatory and inhibitory post-synaptic potentials in the pyramidal cells of the cerebral cortex. The electrical potential generated by the eye is based on the fact that the human eye is a fixed dipole with positive pole at the cornea and negative pole at the retina (Malmivuo & Plonsey, 1995 ). The magnitude of the cornea-retinal potential is in the range of 0.4-1.0 mV and is generated by the metabolic activity of the retina (Malmivuo et al., 1995). The lens of the eye brings illuminated external scenes to focus on the retina. Visual information proceeds from the retina to the central nervous system along the optic nerve. The process sets up a slow varying potential which forms the basis of Electro-oculogram (EOG; du Bois-Reymond, 1848). The cornea-retinal potential is not fixed but vary by the effects of light, fatigue, and other qualities (Carpenter, 1988; Malmivuo & Plonsey, 1995 ). Using the frequency domain of the EEG signals, certain frequency bandwidths can reveal the functional states of the brain. For example, Delta

waves (< 3.99 Hz) are predominantly associated with deep sleep stages; Theta waves (4-7.99 Hz) indicate wake condition; Alpha waves (8-12.99 Hz) for normal relaxed adults; Beta waves (13-29.99 Hz) signify alert or anxious brain (see Table 3).

Table 3

*EEG Frequency Band*

Frequency Band	Range (Hz)	Cognitive State
Delta	0.1-3.99	Preparing a move
Theta	4-7.99	Memory
Alpha	8-12.99	Relaxation
Beta	13-29.99	Motor inactivity
Gamma	> 30	Characteristics association

The relative frequency bandwidths of theta, alpha, and other EEG rhythms may serve to indicate the level of fatigue that subjects experience (Trejo et al., 2005a). For example, Event-Related Potential (ERP) has been used to obtain subjects' attention and focus to task-relevant stimuli. Kramer, Trejo, and Humphrey (1996) observed that the P300 component is known to reflect the allocation of processing resources to task-relevant stimuli, being of larger amplitude in high workload tasks than in low-workload tasks. Studies by Li, Seo, Kham, and Lee (2008) found that the P700 component appears to reflect a high level cognitive activity required at the judgment of 3D depth discrimination. As a 3D visual fatigue increases, cognitive activity to judge 3D depth is delayed. This interpretation is quite consistent with other studies (Chioyenda et al., 2007; Gomas, Althaus, Wijers, & Minderaa, 2006).

### **2.3 Head Mounted Display (HMD) with ViewPoint Eye Tracker Device**

As shown in Figure 3, the HMD-ViewPoint Eye Tracker<sup>®</sup> device provides a complete eye movement evaluation environment.

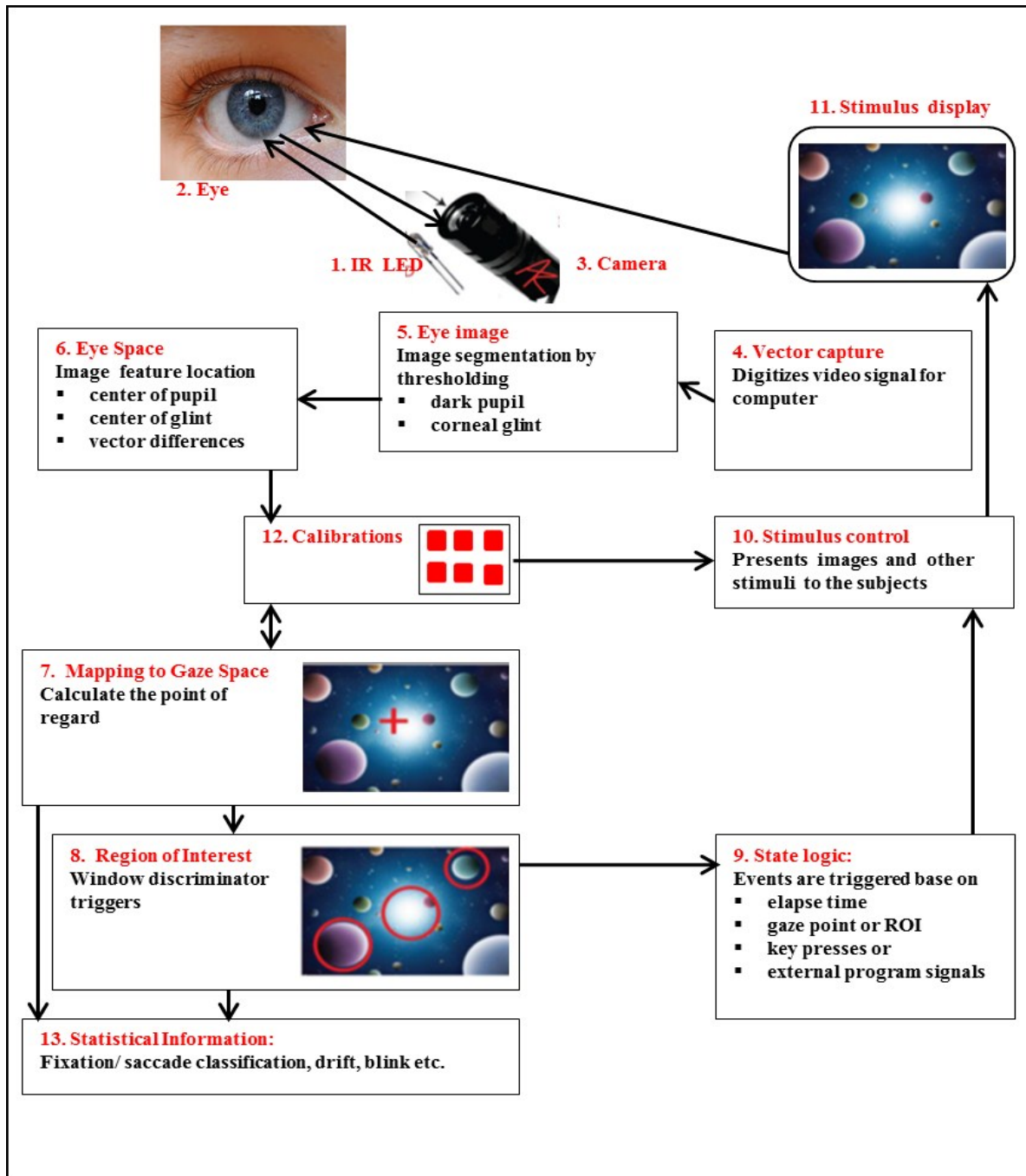


Figure 3. Configuration of the Viewpoint Eye Tracker [ViewPoint EyeTracker® by Arrington Research, 2010].

The device consists of integrated stimulus presentation camera and infra-red LED for simultaneous eye movements and pupil monitoring, and a Software Developer's Kit (SDK) for communicating with other applications. It incorporates several methods from which the user can

make selection to optimize the system for a particular application. The Viewpoint eye tracker system parts consist of the infrared light source (item 1) which serves to both illuminate the eye (item 2) and also to provide specular reflection from the surface of the eye or smooth cornea. In a dark pupil mode, the pupil acts as an infrared sink that appears as a black hole. In a bright pupil mode, the “red eye” effect causes the pupil to appear brighter than the iris. The video signal from the camera (item 3) is digitized by the video capture device (item 4) into a form that can be understood by a computer. The computer takes the digitized image and applies image segmentation algorithms (item 5) to locate the areas of pupil and the bright corneal reflection (glint). An additional image processing (item 6) locates the centers of these areas and also calculates the difference vector between the center locations.

A mapping function (item 7) transforms the eye position signals (item 6) in EyeSpace coordinates to the subject’s GazeSpace coordinates (item 8). Next, the program tests to determine whether the gaze point is inside of any of the region of interest (ROI) that the user has defined. The calibration system (item 12) can be used to present calibration stimuli via (item 10) to the user and to measure the eye position signals (item 6) for each of the stimulus points. These data are then used by (item 12) to compute an optimal mapping function for mapping to position of gaze in GazeSpace (item 7). The equipment was used to collect data on saccade and fixation classifications, drifts, and blink rates.

#### **2.4 Simulator Sickness Questionnaire (SSQ)**

The SSQ as proposed by Kennedy et al. (1993) is comprised of four parts: nausea rating, oculomotor fatigue rating, disorientation rating, and a total score rating. For each component, a higher rating indicates that a participant experienced more symptoms. The symptoms, rated as None = 0; Slight = 1; Moderate = 2; and Severe = 3 of the SSQ, are shown in Appendix D.

## 2.5 Task Simulation Testbed

The task stimulus is an Air Traffic Control Interface Model (ATCIM) developed by Wiyor (2009) and designed with LabView 8.1. provided by National Instrument (Travis & Kring, 2002). The simulated testbed provides a situation awareness (SA) environment similar to an ATC task domain. The use of ATCIM as an ATC simulator is specifically designed to allow for close experimenter control over display features and task performance, while providing a moderate degree of realism. In the ATCM domain, an operator perceives and responds to aircraft conflict separation tasks which occur when two or more aircrafts are in self-separation violation. The separation violation is set to a loss of separation of 5NM laterally or 1000 ft. vertically, or both conditions can occur simultaneously (Hopkins, 1995).

The ATCIM system consists of two main interfaces, namely, the control setting interface and dashboard interface. The control setting interface allows the user to select inputs for the simulation. These as follows: (a) Two closest aircraft color identifications; (b) Color Status Bar which consists of two mutually exclusive red and green color appearance with green for safe mode and red for crash mode; (c) Alert Distance Control that allows the user to preset the minimum safe distance between two planes; (d) Display Time Control which allows for the user to input the minimum time between system collision time and perceived time by the experimenter; (e) Number of Aircraft to Monitor which allows the user to pre select the number of aircraft for the experiment; (f) Sound Control that controls the amount of auditory tones at time of aircraft crash; (g) Collision Alert used by the subjects to respond before collision time; and (h) Aircraft Information-Radii Mode in which the plane path, latitude, longitude, speed and bearing are displayed on the radii and move with the aircraft. The dashboard interface has an output section for data collection during the simulation. This consists of a 30-mile nautical radius

sector in which the number of aircraft is selected to be monitored by the participants. Based on the predetermined mode selected from the setting section, the required output will be shown in the dashboard section at simulation run. Each aircraft is characterized by traffic and conflict information. Within the ATCIM, the minimum safe altitude warning distance is fixed to a default value (see Figures 4 and 5).



Figure 4. ATCM interface design for the study 1. The Interface is designed with LabView 9.1<sup>®</sup> software provided National Instrument.

Throughout the experiments, three ATC tasks were used. They are labeled ATC1, ATC2, and ATC3 to represent the first, second, and third repeated experimental tasks presented in alignment errors. Based on a particular randomization outcome for a particular participant; ATC1 could be vertical shift, ATC2 could be magnification differences, and eventually, ATC3 would be rotational error.

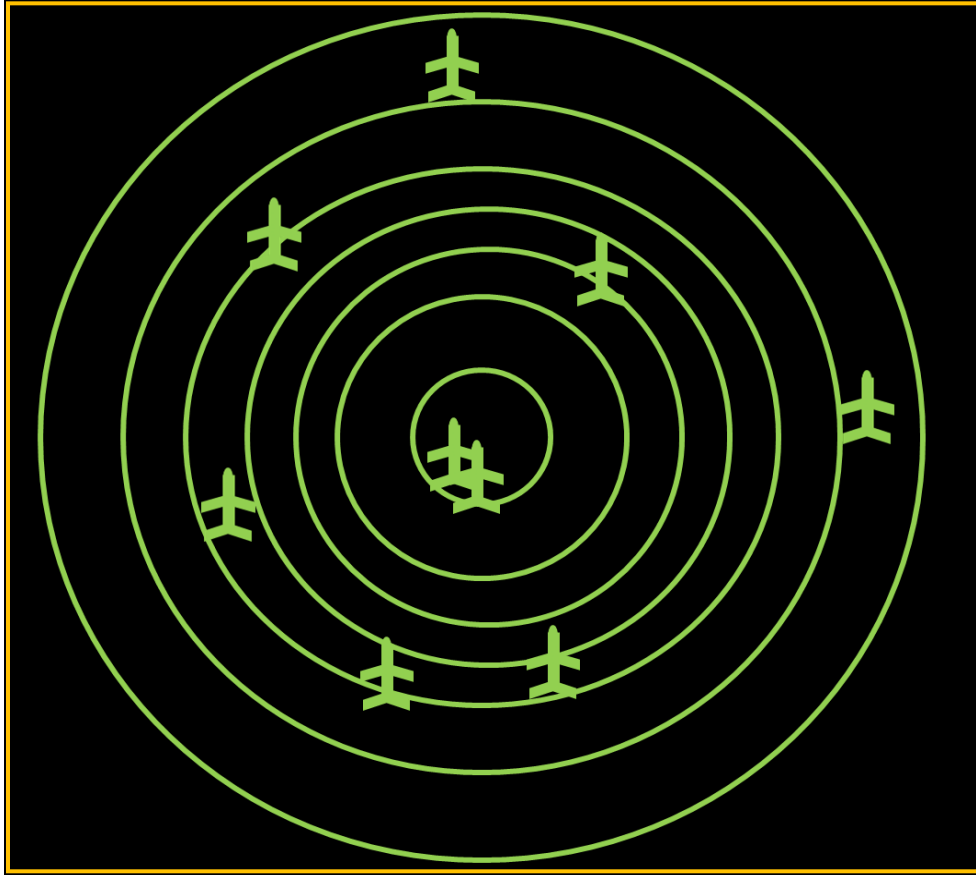


*Figure 5.* ATCM interface design for the study 2. The Interface is designed with E-Prime<sup>®</sup> software provided psychological software tools incorporated.

For study 2, the ATC1, ATC2, and ATC3 are the repeated experimental tasks. The experimental treatments are based on the cognitive loading and task difficulty. The cognitive loading is the number of aircraft on the radar with separation conflicts. The cognitive loading has two levels labeled as low (3) and high (9) while task difficulty has four levels based on the separation conflicts labeled as vertical, horizontal, combined horizontal and vertical, and none. A high maneuver (ATC3) has a maximum number of nine aircraft with either combined horizontal and vertical or none for separation conflicts, and a low maneuver (ATC1) has 2-3 aircraft conflicts in the airspace.

## CHAPTER 3

### Experiment I: The Impact of Alignment Errors on Visual Fatigue

This experimental task investigates the impact of alignment errors on visual fatigue.

Three types of alignment errors in optical systems are defined by Self (1986). Vertical alignment error is an upward or downward tilt in the optical axis of one image resulting in differences of vertical position of an image. Rotational alignment error is a tilt in one of the images with the degree of alignment error increasing from the center. Lastly, magnification difference is an error due to the size difference between the left and right stereo pairs from the field of view.

An issue not often discussed in stereoscopic research is alignment and calibration error. Alignment error has three main sources (Kooi & Toet, 2004). Firstly, errors in the optics are due to shift in the placement for the left and right stereo pairs; optical errors are due to either a shift in rotation, difference in magnification, or difference in reduction. Second, filtration errors in photometry are caused by the difference in luminance, color, contrast, chromatic aberration, or cross talk (images switching back and forth between the eyes). Unfortunately, alignment errors result in binocular asymmetry causing visual discomfort (Kooi & Toet, 2004), shifts in perceived image direction with contrast differences (Mansfield & Legge, 1996) and loss of fusion for stereo pairs (Cheung & Milgram, 2000).

Research has shown that vertical alignment error correlates with degrees of eyestrain (Jin, 2011). Vertical and horizontal alignment error is a well-known problem that causes visual fatigue (Kim, Min, Oh, Jeon, & Sohn, 2009). Vertical alignment errors can be caused by convergence stereoscopic camera structure or caused by slightly tilted stereo camera pair. Panum's fusional area defines the limit of horizontal disparity and vertical disparity in retinal domain (Qin, Takamatsu, & Nakashima, 2004).

For this study, the vertical alignment error is limited within Panum's fusional area to avoid excessive disparity that may likely affect research outcome.

Five hypotheses are investigated in Experiment I.

- 1.1 A prolonged use of stereoscopic display does not cause visual fatigue.
- 1.2 Alignment errors in stereoscopic displays do not increase the prevalence of visual fatigue.
- 1.3 Alignment errors in stereoscopic displays have no effect on workload during visual display tasks.
- 1.4 Alignment errors in stereoscopic displays have no effect on dorsolateral prefrontal cortex hemodynamic responses during visual display tasks.
- 1.5 Alignment errors in stereoscopic displays have no effect on cerebral cortex relative power bands during visual display tasks.

We study the impact of mismatch of right/left images through different magnification of right/left images, vertical and horizontal of right/left image shifts, and mutual rotation of two images on depth perception errors and visual fatigue.

### **3.1 Experimental Design**

The experiment is conducted as completely randomized within subject design. The experimental treatments are the three stereoscopic alignment errors, and each treatment was replicated twice. It should be noted that a particular treatment replication is completed before moving to the next treatment. (For example, if the randomization order is vertical shift, magnification difference, and rotational error). The vertical shift treatment will be replicated twice and each replication lasts for 10 min, hence 20 min for vertical shift as ATC1, followed by magnification difference two replications as ATC2 and lastly, the rotational error two replications

as ATC 3. Table 4 contains the information on the independent variable, levels and measurement units for the experiment.

Table 4

*Experimental Independent Variables, their Levels, and Measurement Units*

Factor	Levels	Measurements
Alignment Errors	Vertical shift	1/2"
	Rotational errors	1/4"
	Magnification differences	6.25%

The independent variable is the stereoscopic alignment errors. The stereoscopic alignment errors had three levels, namely, vertical shift, rotational error, and magnification difference. For the vertical shift, the focused images on the left and right retina are displaced by half inches. For rotational error, the images are displaced from each other in the left and right retina by quarter inches, while for magnification difference, error is caused by 6.25% enlargement in one image. There are five response measures: SSQ, hemodynamic response, electrophysiological response, workload, and visual fatigue ratings. The hemodynamic and electrophysiological responses are continuous variables measured with fNIRS and Biopac MP 150, respectively. The workload and visual fatigue symptoms are subjective ratings measured with NASA-TLX (see Appendix E) and Simulator Sickness Questionnaire (SSQ; see Appendix D).

### **3.2 Apparatus**

The apparatus for the study are an 8ft. x 6ft. NEC LT silver screen, NEC LT 245 DLP projectors, NEC LT 245 polaroid glasses, 22" 1.58 GHz 0.99 GB RAM Gateway DCDi Desktop, Biopac MP 150, Snellen Chart, Measuring tape, Hp 3435A digital Impedance multi-meter, GPM vernier calipers, NASA-Task Load Index (NASA-TLX v.1.0), Simulator Sickness Questionnaire

(SSQ), Neurophysiological Assessments (see Appendix F) and Ophthalmological questionnaire (see Appendix G), and EL-503 and EL-110 Electrodes.

Several software systems are used for the study. These are ATCIM, Cognitive Optical Brain Imaging Studio (COBI) provided by fNIRS Devices LLC (2010) for the fNIRS, and *Acqknowledge*<sup>®</sup> for the Biopac MP drivers (BIOPAC Systems Inc., 2011). Raw materials used include, Nuprep<sup>™</sup>, Ten20<sup>™</sup>, 70% Isopropyl Alcohol Swap, Q-Tips, Cotton Squares, and Ballpin, AstroMed bandage, and Omini gel.

### 3.3 Participants

**3.3.1 Estimating number of subjects.** The estimated number of human subjects for the study is derived from the power of test analysis formula. The power is defined as the probability of not committing type II error, that is, failure to reject null hypothesis when in fact the alternative is true (Cohen, 1977; Dell, Holleran, & Ramakrishnan, 2002; Kupper & Hafner, 1989). Based on the hypotheses, the sample size expression is shown in equation 1.

$$n = \frac{2v\sigma^2\phi^2}{\Delta^2}, \quad (1)$$

where,  $n$  = number of subjects;  $v$  = number of treatments;  $\sigma$  = standard deviation;  $\phi$  = power of the study, and  $\Delta$  = effective size of the study.

Using a power of 0.80 at the 0.05 significant level, a  $\phi$ -value of 1.824 was interpolated from the power of the F-Test table provided by Dean and Voss (1999). A  $v$ -value of 3 was obtained based on the levels of alignment errors. As noted by Sallamander (2010), asthenopia is exacerbated when daily visual display terminal (VDT) tasks last between 4 to 7 hours. We assumed the effect size ( $\Delta$ ) of 7 hrs. Using the experimental data obtained from Lin, Liang, Hwang, and Wang (2010) study, a sample standard deviation of 4.43 is selected because the studied was focused on predicting visual fatigue.

The sample size required is established by

$$n = \frac{2 * 3 * 4.43^2 * 1.824^2}{7^2} = 23.98 \approx 24 \text{ subjects.} \quad (2)$$

Hence 24 participants were used for the study.

### 3.3.2 Visual acuity test and interpupillary distance (IPD) measurements. 24

participants were recruited for the study and consisted of twenty-one males and three females.

The participants were recruited from the college of engineering, and partial credits were awarded to the participating students from their professors. Participants were also screened for color blindness and visual acuity test. The World Health Organization (WHO) specifies blindness as a visual acuity less than 20/400. A visual acuity test was conducted with Snellen chart to screen the participants. The visual acuity score was limited to 20/40. The visual acuity ranges for the participants were between 20/20 to 20/40. Gender and visual acuity composition are shown in Table 5.

Table 5

*Relationship between Gender and Corresponding Visual Acuity Composition*

Gender	Total	Left Eye			Right Eye		
		20/20	20/30	20/40	20/20	20/30	20/40
Male	21	15	6	0	15	5	1
Female	3	3	0	0	3	0	0

The Ophthalmological and Optometric questionnaire (see Appendix G) is used to screen participants for any history of ophthalmological symptoms and optometric corrections. The objective was to eliminate participants with history of ophthalmologic disease and optometric correction which otherwise would have been confounding variables for the study. This was followed with the neurophysiological questionnaire (see Appendix F).

The Interpupillary Distance (IPD) is measured with GPM vernier calipers. Figure 6 shows the Limbus method from International Centre for Eyecare Education (ICEE) (2009) used for IPD measurement.

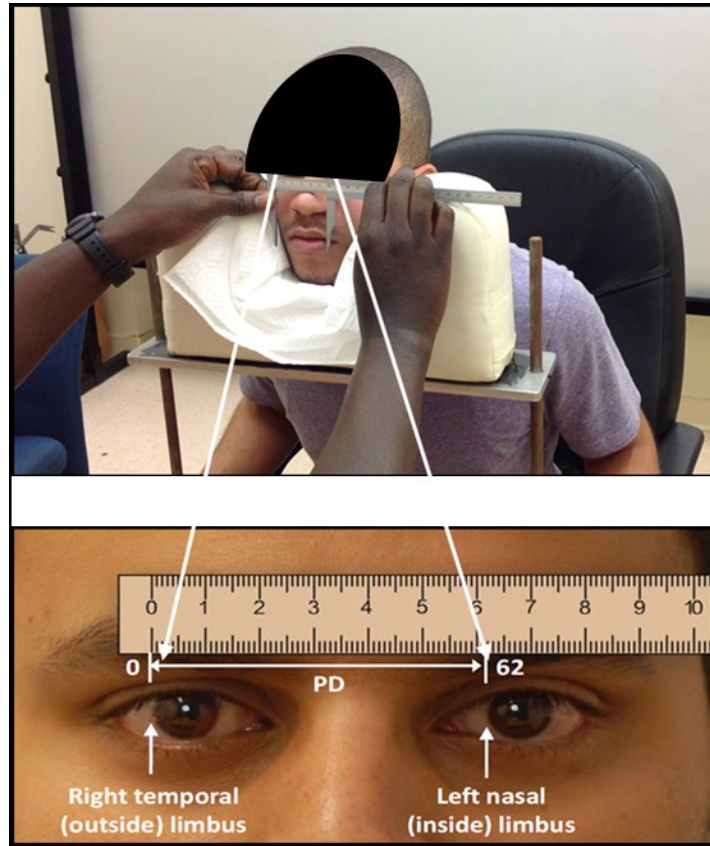


*Figure 6.* Interpupillary Distance (IPD) measurements using the Limbus method.

Participants were asked to place their chin in an eye tracker chin rest and asked to close their eyes; the vernier caliper was placed just above the participant's nose and aligned parallel to the eyes. The participants were asked to open their eyes and maintain no blink for 10 seconds during which the inside edge of the fixed jaw of caliper was aligned to the right eye's temporal (outer) limbus and the inside edge of the movable jaw was slid to left until it was aligned to left eye's nasal (inner) limbus.

**3.3.3 Participants' preparation.** Participants were prepped for electrode placements. The nasion-inion distance of each participant's head was measured with measuring tape. Using

the 10-20 nomenclature for EEG electrode placement, EEG markings for  $O_z$ ,  $O_1$ , and  $O_2$  positions were determined by calculating 90% for  $O_z$  from nasion. For  $O_1$  and  $O_2$ , the nasion-inion distance was measured on the lateral side of the head at 90% from nasion on the left and right hemisphere of the head as  $O_1$  and  $O_2$ , respectively. The positions were marked with colored marks. The 70% Isopropyl Alcohol to clean the landmarks and then followed with Nuprep™ cream to clean the dirt from the skin. Further, the Omni gel was used to wipe clean the skin. The Grass shielded EL-110 electrodes cup was filled with EC2® electrode cream provided by GRASS (GRASS Technologies, 2012). The EC2® electrode was placed on the prepared surfaces and held in place by AstroMed bandage. The EC2® Electrode is used to reduce noise in the EEG recording.

As shown in Figure 7, participants were seated at 120 inches from the silver screen. The Ground electrode was placed on the forehead and connected to 100EEG amplifier No.2 GND port; Reference electrode was placed behind the right ears and connected to 100EEG amplifier No.2 VIN- port;  $O_z$  electrode was connected to 100EEG amplifier No.2 VIN+ port;  $O_1$  electrode was connected to 100EEG amplifier No.1 VIN+ port; and,  $O_2$  was connected to 100EEG amplifier No.3 VIN+ port. The impedance between EEG electrodes and skin was kept to less than 5k $\Omega$  by using Hp 3435A Digital Impedance Multimeter, and any reading above 5k $\Omega$  was reduced by recleaning the skin and/or refilling the EEG cap. The participants' forehead was cleaned with 70% Isopropyl alcohol swap and air dried for two minutes. The fNIRS sensor pad was placed on the participant's forehead and held in place by a head band

### **3.4 Procedure**

The experimental procedure is shown in Figure 7. The experiment was approved by the office of Institutional Review Board of North Carolina Agricultural and Technical State

University. Participants were introduced and welcomed to the experimental station. Each participant was assigned alphanumeric identification number instead of using their real names; the same identification number was also assigned to a particular randomized experimental treatment in accordance with the IRB protocol.

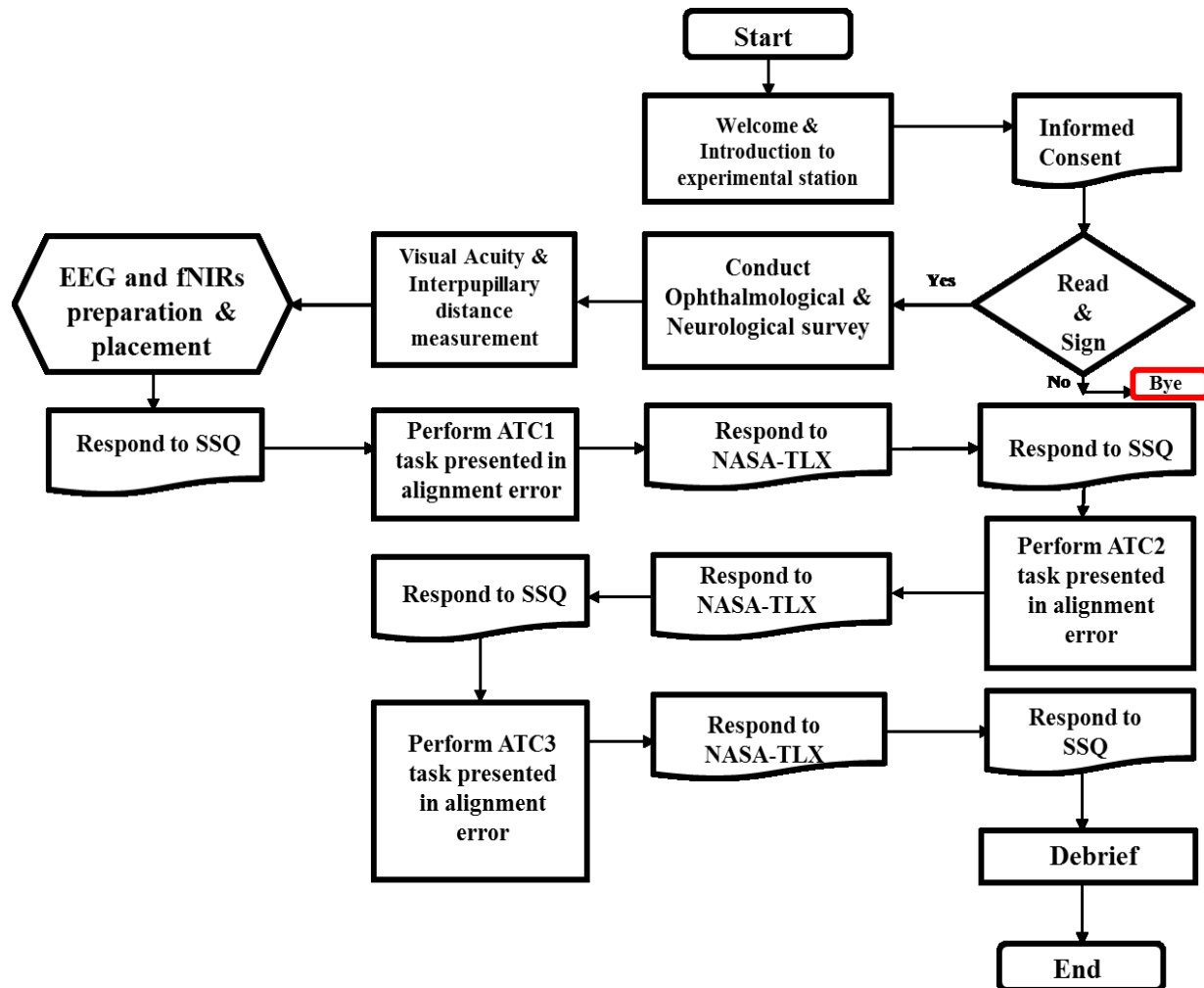


*Figure 7.* Experimental procedure with three ATC task sessions, four sets of SSQ questionnaires, and three sets of NASA-TLX questionnaires.

Each participant was given an Inform Consent to read and sign. Verbal explanations were provided to clarify concepts and terminologies. The neurophysiological assessment (see Appendix F) and ophthalmological assessments (see Appendix G) survey questionnaires were

administered. The ophthalmological survey was used to ensure that the participants under 40 years had no optometric and/or ophthalmological symptoms. Available studies have shown that after the age 40, most people experience the onset of ocular-motor problems, such as accommodations and convergence (Millodot & Newton, 1981; Stein & Stein, 1994). The National Eye Institute (2002) estimates that, currently, more than 38 million Americans age 40 and older experience blindness, low vision or an age-related eye disease, such as age-related macular degeneration (AMD), glaucoma, diabetic retinopathy, or cataracts. This is expected to grow to more than 50 million by year 2020 (National Eye Institute, 2002). In addition, subjective neurological questionnaire was administered to participants for life styles and/or accidental damage that might affect the brain electrophysiological data. Alcohol, smoking, and dominate/preferred hands have effects on especially alpha and beta brain waves (Wong, Maini, Rousset, & Brasic, 2003).

The participants were prepared for the EEG electrodes and fNIRS sensor pad placement as discussed in section 3.3.3. The participants were then seated at about 120 inches in front of the 8ft x 6ft silver screen. They were then given simulator sickness questionnaire (SSQ) consisting of 32 symptoms to rate their perception of visual fatigue as none (0), slight (1), moderate (2), and severe (3). The participants proceeded to perform the ATC task presented in alignment error labeled as ATC1. After ATC1, participants rated the workload using NASA-TLX then followed by SSQ. Subsequently, they proceeded to perform the same ATC task but in different alignment error labeled as ATC2. The procedure was followed by NASA-TLX and SSQ ratings. Further, participants performed the last ATC presented in the last alignment error followed by NASA-TLX and SSQ ratings. It should be noted that, throughout the experiment, participants were continuously asked if they were willing to continue the experiment.

### 3.5 Task

Figure 8 shows a participant performing ATC task with experimental treatments. The participant performed three ATC tasks sessions labeled as ATC1, ATC2, and ATC3, consecutively.

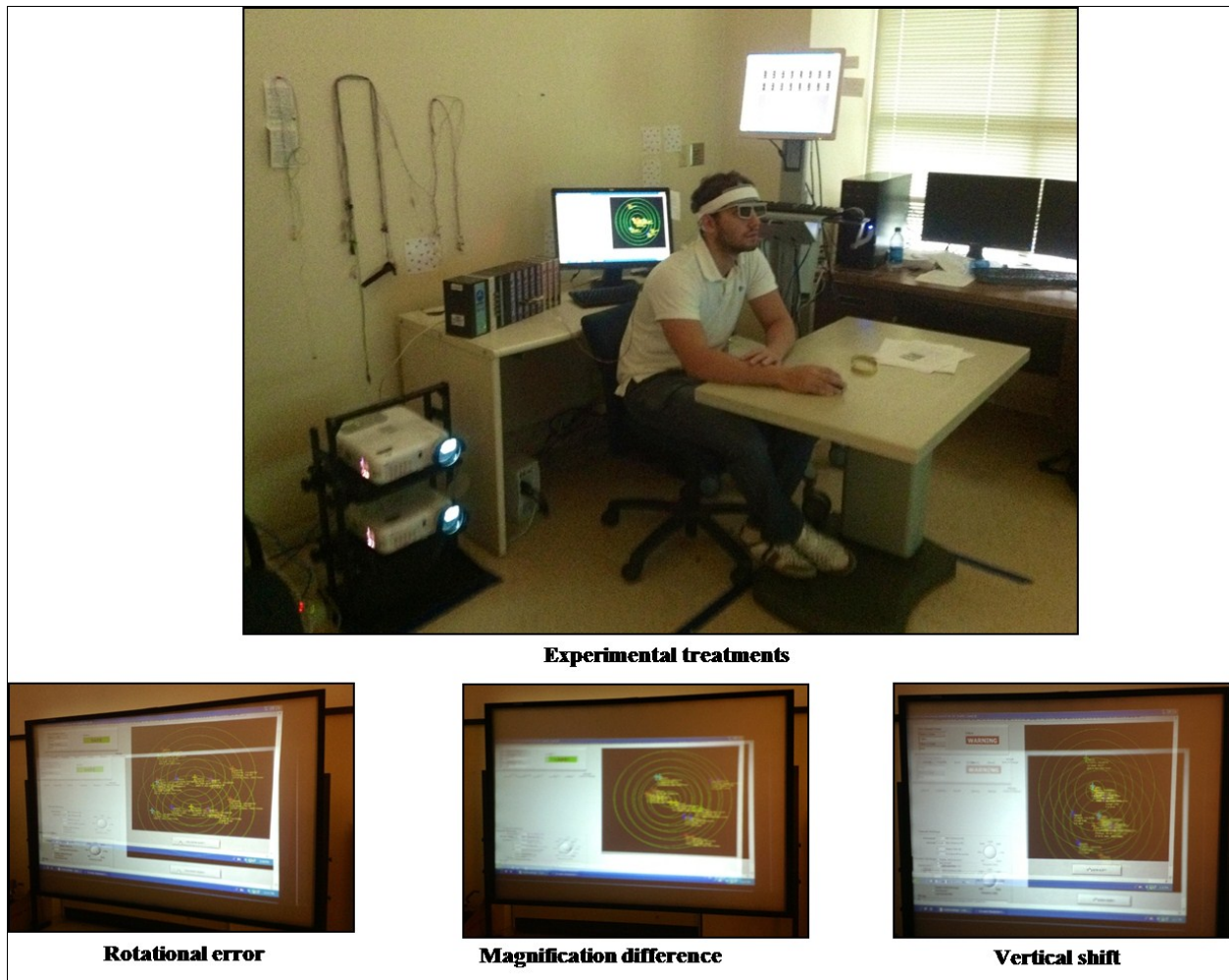


*Figure 8.* Participant performing experimental tasks with various alignment error conditions.

The ATC task was kept the same for all the three tasks sessions; however, based on particular randomization outcome for experimental treatments, for example vertical shift, rotational error, and magnification difference, ATC1 was presented in vertical shift alignment error, ATC2 was presented in rotational error alignment error, and ATC 3 was presented in

magnification difference alignment error, respectively. A summary of the experimental randomization outcome for the twenty-four participants and the corresponding ATC is shown in Appendix D. It should be noted that a particular treatment replications was completed before moving to the next treatment. For example, if the randomization order was vertical shift, rotational error, and magnification difference. The vertical shift treatment was replicated twice and each replication lasted for 10 min; hence, there were 20 min for vertical shift as ATC1, which was followed by rotational error replications as ATC2 and finally, the magnification difference error replications as ATC 3. The tasks involve continuous monitoring, that is, the participants visually scanned the display and if they detected any two or more self-separation violations, they responded by pressing a “CLICK BUTTON” located at the interface of the ATCIM. However, if they detected no self-separation violations, no response were issued and after 20 seconds, the display refreshed itself for a new display.

The self-separation violation was set to a loss of separation of 5nmi laterally or 500 ft. vertically (Nolan, 1994). After the completion of each session, subjects were asked to rate their perception of visual fatigue and workload. The subjects were required to perform the experimental tasks as quickly and as accurately as possible. The average time for the experiment was 1 hr. 45mins, inclusive of IRB briefing, visual acuity test, IPD measurement, conduct the ophthalmological and neurological survey questionnaire, performing the experiments, and clean participants, and debrief.

### **3.6 Data Acquisition**

Data were amplified and recorded by the Biopac MP 150 system (BIOPAC Systems Inc., 2011) with a high-quality 16-channel digital EEG 100C amplifier. Figure 8 shows a participant during an experiment. The EEG data were recorded with a sampling rate of 1000 Hz

in the experiment. Data were preprocessed using a gain of 500, and output selection set to normal and low-pass filter with a cut-off frequency of 35 Hz in order to remove the power line noise and other high-frequency noise. Similarly, a high-pass filter with a cut-off frequency at 0.1 Hz was applied to remove baseline drifts. The hemodynamic data were recorded with a sampling rate of 100Hz, a frame rate of 500ms, and 25 samples per voxels. The data acquisition settings include LED drive current of 10mA, an Analog-to-Digital (A/D) gain of 1mA, and initial gain drift of 1 with a balance of 4000. The participants put on NEC LT 245 polaroid glasses. NEC LT 245 DLP projector is turned on which projects the ATCIM image on a 8 x 6' NEC LT silver screen located at 120 inches. The lighting system in the experimental setting was turned off to create an ambient illumination of 28 lux and also to reduce reflections from surrounding surfaces, including that of the silver screen. Len and Huang (2006) noted that higher levels of ambient illumination cause display images to fade and ultimately induce visual discomfort.

## CHAPTER 4

### Data Analyses and Results for Study Experiment I

#### 4.1 Data Pre-Processing

The data pre-processing consisted of two steps. First, each of the dependent variables were preprocessed for outliers, missing values, or non-responses. The missing values, they were replaced by the computed average of the values (Pang-Ning, Steinbach, & Kumar, 2006). The second approach involved applying the appropriate software and technique to each dependent variable to make it suitable for statistical analysis.

**4.1.1 Simulator sickness questionnaire (SSQ) ratings.** Four SSQ instruments were administered per subject after each experimental treatment. The responses were scored on visual fatigue as: 0 (for none), 1 (slight), 2(moderate), and 3(severe), respectively. The SSQ data was generated and stored in Microsoft<sup>®</sup> Excel file. For analyses, the files were generated by conducting frequency tallying on each subject's responses for each experimental treatment. After obtaining the total number of responses per symptom per treatment, the total adjusted rating for each symptom was calculated as:

$$\text{Adjusted ratings for symptoms} = \frac{\sum_{n=0}^3 W_n X_n}{\sum_{n=0}^3 X_n}, \quad (3)$$

where,  $n = 0, 1, 2,$  and  $3$  are the index counts for None, Slight, Moderate, and Severe SSQ ratings of visual fatigue for a particular symptom,  $W_n$  is the total rating for  $X_n$ ; and  $X_n$  has the values

$$X_n = \begin{cases} X_0 = 0; \text{None} \\ X_1 = 1; \text{Slight} \\ X_2 = 2; \text{Moderate} \\ X_3 = 3; \text{Severe} \end{cases} \quad (4)$$

The total weighted rating across all 32 symptoms per treatment was calculated as shown in equation 5:

$$\frac{\left\{ \left( \frac{\sum_{n=0}^3 W_n X_n}{\sum_{n=0}^3 X_n} \right)_{S1} \dots + \left( \frac{\sum_{n=0}^3 W_n X_n}{\sum_{n=0}^3 X_n} \right)_{S32} \right\}}{N = 24}, \quad (5)$$

where,  $N$  = total number of participants;  $S1, S2, \dots, S32$  represent the types of symptoms rated.

Tables 6 through 9 present the sample SSQ data after each ATC session.

Table 6

*Pre-Experimental SSQ Rating Data Before Air Traffic Control Task (BATC)*

No.	Symptoms(BATC)	0 = None	1 = Slight	2 = Moderate	3 = Severe	SSQ
1	Ache	23	1			0.17
2	Blurred vision	24				0.00
3	Boredom	17	5	2		1.50
4	Confusion	24				0.00
5	Difficulty concentrating	21	3			0.50
6	Difficulty focusing	22	2			0.33
7	Dizziness eyes closed	24				0.00
8	Dizziness eyes open	24				0.00
9	Double vision	24				0.00
10	Drowsiness	19	5			0.83

Table 7

*Sample SSQ Ratings After Air Traffic Control Task Session 1 (ATC1)*

No.	Symptoms(ATC1)	0 = None	1 = Slight	2 = Moderate	3 = Severe	SSQ
1	Ache	21	3	0	0	0.50
2	Blurred vision	14	7	3	0	2.17
3	Boredom	23	1	0	0	0.17
4	Confusion	23	1	0	0	0.17
5	Difficulty concentrating	12	8	4	0	2.67

Table 7

*(cont.)*

No.	Symptoms(ATC1)	0 = None	1 = Slight	2 = Moderate	3 = Severe	SSQ
6	Difficulty focusing	15	6	3	0	2.00
7	Dizziness eyes closed	0	1	0	0	0.17
8	Dizziness eyes open	22	1	1	0	0.50
9	Double vision	18	3	2	1	1.67
10	Drowsiness	13	5	5	1	3.00

Cronbach's alpha reliability test was applied to the SSQ responses using SAS. The Cronbach was evaluated based on participants' overall SSQ scores for each ATC tasks sessions (alignment errors). Thus, the dataset consisted of 24 observations and 4 attributes representing BATC, ATC1, ATCF2, and ATC3. A Cronbach alpha 0.961 was obtained. This shows stable responses considering 0.7 as cut off for acceptable response (Cronbach, 1951; Hatcher, 1994; Nunnaly, 1978; Santos et al., 1998).

Table 8

*Sample SSQ Ratings After Air Traffic Control Task Session 2 (ATC2)*

No.	Symptoms(ATC2)	0 = None	1 = Slight	2 = Moderate	3 = Severe	SSQ
1	Ache	0	5	3	0	1.83
2	Blurred vision	11	5	8	1	3.00
3	Boredom	5	4	9	6	2.67
4	Confusion	22	1	1	0	0.50
5	Difficulty concentrating	8	8	7	1	1.17
6	Difficulty focusing	9	7	7	1	2.00
7	Dizziness eyes closed	23	1	0	0	0.17
8	Dizziness eyes open	22	1	1	0	0.50
9	Double vision	14	4	5	1	2.83
10	Drowsiness	11	6	5	2	1.67

Table 9

*Sample SSQ Ratings After Air Traffic Control Task Session 3 (ATC3)*

No.	Symptoms (ATC3)	0 = None	1 = Slight	2 = Moderate	3 = Severe	SSQ
1	Ache	14	9	1	0	1.83
2	Blurred vision	11	9	3	1	3.00
3	Boredom	4	3	12	5	2.04
4	Confusion	22	2	0	0	0.33
5	Difficulty concentrating	13	5	4	2	2.17
6	Difficulty focusing	12	8	3	1	2.83
7	Dizziness eyes closed	21	3	0	0	0.50
8	Dizziness eyes open	20	3	1	0	0.83
9	Double vision	18	2	4	1	2.17
10	Drowsiness	11	8	4	1	1.17

**4.1.2 Electroencephalogram (EEG).** The EEG signal was divided into five bands, namely delta (1-3.5Hz), theta (4-8 Hz), alpha (8-13 Hz), beta (13-30 Hz) and gamma (> 30 Hz). Hence, the time series EEG signal was divided into the five bands by using an elliptic Infinite Impulse Response (IIR) low pass and high pass combination filters (Adikarapatti, 2007).

Filtering the EEG signal removes any artifacts that may influence the quality of the signal, which might influence the characteristics of the signal (Adikarapatti, 2007). Fast Fourier Transform (FFT) was then used to obtain the power spectrum for each band. The power spectrum was used in the computation of the total power of each band, which was then extracted for further statistical analyses. The time documented for each activity in the time study was used to calculate the mean power of each band. The resulting total power epoch mean for each activity was then normalized for all channels between 1-50 Hz to obtain relative power (Wyczesany, Kaiser, & Coenen, 2008). The relative power for each visual display task was used to determine the influence of various alignment errors on mental activity. Relative power for each band was calculated using equation 6 (Wyczesany et al., 2008).

$$\text{Relative Power for Band X} = \frac{\text{Total power epoch mean of band X}}{\text{Sum of totalepoch mean of all bands in channel}(i)}, \quad (6)$$

where X represents delta, theta, alpha, beta and gamma bands;  $i$  = sampled channels 1,2, 3.

An example of sampled raw EEG data plot for participant 12 is shown in Figures 9 through 11. The processed sample data for each relative band power is shown in Appendix I.

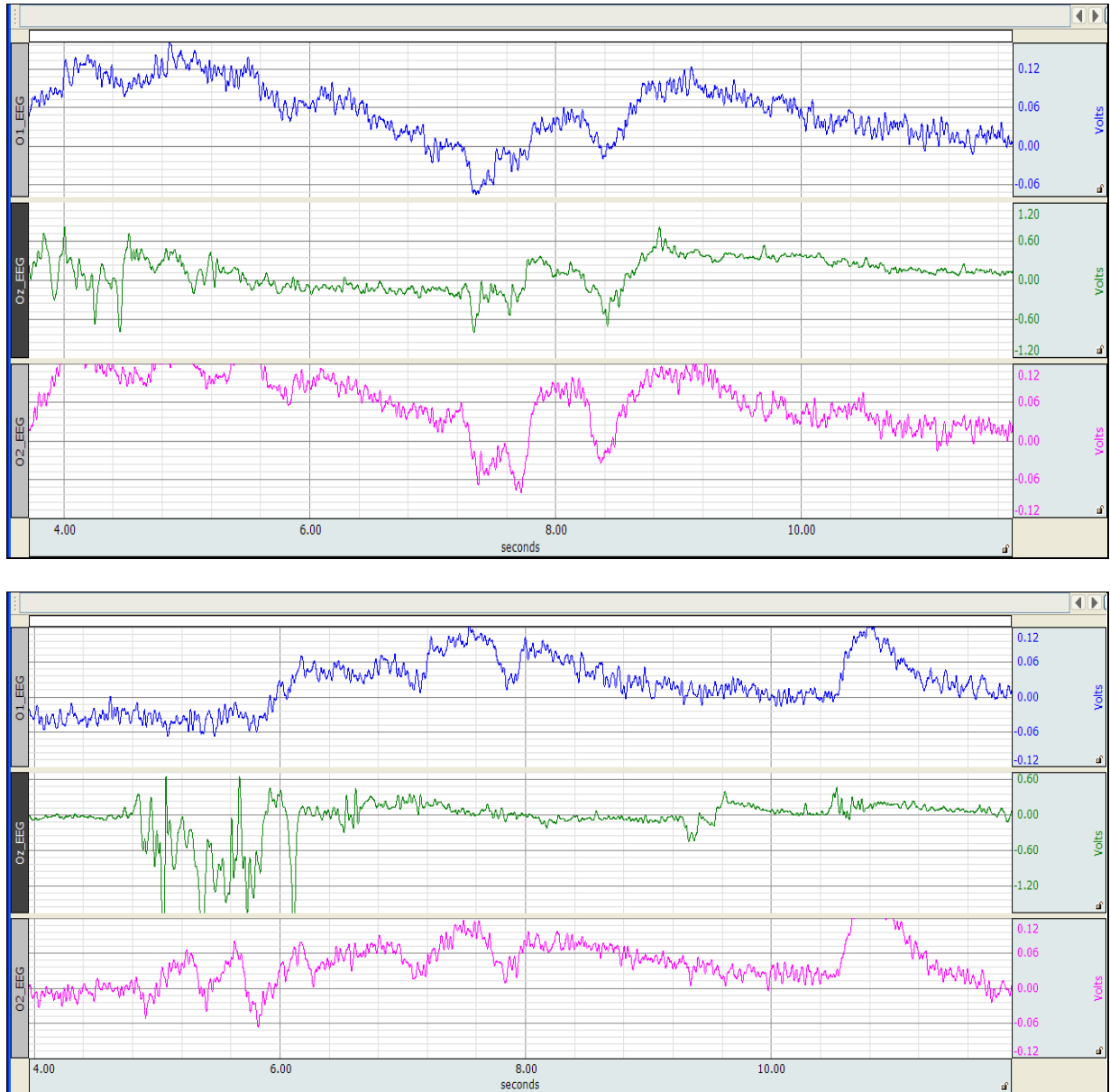
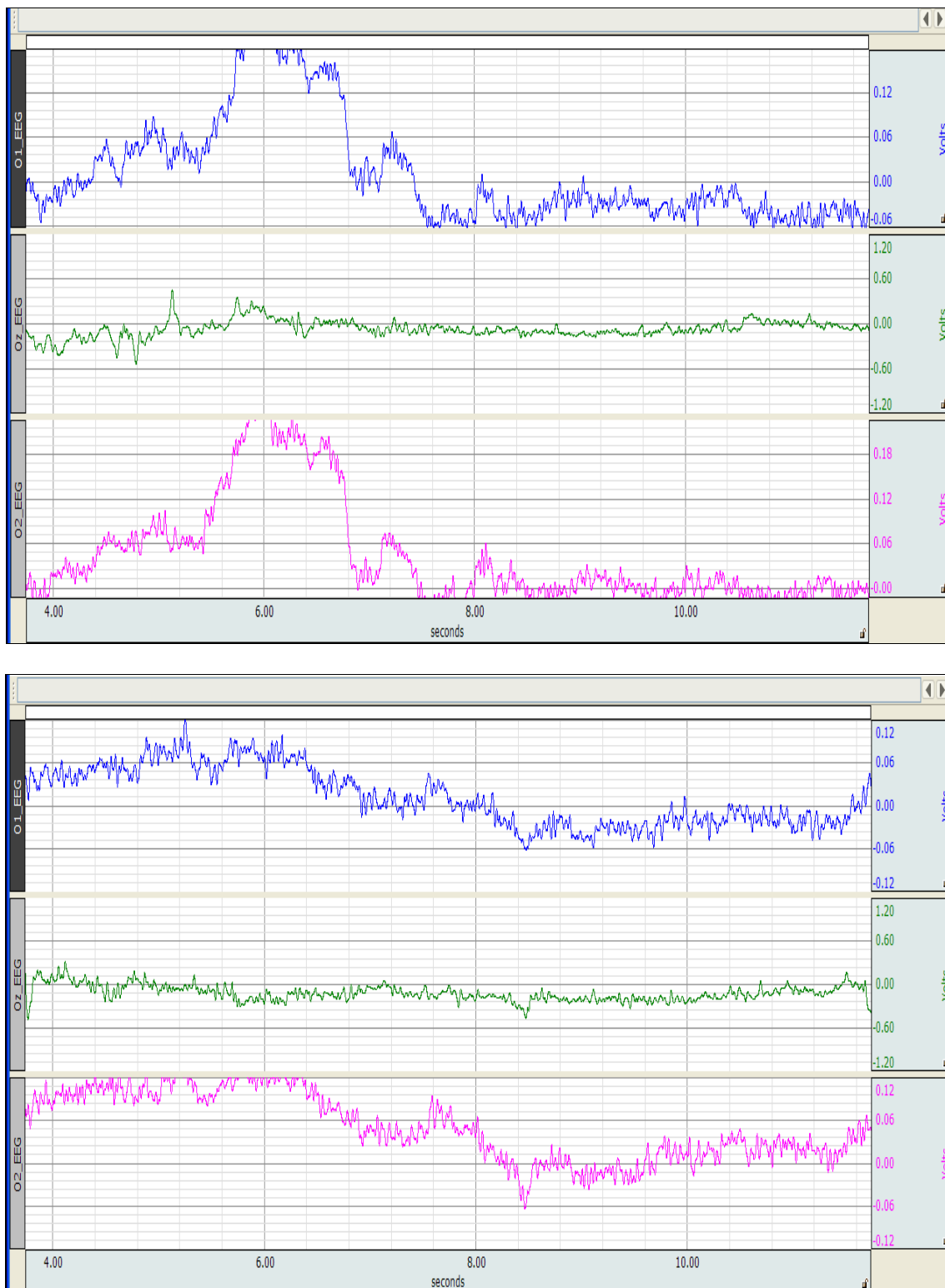


Figure 9. Sample 4s-12s raw EEG plot for participant 12 during magnification difference treatment 1 and 2 on channels  $O_1$ ,  $O_z$ , and  $O_2$ .



*Figure 10.* Sample 4s-12s raw EEG plot for participant 12 rotational error for treatment 1 and 2 on channels O<sub>1</sub>, O<sub>z</sub>, and O<sub>2</sub>.

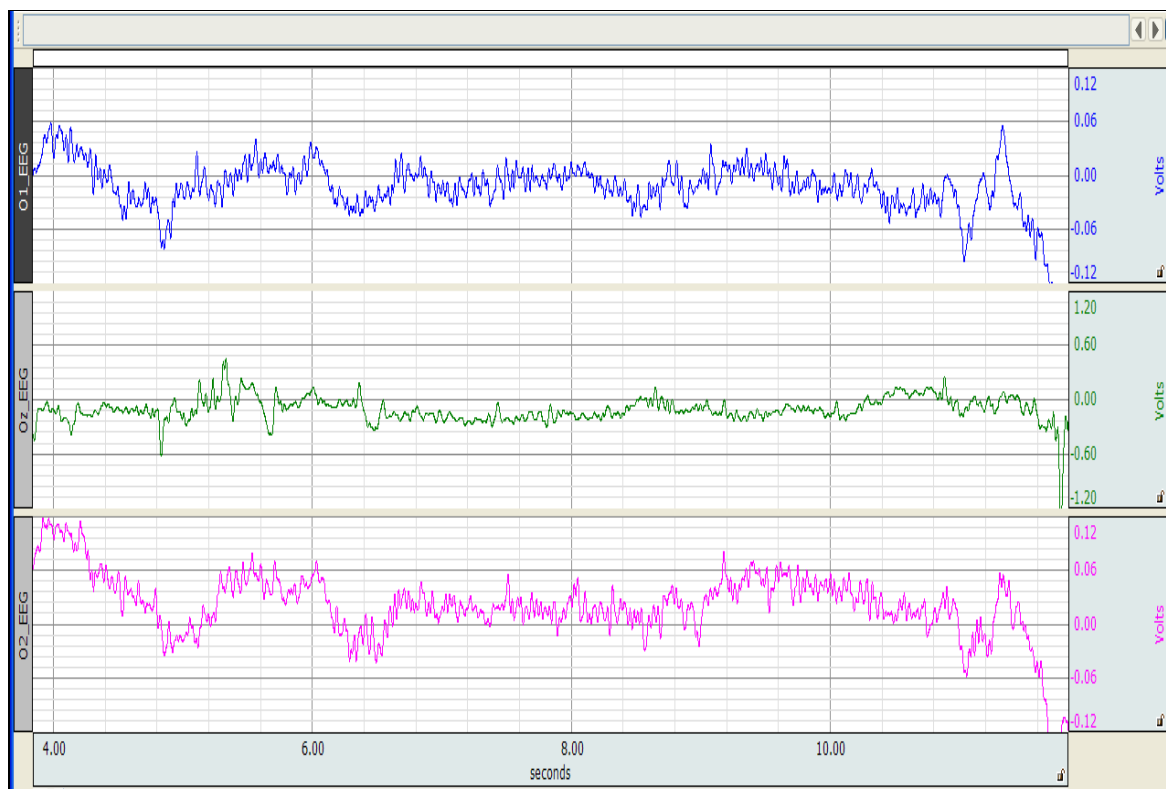
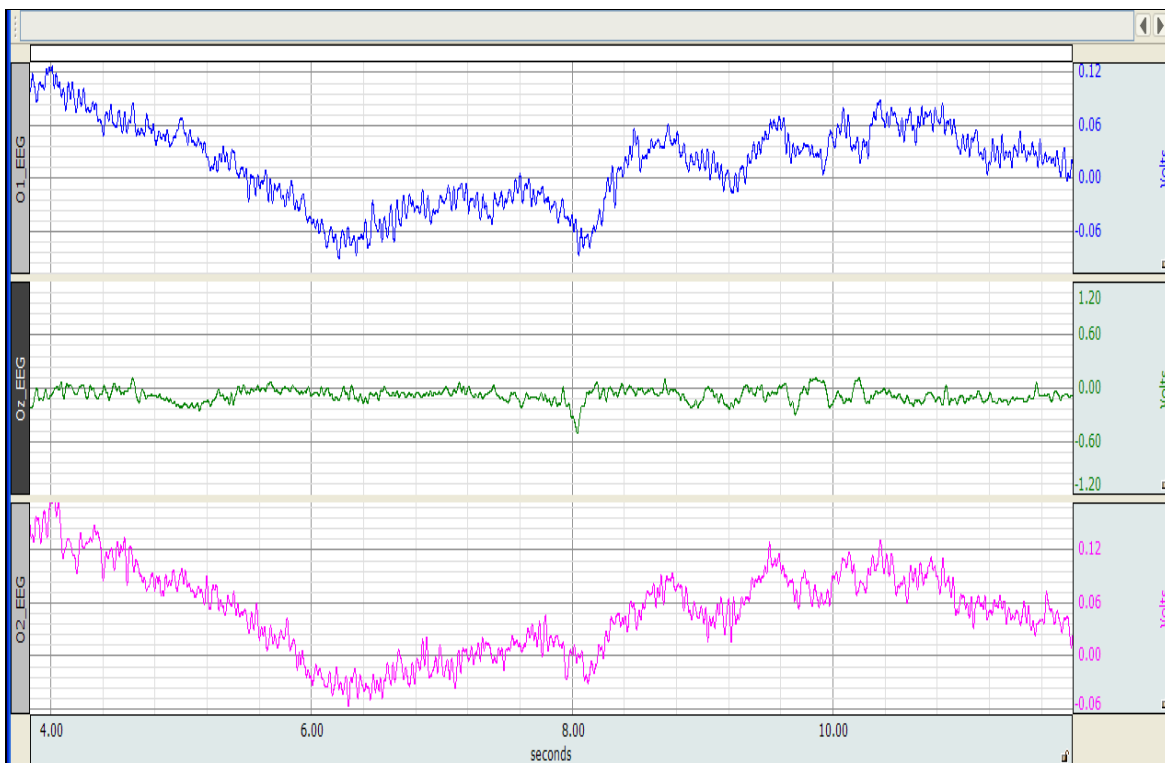


Figure 11. Sample 4s-12s raw EEG plot for participant 12 vertical shifts for treatment 1 and 2 on channels O<sub>1</sub>, O<sub>z</sub>, and O<sub>2</sub>.

**4.1.3 Hemodynamic responses.** There were two main hemodynamic responses measured by fNIRS. These responses were changes in oxyhemoglobin concentration  $\Delta C_{\text{HbO}_2}(t)$  and deoxyhemoglobin concentration  $\Delta C_{\text{Hbb}}(t)$  from the 16 voxels. The recordings cover the area of dorsolateral prefrontal cortex (DLPFC). The DLPFC roughly corresponds to Broadman areas 9 and 46, and it covers portions of the middle and inferior frontal gyri (Merzagora, Maria, Onaral, & Izzetoglu, 2011). These regions of interest for task execution in the prefrontal area had been identified based on a previous fNIRS study by Izzetoglu et al. (2003) and based on a meta-analysis of other neuroimaging studies performed by Cabeza and Nyberg (2000). In order to reduce the data dimensionality, within subject averages were computed using Microsoft Excel<sup>®</sup>2009 for both oxyhemoglobin and deoxyhemoglobin concentration for the 16 voxels as  $\text{HbO}_2(\text{mean})$  and  $\text{Hbb}(\text{mean})$ , respectively. As indicated by fNIR Devices LLC (2010), the voxels 1 through to 8 correspond to the left (*l*) DLPFC while voxels 9 through to 16 corresponds to right (*r*) DLPFC. A summary of the hemodynamic responses is shown in Table 10.

Table 10

*Descriptive Statistics for Hemodynamic Responses*

Alignment Errors	Statistic	<i>l</i> DLPFC		<i>r</i> DLPFC	
		Hbb	HbO2	Hbb	HbO2
Vertical shift	Hmax	1.199	0.955	1.054	1.597
	Hmean	-0.29	-0.625	-0.25	-0.308
	Hstdev	0.666	0.608	0.717	0.781
Rotational error	Hmax	0.916	1.199	1.43	1.561
	Hmean	-0.204	-0.523	0.068	-0.665
	Hstdev	0.766	0.656	0.857	0.873
Magnification difference	Hmax	0.914	0.928	0.855	1.514
	Hmean	0.276	-0.563	0.151	-0.413
	Hstdev	0.641	0.657	0.71	0.764

**4.1.4 NASA task load index (NASA- TLX).** NASA-TLX is a multi-dimensional rating procedure for the overall workload score based on the weighted average of ratings on six subscales (So, 2010). The six subscales are clustered into two groups: 1) relates to the demands imposed on the subjects. These demand factors are Mental, Physical, and Temporal, and 2) relates to the interaction of the subjects. Here the interaction factors are Effort, Frustration, and Performance (So, 2010).

The degree to which each of the six factors contributed to the workload of a specific task was grounded on pair-wise comparisons among the six factors as weights and the magnitude of each subscale as ratings from a particular participant of the task (Hart, 2006). The overall workload scores for each subject were computed by multiplying the ratings by the weight for a particular subscale (factor) for each subject to obtain the individual adjusted ratings for a particular subscale. Figure 12 is the sample plot for participants 6 and 22, showing their variations of ratings and weights under each experimental condition.

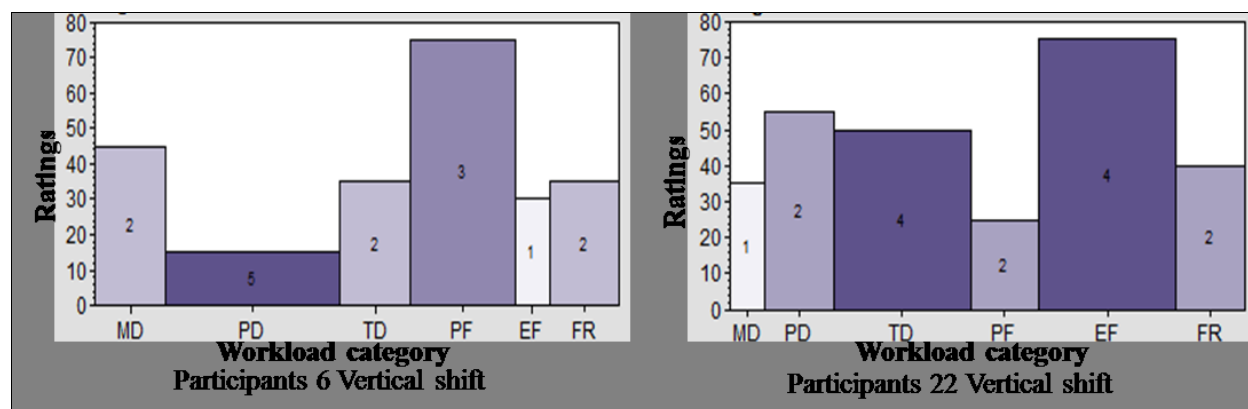


*Figure 12.* Graphical composition of workloads for subjects ID 6 and 22. The sources of workload were Mental Demand (MD), Physical Demand (PD), Temporal Demand (TD), Performance (PF), Effort (EF) and Frustration (FR). The weight was scaled between 0-5, and ratings are scaled between 0-100.

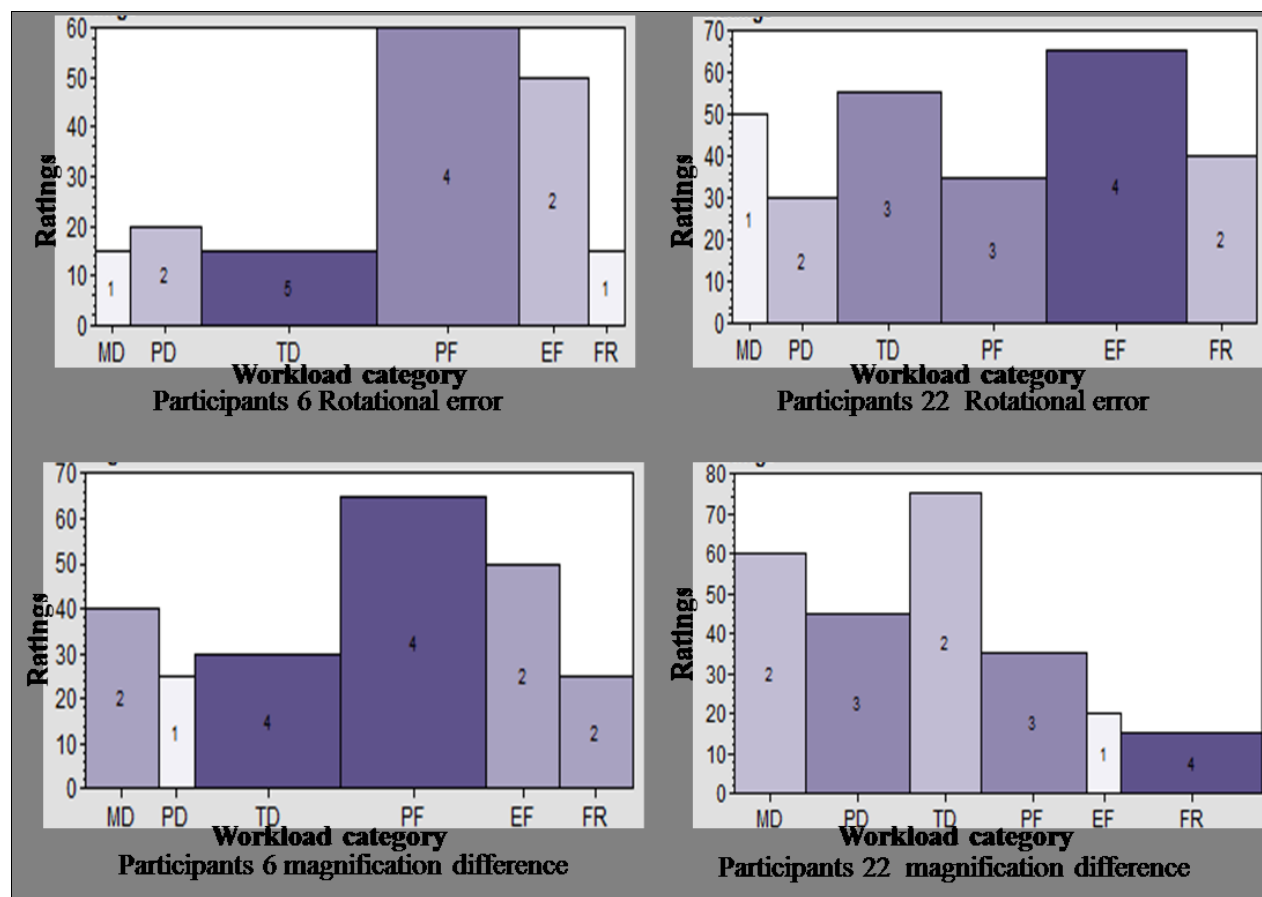


Figure 12. (cont.)

#### 4.2 Experimental Hypotheses Testing

There were five hypotheses for the study. A model adequacy checks were performed to test for the three ANOVA assumptions of normality, independence, and homogeneity of variance. If the original data violated any of the assumptions, an appropriate transformation was applied to the data until all the assumptions were met. The model adequacy was analyzed with SAS. The normality test showed that the SSQ dataset was normally distributed with Shapiro-Wilk,  $W = 0.816, p = 0.471$ . The Levene's test for homogeneity of variance for SSQ responses were not significantly different,  $F(3, 69) = 0.94, p = 0.064$ . For workload, the dataset was normally distributed with Shapiro-Wilk,  $W = 0.246, p = 0.142$ , and the Levene's test for homogeneity of variance for workload dataset was not significantly different,  $F(2, 69) = 3.49, p$

= 0.251. For EEG, the Shapiro-Wilks showed that the EEG data was normally distributed with Shapiro-Wilk's  $(W) = 0.866, p = 0.214$ , and the Levene test showed no significant difference,  $F(2, 69) = 7.21, p = 0.984$ .

For the hemodynamic responses, for Hbb variable,  $W = 0.406, p < 0.05$ ; For HbO<sub>2</sub> variable  $W = 0.476, p < 0.05$ . The normality tests were violated for hemodynamic response variables. As a result of significant violations of the model adequacy checks by the hemodynamic responses, the data underwent some transformations. The various transformation approaches were applied to the hemodynamic response data that further analyzed for model adequacy check. Eventually, the box-cox transformation yielded the best results. The dataset was transformed by a power of 1/3 (that is  $X^{1/3}$ ). After the data transformation, Shapiro-Wilks test showed that  $W = 0.04, p > 0.05$ ; for HbO<sub>2</sub> variable,  $W = 0.015, p = 0.548$ . Levene's test for homogeneity of variance for Hbb and HbO<sub>2</sub> variables, analyzed with ANOVA of squared deviations from group mean, was significant resulting for Hbb,  $F(5,272) = 1.23, p = 0.541$  and HbO<sub>2</sub>,  $F(5,272) = 0.74, p > 0.05$

Hypothesis 1.1: A prolonged use of stereoscopic display does not cause visual fatigue

$$H_0: \mu_{\text{BATC}} = \mu_{\text{ATC3}}$$

$$H_a: \mu_{\text{BATC}} < \mu_{\text{ATC3}}$$

That is, the mean SSQ responses to display alignment errors before tasks are the same as mean display alignment errors after tasks.

Using Simulator Sickness Questionnaire (SSQ), the response variable for the hypothesis was a computed total weighted SSQ rating across all 32 symptoms before air traffic control task (BATC) and after the air traffic control 3 (ATC 3). The descriptive statistics for SSQ was summarized as shown in Figure 13.

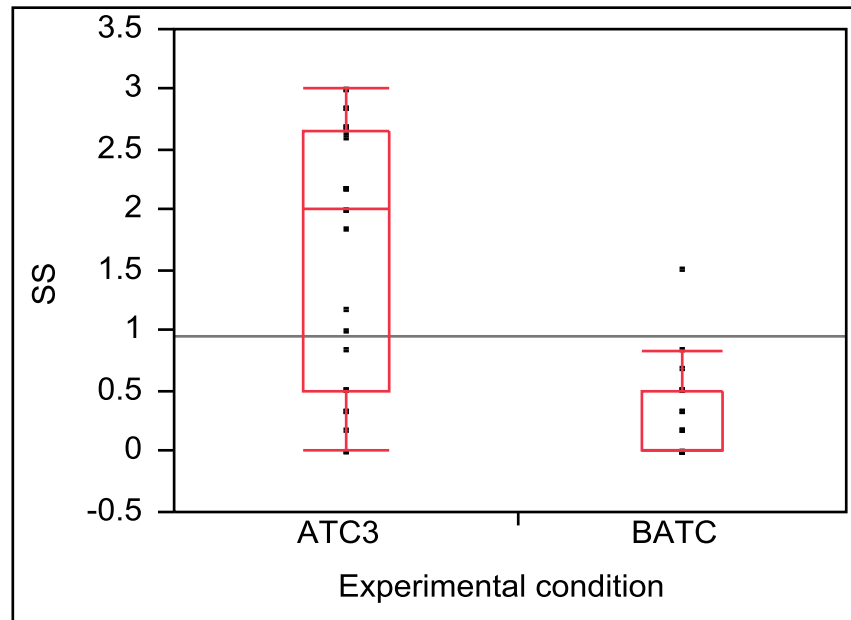


Figure 13. Side-by-side box plot of SSQ ratings for BATC and ATC 3.

The SSQ ratings consist of 34 symptoms. In this study, the ATC 3 task consisted of two replications. At BATC, there was no stereoscopic display. The SSQ responses at ATC 3 were influenced by the combined effect of alignment errors in stereoscopic displays.

A paired *t*-test statistical technique was used, and the data was analyzed by statistical analyses software (SAS Institute Inc., 2008). The null hypothesis was rejected. At 5% significance level, there was enough evidence to conclude that a prolonged use of stereoscopic display was likely to induce visual fatigue as there was a significant difference between the SSQ responses between before air traffic control task (BATC) and after air traffic control task (ATC 3),  $t(23) = -15.27, p < 0.05$ . An exploratory analysis revealed that twenty-one of the thirty-two symptoms were pronounced after the ATC 3. This is shown in Figure 14.

The observed significant symptoms include ache, blurred vision, boredom, difficult concentrating, difficult focusing, dizziness eye open, dizziness eye closed, double vision, drowsiness, eyestrain, faintness, fatigue, fullness of the head, general discomfort, headache, loss

of appetite, increased appetite, mental depression, salivation increase, salivation decrease, and tearing.

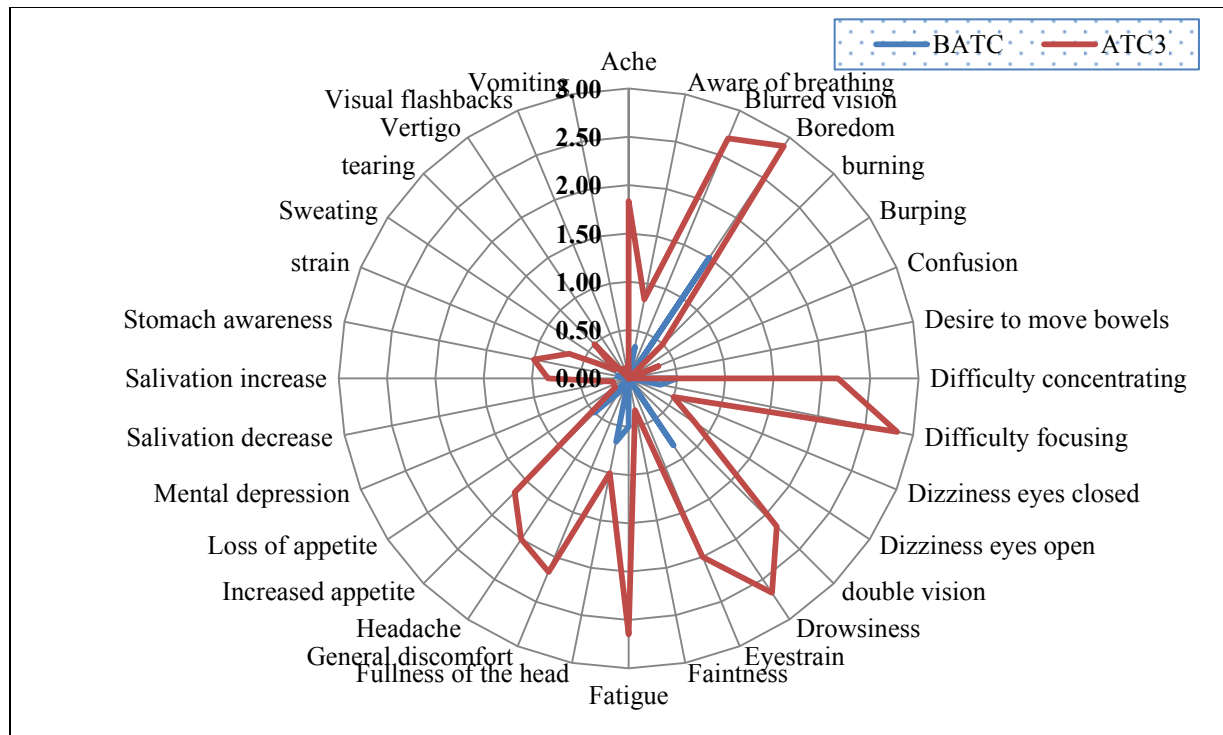


Figure 14. A radial plot of SSQ rated symptoms on ATC task sessions.

Hypothesis 1.2: Alignment errors in stereoscopic displays do not increase the prevalence of visual fatigue

$$H_0: \mu_{\text{vertical shift}} = \mu_{\text{rotational error}} = \mu_{\text{magnification difference}}$$

$H_a$ : At least one mean is different

That is, the mean SSQ responses across the display alignment errors are the same. Significant level ( $\alpha$ ) = 0.05. The One-way ANOVA results,  $F(2, 69) = 35.38, p < 0.05$ . The null hypothesis was rejected. At 0.05 level of significance, there was enough evidence to conclude that at least one of the stereoscopic alignment error is different. A Tukey post ad hoc analyses revealed that there was a significant difference between magnification difference and vertical shift ( $p < 0.05$ ), magnification difference and rotational error ( $p < 0.05$ ), and there was no significant difference

between vertical shift and rotational error. Figure 15 shows the line graph of the SSQ responses for each alignment error and ATC task.

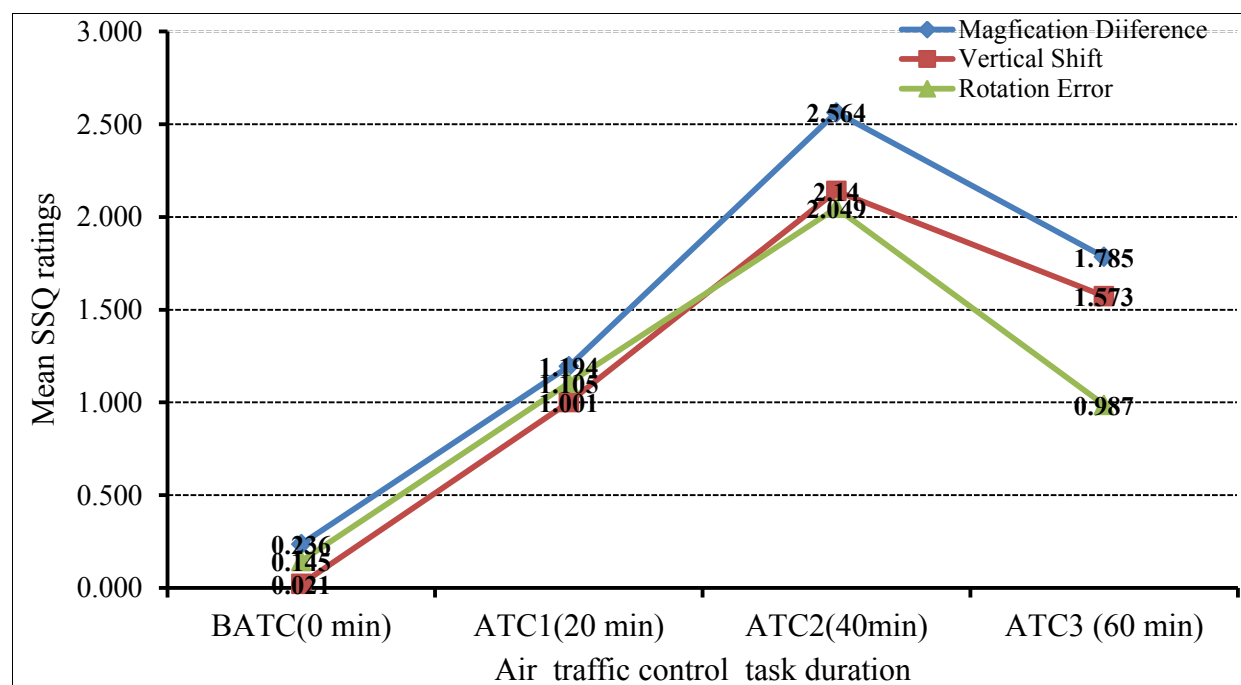


Figure 15. Mean SSQ ratings for Air Traffic Control (ACT) tasks. The SSQ ratings are from 0 to 3 for 34 symptoms, and  $N = 24$  subjects.

The perceptual ratings of visual fatigue for all the alignment error types occurred at ATC 2. At the peak, the highest overall SSQ ratings was magnification difference (SSQ = 2.56), followed by vertical shift (SSQ = 2.14), and rotational error (SSQ = 2.049). Between ATC 1 and ATC 2, there was an interaction between vertical shift and rotational error. The frequency of the SSQ responses for the alignment errors across the ATC task are shown in Figures 16, 17, and 18. The common symptoms across the alignment errors were difficulty in concentrating, difficulty in focusing, drowsiness, and fatigue. The high frequencies of difficulty in concentrating and in focusing symptoms occurred at magnification difference while fatigue occurred at rotational error and drowsiness was observed to be high at both magnification difference and rotational error.

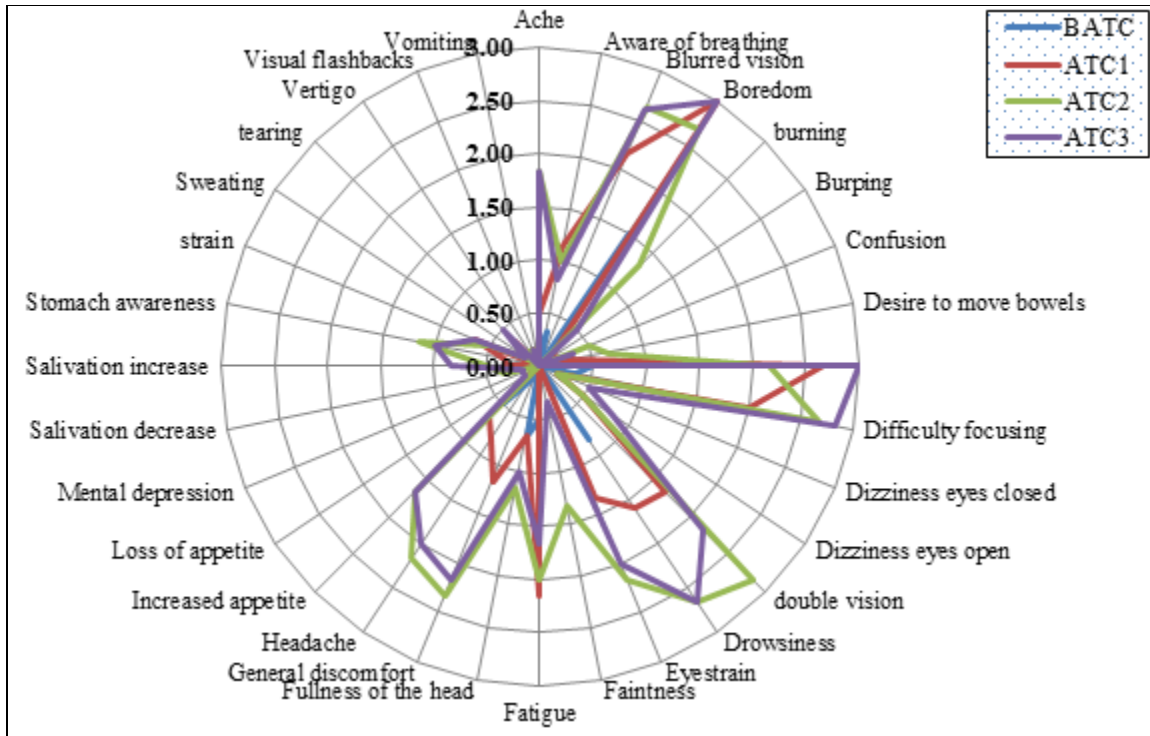


Figure 16. A radial plot of SSQ rated symptoms on ATC task session during magnification difference.

Hypothesis 1.3: Alignment errors in stereoscopic displays have no effect on workload during visual display tasks

$$H_0: \mu_{\text{vertical shift}} = \mu_{\text{rotational error}} = \mu_{\text{magnification difference}}$$

$H_a$ : At least one mean is different

That is, the workload effects across alignment errors are the same. The response variable for this hypothesis is workload, using NASA-TLX. The significance level ( $\alpha$ ) = 0.05.

The One-way ANOVA results,  $F(2, 69) = 0.74, p < 0.05$ . The null hypothesis was rejected. At the level of significance ( $\alpha$ ) = 0.05, there was enough evidence to conclude that at least one of the stereoscopic alignment errors was different. A Tukey post ad hoc analyses revealed that there was a significant difference between magnification difference and vertical shift ( $p < 0.05$ ). However, there was no significant difference between magnification difference

and rotational error ( $p < 0.05$ ), and there was no significant difference between vertical shift and rotational error. This is depicted in Figure 19.

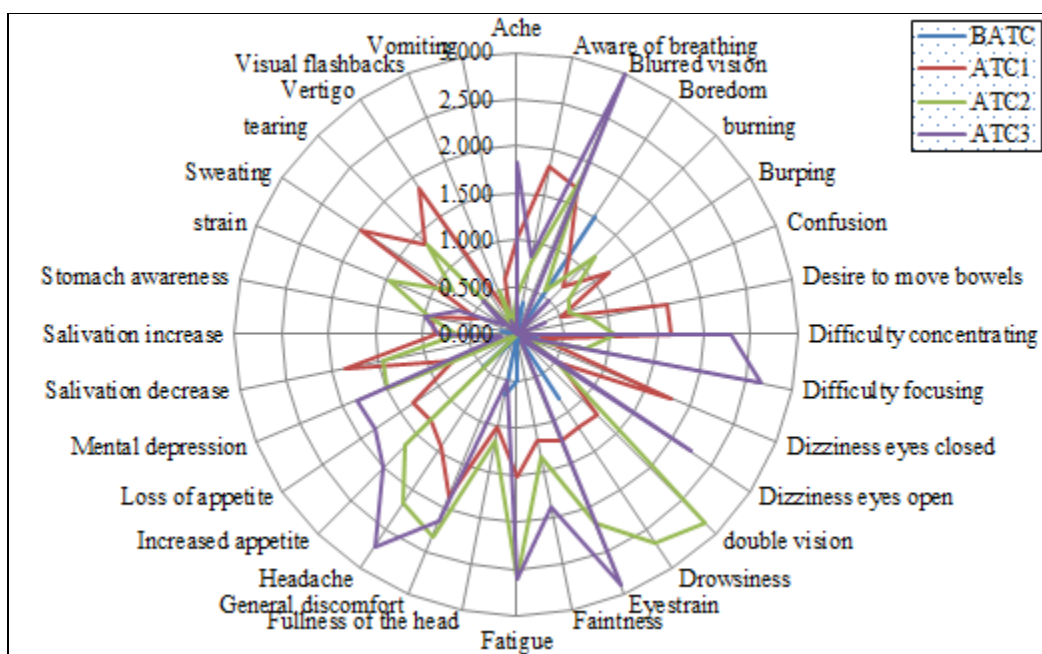


Figure 17. A radial plot of SSQ rated symptoms on ATC task session during rotational error.

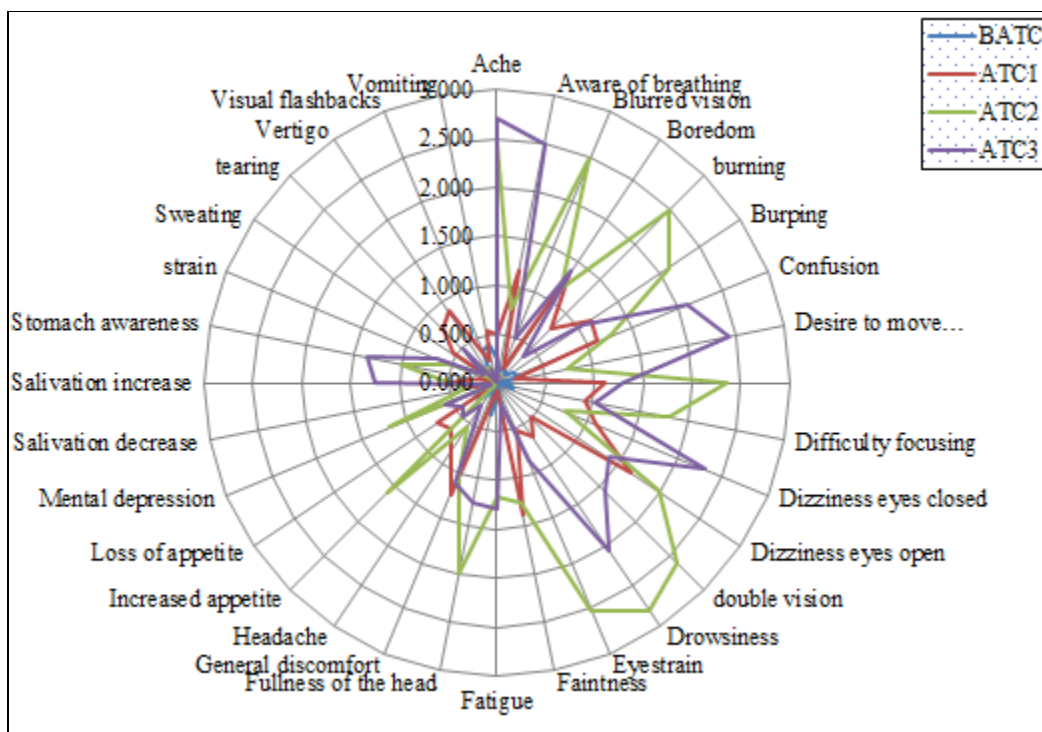


Figure 18. A Radial plot of SSQ rated symptoms on ATC task session during vertical shift.

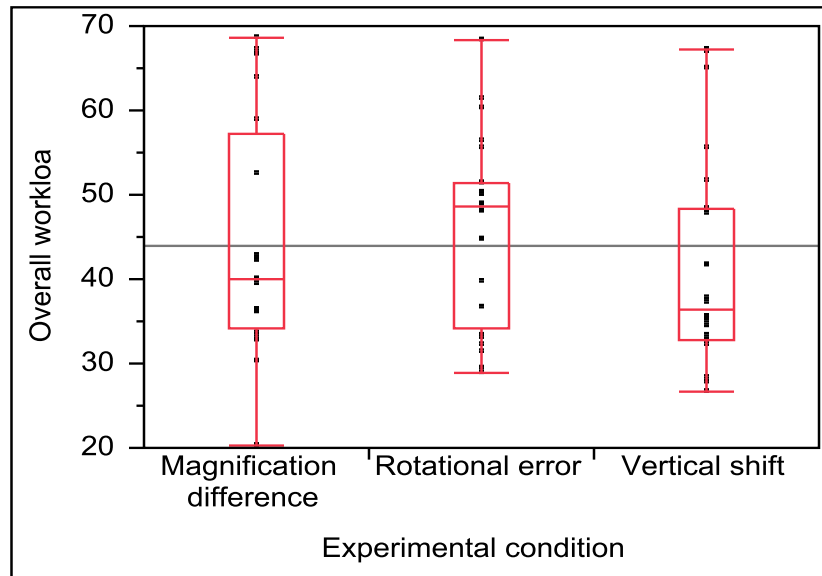


Figure 19. Side-by-side box plots for the alignment errors based on NASA workload.

Overall workload for magnification alignment error was higher than rotational and vertical shift alignment display errors. The result shows that low ratings for the overall workload occurred when vertical alignment display error display was used. Thus, magnification difference display error was likely to have the most impact on participants' visual loadings. Generally, the alignment display errors had an impact on the overall workload. It was also observed in the NASA-TLX component scores that the contributions of the six components on the overall workload were different for the stereoscopic display alignment errors. As shown in Table 11, there was a positive correlation between overall workload (NASA-TLX) and perceptual ratings of visual fatigue (SSQ),  $r = 0.89$ ,  $p < 0.05$ . As the ATC task sessions progressed toward a higher workload (NASA-TLX), the weighted ratings for SSQ and overall mental workload increased.

Hypothesis 1.4: Alignment errors in stereoscopic displays have no effect on dorsolateral prefrontal cortex hemodynamic responses during visual display tasks

$$H_0: \mu_{\text{vertical shift}} = \mu_{\text{rotational error}} = \mu_{\text{magnification difference}}$$

$H_a$ : At least one mean is different

That is, the mean dorsolateral prefrontal cortex hemodynamic response is the same across alignment errors. The significance level ( $\alpha$ ) = 0.05.

Table 11

*Subjective Responses for Overall Workload (WL<sup>1</sup>) Using NASA-TLX and Perceptual Ratings of Visual Fatigue Symptoms Using SSQ<sup>2</sup>*

Alignment Error	Task Sessions Mean							
	BATC		ATC1		ATC2		ATC3	
	NASA TLX	SSQ	NASA TLX	SSQ	NASA TLX	SSQ	NASA TLX	SSQ
Vertical Shift	-	0.021	48.36	1.001	63.24	2.004	60.52	1.573
Rotational error	-	0.145	34.89	1.015	55.98	2.049	68.14	0.987
Magnification differences	-	0.236	39.28	1.197	67.14	2.564	69.21	1.785

<sup>1</sup>( $0 \leq WL \leq 100$ ) and <sup>2</sup>( $0 \leq WL \leq 3$ )

There was low to moderate correlation between hemodynamic responses. The coefficients of correlation ( $r$ ) are;  $r_{/DLPFC-Hbb \text{ and } /DLPFC-HbO_2} = 0.37$ ;  $r_{/DLPFC-Hbb \text{ and } r_{DLPFC-Hbb}} = 0.55$ ;  $r_{/DLPFC-Hbb \text{ and } r_{DLPFC-HbO_2}} = -0.43$ ;  $r_{/DLPFC-HbO_2 \text{ and } r_{DLPFC-Hbb}} = 0.39$ ;  $r_{/DLPFC-HbO_2 \text{ and } r_{DLPFC-HbO_2}} = 0.44$ ; and  $r_{r_{DLPFC-Hbb} \text{ and } r_{DLPFC-HbO_2}} = 0.64$ . As a result, One-way MANOVA statistical technique was used, and the data was analyzed with SAS. For any significance, a Tukey post ad hoc analyses was conducted to reveal the significant difference. The One-way MANOVA results showed Wilk's Lambda = 0.924,  $F(8, 132) = 0.66$ ,  $p < 0.05$ . At 0.05 level of significance, there was enough evidence to conclude that the transformed hemodynamic response as composite score was significant. For  $/DLPFC-Hbb$  transformed dataset, the ANOVA results were,  $F(2, 69) = 0.10$ ,  $p < 0.05$ . Hence, the null hypothesis was rejected. At 0.05 level of significance, there was enough evidence to conclude that at least one of the stereoscopic alignment errors was different.  $/DLPFC-HbO_2$

transformed dataset, the ANOVA results were,  $F(2, 69) = 0.15, p < 0.05$ . Hence, the null hypothesis was rejected. At 0.05 level of significance, there was enough evidence to conclude that at least one of the stereoscopic alignment errors was different. Further, for  $r$ DLPFC-Hbb transformed dataset, the ANOVA results were,  $F(2, 69) = 1.09, p < 0.05$ . Hence, the null hypothesis was rejected. Thus, at 0.05 level of significant, there was enough evidence to conclude that at least one of the alignment error effects was different. For  $r$ DLPFC-HbO<sub>2</sub>, the ANOVA results were,  $F(2, 69) = 1.24, p = 0.2966$ . Hence, failed to reject the null hypothesis. At 0.05 significant level, there was not enough evidence to conclude that different alignment error effects on  $r$ DLPFC-HbO<sub>2</sub> transformed dataset. Tukey analyses  $l$ DLPFC-Hbb,  $l$ DLPFC-HbO<sub>2</sub>, and  $r$ DLPFC-Hbb results are shown in Table 12.

Table 12

*ANOVA Summary of Significant Effect of Hemodynamic Responses for the Alignment Errors*

Location	Hemodynamic Responses	Tukey post ad hoc analyses for alignment display errors ( $p < 0.05$ )
$r$ DLPFC	Deoxygenated hemoglobin (Hbb)	(Magnification difference and Rotation error) and (Magnification difference and Vertical Shift)
$l$ DLPFC	Oxygenated Hemoglobin (HbO <sub>2</sub> )	(Magnification difference and Rotation error) and (Magnification difference and Vertical Shift)
	Oxygenation (Hbb)	(Magnification difference and Rotation error) and (Magnification difference and Vertical Shift)

Hypothesis 1.5: Alignment errors in stereoscopic displays have no effect on cerebral cortex relative power bands during visual display tasks.

$$H_0: \mu_{\text{vertical shift}} = \mu_{\text{rotational error}} = \mu_{\text{magnification difference}}$$

$H_a$ : At least one mean is different

That is, the mean cerebral cortex relative power bands are the same across alignment errors. The significance level ( $\alpha$ ) = 0.05. There were low to medium correlations between the fifteen relative

power bands (that is, five relative power bands and three channels labeled  $O_1$ ,  $O_z$ , and  $O_2$ ).

Similarly, One-way MANOVA statistical technique was used. For any significance, a Tukey post ad hoc analyses was conducted to reveal any significant differences.

The One-way MANOVA results showed that Wilk's Lambda = 0.0349,  $F(30, 110) = 15.96$ ,  $p < 0.05$ . At level of significance ( $\alpha$ ) = 0.05, there was enough evidence to conclude that the cerebral cortex relative power as composite score was significant and the summary of the ANOVA results for the individual relative power bands are shown in Table 13. The summary of the Tukey results is shown in Tables 14 and 15.

Table 13

*ANOVA Results Based on Alignment Error Using EEG Data*

Effects	ANOVA				
	Alpha	Beta	Theta	Delta	Gamma
Left Occipital Cerebral Cortex Hemisphere ( <i>l</i> OCCH)					
Alignment Errors	F(2, 69) = 0.035 $p = 0.7087$	F(2, 69) = 0.05 $p = 0.954$	F(2, 69) = 2.26 $p = 0.1116$	F(2, 69) = 0.05 $p = 0.087$	F(2, 69) = 0.30 $p = 0.614$
Effects	ANOVA				
	Alpha	Beta	Theta	Delta*	Gamma
Midline Occipital Cerebral Cortex ( <i>m</i> OCC)					
Alignment Errors	F(2, 69) = 0.32 $p = 0.7303$	F(2, 69) = 0.37 $p = 0.6941$	F(2, 69) = 206.91 $p = 0.154$	F(2, 96) = 18.8 $p < 0.05$	F(2, 69) = 93.52 $p = 0.225$
Effects	Alpha*	Beta	Theta*	Delta*	Gamma
Right Occipital Cerebral Cortex Hemisphere ( <i>r</i> CCH)					
Alignment Errors	F(2, 69) = 139.26 $p < 0.05$	F(2, 69) = 139.6 $p = 0.057$	F(2, 69) = 18.98 $p < 0.05$	F(2, 69) = 0.5 $p < 0.05$	F(2, 69) = 4.7 $p = 0.125$

\*significant, the null hypothesis is rejected.

Table 14

*Tukey Post Ad Hoc Analyses of EEG Data for Alignment Errors on the Midline Cerebral Cortex Hemisphere*

Hemisphere	Band Waves	Tukey post ad hoc analyses for alignment errors, ( $p < 0.05$ )
<i>c</i> CCH	Delta	Magnification difference and Rotation error

Table 15

*Tukey Post Ad Hoc Analyses of EEG data for Alignment Errors on the Right Cerebral Cortex Hemisphere*

Hemisphere	Band Waves	Tukey post ad hoc analyses for alignment errors, ( $p < 0.05$ )
<i>r</i> CCH	Alpha	Magnification difference and Rotation error
	Delta	Magnification difference and Vertical shift
	Delta	Magnification difference and Vertical Shift

Generally, all the subjective responses measured by SSQ and NASA-TLX and eight physiological responses were significant, while eleven physiological responses were not. The stereoscopic alignment errors had great impact the SSQ responses. From the second to the third experimental sessions, the participants' perceptual ratings of visual fatigue increased from slight to moderate or moderate to severe. The left dorsolateral prefrontal cortex was affected more than the right dorsolateral prefrontal cortex. Both oxygenated hemoglobin and deoxygenated hemoglobin in the left dorsolateral prefrontal cortex were significantly affected by the stereoscopic display alignment error, while in the right dorsolateral prefrontal cortex, the stereoscopic display alignment error had an impact on only the deoxygenated hemoglobin. As stated by Buxton, Uludag, Dubowitz, and Liu (2004), responses to stimuli changes result in increase or decrease of regional Cerebral Blood Flow (rCBF) to this localized brain region. It

increases with the increase in demand for decision making processes. Thus, cortical tissue oxygenation requirement in the left hemisphere indicates that the effect of visual fatigue is more pronounced in the left dorsolateral prefrontal cortex. The EEG spectrum was divided into five components including Delta (1-3.99Hz), Theta (4-7.99 Hz), Alpha (8- 12.99 Hz), Beta (13-29.99 Hz) and Gamma (> 30Hz) (Dussault, Jouanin, Philippe, & Guezennec, 2005). Higher power for delta, theta, alpha, and beta bands suggest higher mental loading, task manipulations, increased level of complexity, and anxiety (Demos, 2005). The delta bands in the occipital lobe were significant for midline occipital lobe and left occipital lobe. Delta bands are influenced by cognitive loading. As cognitive loading increases, delta band power also increases (Dussault et al., 2005). The level of experience significantly influenced delta band power, indicating that lower delta band power was associated with individuals with a higher experience level (Dussault et al., 2005). As participants continued to engage in the experiment, their alertness decreased with time as explained in Table 6. The decrease in alertness might be attributed to the onset of visual fatigue.

In addition to the delta band, alpha, beta, and theta bands were significant at right occipital lobe. Serman and Mann (1995) suggested that higher alpha band activity may be associated with visuomotor tasks. Hence, the onset of visual fatigue had great impact on hand and eye coordination during the ATC tasks. A stereoscopic display alignment error increased with the level of task difficulty since task difficulty directly influences the power of theta band power in the EEG spectrum. Brookings, Wilson, and Swain (1996) noted that activities requiring continuous monitoring resulted in increased theta band power, which may be attributed to fatigue associated with lower arousal. Beta and gamma are distinguished by motor inactivity and learning process, respectively. Clearly, experimental conditions were contrary to the

cognitive state of beta and gamma, which was supported by the analyses. Finally, beta and gamma bands were not significant in any of the regional occipital lobe.

As shown in Figure 20, the profiles plots for alpha, beta, theta, and gamma bands had similar patterns. These bands have high relative powers at both left and right hemispheres and reduce toward mid line section of the occipital lobes of the brain. The power plots show that delta band had a low relative power at the mid line section and high relative band power at the left and right hemisphere. There was a noticeable variability in all frequency bands in the experimental conditions. The same distribution pattern existed for channel  $O_z$  and  $O_2$ . There were noticeably higher powers for delta, theta, alpha, and beta bands. These suggested higher mental loading, task manipulations, increased level of complexity, and anxiety (Damos & Wickens, 1980; Dussault et al., 2005; Gundel & Wilson, 1992; Petsche & Rappelsberger, 1992)

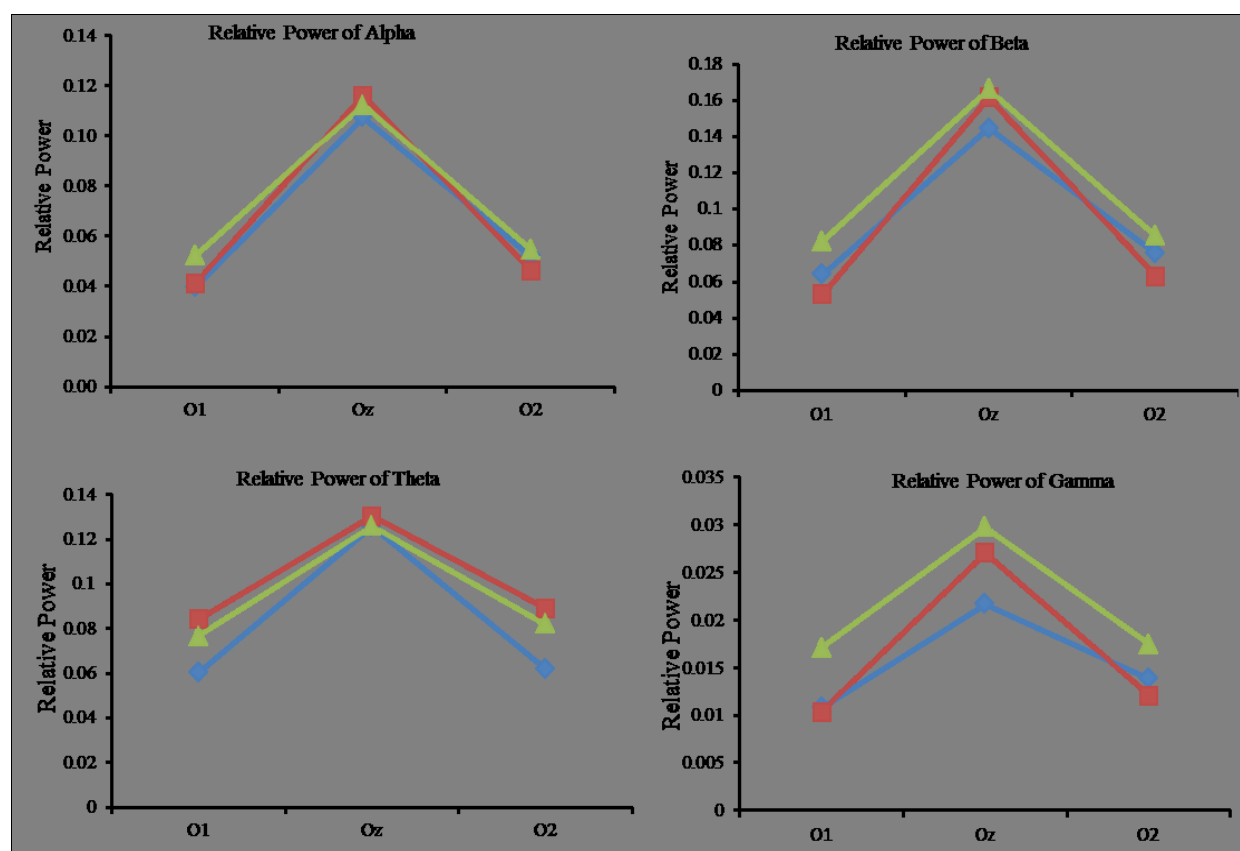


Figure 20. Profile plot of EEG band relative at the three alignment display error type.

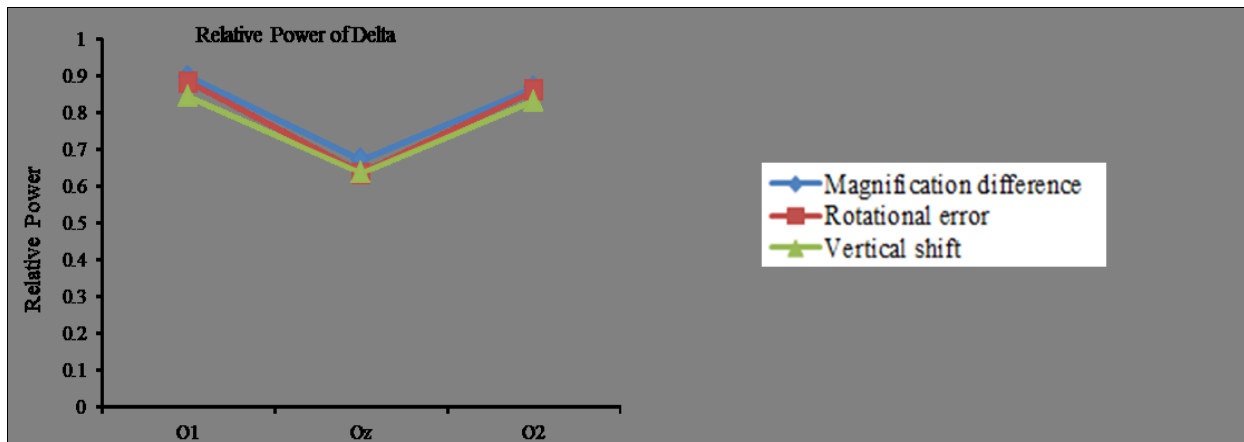
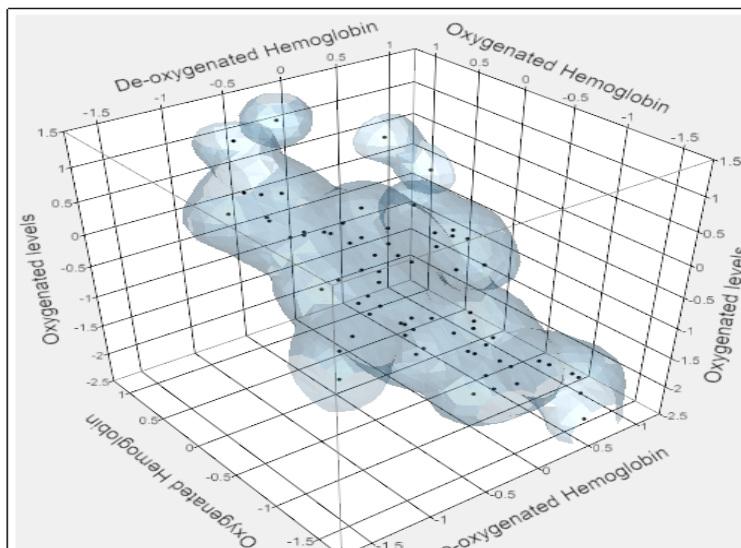


Figure 20. (cont.)

Using the oxygenated hemoglobin and deoxygenated hemoglobin, blood volume, and oxygenation levels, a 3D scatter plot for neuroimaging data comprising of de-oxygenated hemoglobin, oxygenated hemoglobin, and oxygenation level were plotted as shown in Figure 21. Increase in the oxygenated hemoglobin resulted in a corresponding increase in the oxygenated levels. This was depicted by the upward movements toward the vertex of the oxygenation level and oxygenated hemoglobin variables.



(a) /DLPFC

Figure 21. Temporal patterns for hemodynamic responses for the dorsolateral prefrontal cortex for all the alignment errors in the ATCIM display.

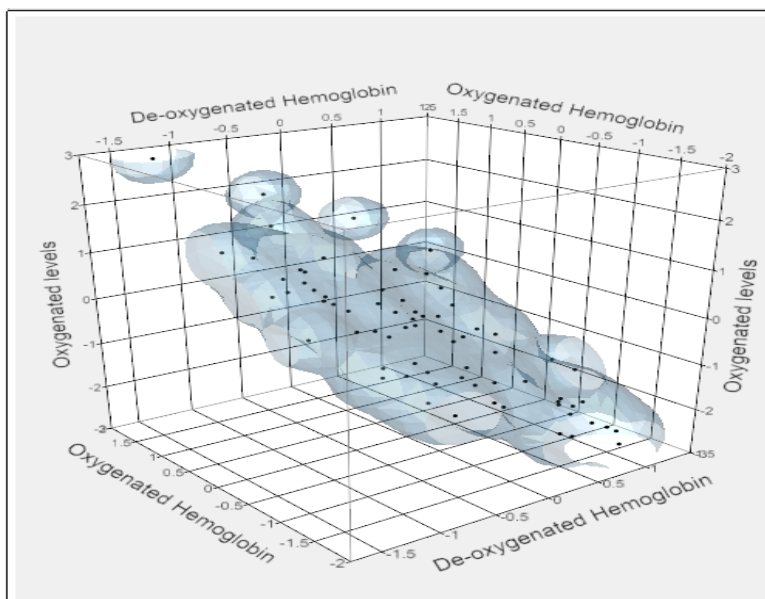
(b) *rDLPFC*

Figure 21. (cont.)

The same pattern was depicted in the right dorsolateral prefrontal cortex. However, for the right dorsolateral prefrontal cortex, the distribution was narrower than the left dorsolateral prefrontal cortex. The ATC tasks induced more cognitive processes in the left dorsolateral prefrontal cortex than the right dorsolateral prefrontal cortex.

As result of the cognitive load, more energy was required by the brain and thus more oxygen requirements. According to Hansen (1987), the concentration of oxygen in the brain is about  $0.1 \mu\text{mol g}^{-1}$ , of which 90% is in oxy-Hb in brain capillaries. This concentration can support the normal oxygen consumption of about  $3.5 \mu\text{mol g}^{-1} \text{min}^{-1}$  for two seconds (Ames III, 2004). For this reason, any increase in neural activity in the brain is followed by the rise in regional cerebral blood flow (CBF) (Buxton et al., 2004). Oxygen is transported to neural tissue via oxygenated hemoglobin (oxy-Hb) in the blood. The demand for glucose and oxygen by neuronal tissues in a particular brain region may vary due to particular processing requirements at a particular time.

Increases in hemoglobin and oxygenation levels in left dorsolateral prefrontal cortex mean that the left side of the brain is more engaged with visiomotor cognitive processes than the right side of the brain. The continual engagement of the left brain may lead to the mental fatigue. Post ad hoc analyses revealed that there were significant differences between magnification error and rotational error, and magnification error and vertical shift error. However, there was no significant difference between rotational error and vertical shift error. For the right hemisphere of the dorsolateral prefrontal cortex, oxygenated hemoglobin, blood volume level, and oxygenation levels were significant.

### 4.3 Prediction Equations for Visual Fatigue

The main premise of this study was to develop models to predict the on-set of visual fatigue using alignment errors as dependent variables and workload and hemodynamic responses as the independent variables. The general criteria used to determine the efficiency of the prediction equations have been detailed in the following sections. The data were checked for multicollinearity using correlations and variance inflation factor (VIF). A stepwise regressions technique with SAS was used for the analysis. Stepwise regression is an efficient method that adds one variable at each step until no more variables may be included in the model that may improve the  $R^2$  value. The models obtained are shown in equations 7 to 9.

$$\begin{aligned}
 SSQ_{(Vertical\ Shift)} = & 0.47089 + [0.04081 * NASA-Workload + 447.41 * Deoxygenated\ hemoglobin \\
 & + 569.59 * Oxygenated\ hemoglobin - 508.51336 * Blood\ Volume \\
 & - 61.20 * Oxygenation]_{(l)DLPFC} + [423.86 * Deoxygenated\ hemoglobin \\
 & + 597.52 * Oxygenated\ hemoglobin - 510.85 * Blood\ Volume \\
 & - 86.87 * Oxygenation]_{(r)DLPFC}
 \end{aligned} \tag{7}$$

$$R^2 = 0.818 \text{ and } VIF \leq 1.7$$

$$\begin{aligned}
SSQ_{\text{(Magnification Difference)}} = & 0.7932 + [0.01989 * \text{NASA-Workload} + 497.039 * \text{Deoxygenated} \\
& \text{hemoglobin} - 295.19 * \text{Oxygenated hemoglobin} - 100.94 * \text{Blood Volume} \\
& + 369.54 * \text{Oxygenation}]_{(l)DLPFC} + [-1505.08 * \text{Deoxygenated hemoglobin} \\
& + 235.76 * \text{Oxygenated hemoglobin} + 634.96 * \text{Blood Volume} \\
& - 870.62 * \text{Oxygenation}]_{(r)DLPFC} \quad (8)
\end{aligned}$$

$$R^2 = 0.794, \text{ VIF} \leq 1.4$$

$$\begin{aligned}
SSQ_{\text{(Rotational Error)}} = & 0.5508 + [0.01882 * \text{NASA-Workload} + 17.89 * \text{Deoxygenated hemoglobin} \\
& - 729.233 * \text{Oxygenated hemoglobin} + 355.68 * \text{Blood Volume} \\
& + 373.40 * \text{Oxygenation}]_{(l)DLPFC} + [57.30 * \text{Deoxygenated hemoglobin} \\
& + 409.86 * \text{Oxygenated hemoglobin} - 233.44 * \text{Blood Volume} \\
& - 176.26 * \text{Oxygenation}]_{(r)DLPFC} \quad (9)
\end{aligned}$$

$$R^2 = 0.4593 \text{ and } \text{VIF} \leq 6.7$$

Where

Workload = Overall NASA-TLX workload scaled between 0-100

Deoxygenated hemoglobin = grams per deciliter (gm/dL)

Oxygenated hemoglobin = grams per deciliter (gm/dL)

Blood Volume =  $\mu\text{M}$

Oxygenation =  $\mu\text{M}$

(*l*)DLPFC = left Dorsolateral Prefrontal Cortex

(*r*)DLPFC = right Dorsolateral Prefrontal Cortex

For the vertical shift, the overall model was statistically significant,  $F(9, 14) = 3.33, p < 0.05$ , and model accounts for 81% of the variability observed in the SSQ perception of visual fatigue. For magnification differences, the model was significant  $F(9, 14) = 0.80, p < 0.05$  with the model accounting for 79% of the variability observed in the SSQ perception of visual fatigue.

As shown in Figure 20, the profiles plots for alpha, beta, theta, and gamma bands had similar patterns. These bands had high relative powers at both left and right hemispheres and reduced towards mid line section of the occipital lobes of the brain. The power plots show that delta band had a low relative power at the mid line section and high relative band power at the left and right hemisphere. There was a noticeable variability in all frequency bands in the experimental conditions. The same distribution pattern existed for channel  $O_z$  and  $O_2$ . There were noticeably higher powers for delta, theta, alpha, and beta bands. These results suggested higher mental loading, task manipulations, increased level of complexity, and anxiety, which agree with previous researches (Damos & Wickens, 1980; Dussault et al., 2005; Gundel & Wilson, 1992; Petsche & Rappelsberger, 1992).

#### **4.4 Analysis on Magnification Differences Error**

Since magnification difference errors were significant, further analysis was conducted to identify the likely points of visual fatigue. The hemodynamic responses revealed that significant differences exists between left and right dorsolateral prefrontal in the alignment errors in visual attention tasks,  $F(1, 47) = 0.034, p < 0.05$ . Generally, oxygenation levels were increased in both left and right dorsolateral prefrontal; however, it was more pronounced in the left dorsolateral prefrontal. In the left dorsolateral prefrontal, the increased oxygenation levels resulted from the corresponding increased oxygenated hemoglobin and blood volume. Contrasting to the left dorsolateral prefrontal, oxygenated levels increased without any blood flow to that region. More interestingly, the pronouncements in left dorsolateral prefrontal can be traced to the fact that all participants were right-handed. This is consistent with Springer and Deutsch (1989) observations. The left hemisphere controls the right side of the body, and the right hemisphere controls the left side of the body (Springer & Deutsch, 1989).

The ANOVA Table 16 shows that there was a significant difference between the power spectrums from left to right channels. With a level of significance of  $(\alpha) = 0.05$ , there was enough evidence to suggest some interaction between left, middle, and right sides of the brain and the magnification difference during the ATC task sessions as a result of magnification difference display. There was also a significant difference between the main effect for power band hemisphere and the magnification difference due to ATC task sessions,  $F(2,47) = 0.87, p < 0.05$  and interaction effects between the processing lobes and tasks  $F(8, 47) = 3.306, p < 0.05$ . The summary of major findings in this study was summarized in Table 17.

Table 16

*ANOVA Results for Hemodynamics Data on the Dorsolateral Prefrontal Cortex Location during ATC Tasks*

Source	<i>df</i>	Sum of Square	Mean Square	<i>F</i> Value	<i>p &gt; F</i>
<i>DLPFC</i> Location	1	1.25	1.25	0.034	< 0.05
Magnification difference	2	0.005	0.104	0.76	< 0.05
<i>DLPFC</i> Location* Magnification difference	8	0.096	0.012	3.306	< 0.05
Error	47	3.025	36.3		
Corrected Total	56				

*Industrial Relevance:* From the empirical findings, stereoscopic display alignment errors can induce visual fatigue due to workload and other underpinning neurophysiological effects associated with visual task performance. Visual fatigue is likely to increase the hemodynamic response in the left dorsolateral prefrontal cortex of the brain and delta band waves can be used to predict cognitive fatigue across all the occipital cerebral cortex. Thus, visual fatigue can lead to mental fatigue. To improve HMD design for minimum visual fatigue to the users, the optical

axes system in HMD devices should be designed with minimum magnification difference and rotational error, as these errors were observed to be most prevalent. HMD designs with minimum magnification difference and rotational error is more likely to reduce visual fatigue, increase performances, and satisfaction of the users such as aviators and flight pilots.

Table 17

*Summary of Major Findings from Hypotheses in Study I*

<p>Hypothesis 1.1: A prolong use of stereoscopic display does not induce visual performance.</p>	
Dependent variable:	SSQ
Independent variable	BATC and ATC 3
Outcome	Yes, at 0.05 level of significance a prolong use of stereoscopic is likely to cause visual fatigue, $t(23) = -15.27, p < 0.05$ .
<p>Hypothesis 1.2: Alignment errors in stereoscopic displays do not increase the prevalence of visual fatigue.</p>	
Dependent variable:	SSQ
Independent variable	Alignment errors
Outcome	Yes, at 0.05 level of significance, there is enough evidence to conclude that at least one of the stereoscopic alignment is likely to increase the prevalence of visual fatigue, $F(2, 69) = 35.38, p < 0.05$ .
<p>Hypothesis 1.3: Alignment errors in stereoscopic displays have no effect on workload during visual display task.</p>	
Dependent variable:	NASA-TLX Workload
Independent variable	Alignment errors
Outcome	Yes, at 0.05 level of significance, there is enough evidence to conclude that at least one of the stereoscopic alignment error had effect on workload, $F(2, 69) = 0.74, p < 0.05$ .

Table 17

(cont.)

Hypothesis 1.4: Alignment errors in stereoscopic displays have no effect on dorsolateral prefrontal cortex hemodynamic responses during visual display task.	
Dependent variable:	Transformed hemodynamic responses
Independent variable	Alignment errors
Outcome	Yes, at 0.05 level of significance, there is enough evidence to conclude that the transformed hemodynamic response as composite score was significant, Wilk's Lambda = 0.924, $F(8, 132) = 0.66, p < 0.05$ . a. $l$ DLPFC-Hbb transformed dataset $F(2, 69) = 0.10, p < 0.05$ b. $l$ DLPFC-HbO <sub>2</sub> transformed dataset $F(2, 69) = 0.15, p < 0.05$ c. $r$ DLPFC-Hbb transformed dataset, $F(2, 69) = 1.09, p < 0.05$
Hypothesis 1.5: Alignment errors in stereoscopic displays have no effect on cerebral cortex relative power bands during visual display task.	
Dependent variable:	Cerebral cortex relative power bands
Independent variable	Alignment errors
Outcome	Yes, at 0.05 level of significance, there is enough evidence to conclude that the cerebral cortex relative power as composite score was significant, Wilk's Lambda = 0.0349, $F(30, 110) = 15.96, p < 0.05$ a. $m$ OCCH (O <sub>z</sub> ): Delta, $F(2, 96) = 18.8, p < 0.05$ b. $r$ OCCH (O <sub>2</sub> ): Alpha, $F(2, 69) = 139.26, p < 0.05$ c. $r$ OCCH (O <sub>2</sub> ): Theta, $F(2, 69) = 18.98, p < 0.05$ $r$ OCCH (O <sub>2</sub> ): Delta, $F(2, 69) = 0.5, p < 0.05$

## CHAPTER 5

### Experiment II: Cognitive Neuroscience for Visual Fatigue

Visual processing occurs in a series of hierarchical steps involving photoreceptors, retinal bipolar cells, ganglion cells, the lateral geniculate nucleus (LGN), and the primary visual cortex (V1) (Kaplan & Shapley, 1986). The neurons in primary visual cortex (V1) are selective for binocular disparity. Backus, Fleet, Parker, and Heeger (2001) discovered that the V1 neurons do not explicitly code perceived depth. It has concluded that stereoscopic pathways include additional processing beyond V1. Backus et al. (2001) found cortical activities in areas of V3A (texture), MT+ (motion direction), and frontal eye field (FEF) of the human brain when presented with 3D images. The FEF is known to be involved in eye movement control. It also appears to have correlation with the visual fatigue caused by the stereoscopic depth perception (Kim, Jung, Kim, Man Ro, & Park, 2011). Tsao, Vanduffel, Sasaki, Fize, Knutsen, Mandeville, Wald, Dale, Rosen, Van Essen, Livingstone, Orban, Tootell, (2003) concluded that the stereoscopic processing occurs in the V3A , V7 (working memory), V2 (stereo), V4d topology (kinetic motion), and the caudal parietal disparity region (CPDR).

Studies have noted that visual fatigue induces concentration and focusing attention difficulty, and can eventually lead to VDT performance decrement. For example, Palaniappan and Jayant (2006) concluded that the additional cognitive processing required for depth perception is the major cause of visual fatigue for 3D viewing. According to Harrison and Home (1999) and Harrison and Home (2000), both mental and/or visual fatigues are responsible for deficient functioning of prefrontal cortex.

Four hypotheses were studied in Experiment II:

2.1 A prolonged use of stereoscopic display does not cause visual fatigue.

- 2.2 A prolonged use of stereoscopic display has no effect on response time.
- 2.3 Cognitive loadings have no effects on response time.
- 2.4 Task difficulty (i.e., aircraft separation types) has no effects on response time.
- 2.5 There is no effect of interaction between cognitive workload response variables and task difficulty on response time.

## 5.1 Experimental Design

The purpose of the experiment was to elicit real-time neurophysiologic and psychophysiological data during task performance. The experiment used a 2 x 4 within subject repeated randomized factorial design. Table 18 describes the experimental treatment, displaying the levels for each treatment, and the measurement units for the experiment.

Table 18

*List of Factors and Their Levels for Experiment II*

Factors	Levels	Measurements
Cognitive loading	3	Low
	9	High
Task difficulty	Vertical	Low
	Horizontal	Medium
	Combined vertical and horizontal	High
	None	High

The objective data was response time for the evaluation of human performance from varied cognitive loadings using dynamic SA with sample ATC tasks. There were five dependent variables for the study. These are response time, hemodynamic response, electrophysiological responses, eye responses, and SSQ. The hemodynamic and electrophysiological responses are continuous variables measured with fNIRS and Biopac MP 150, respectively. The eyes responses

wer measured with ViewPont Eye Tracker. Response Time (RT) in the study is defined as the time lag between the moment when the subject clicks the ‘COLLISION ALERT’ button and the moment the subject is presented with the type of system alert at the point of aircraft self-separation violation. Response Time is measured in milliseconds.

## 5.2 Apparatus and Experimental Set up

The apparatus and experimental set up used were identical to task I. However, due to software incompatibility, the ATCIM was designed using E-Prime<sup>®</sup> 2.0 software (Psychological Software Tools Inc., 2010) and the stimuli was delivered through the HMD-Viewpoint Eye tracker (Arrington Research Inc., 2010).

The literature (van der Linden, Frese, and Meijman (2003) indicated that a cognitively demanding task involving human visual systems induces visual fatigue after 2.5 hours. By using equation 1 of Chapter 3, the number of subjects for the study was computed as:

$$n = \frac{2 * 3 * 2.5^2 * 1.824^2}{7^2} = 7.638 \approx 8 \text{ subjects} \quad (10)$$

## 5.3 Participant Preparation and Procedure

The subjects were introduced to the workstation and briefed on the experimental protocol based on the Institutional Review Board requirements. They read the informed consent form and signed it upon agreeing to participate in the experiment. Verbal explanations were occasionally offered for clarification. Each of the participants were assigned an alphanumeric identification number, rather than using their real name. Participants’ foreheads were cleaned with 70% Isopropyl alcohol swap wipes and air dried. Using the 10-20 system, the  $F_{p1}$ ,  $F_z$ ,  $C_z$ , and  $O_z$ , were measured with measuring tape and marked with washable markers. The positions for  $F_{p1}$ ,  $F_z$ ,  $C_z$ , and  $O_z$ , were cleaned with 70% Isopropyl alcohol swap, and Nuprep cream was used to clean the dirty skin. The EL-110 electrodes were filled with the EC<sup>®</sup> cream and placed on the prepared

skin surfaces. Further, another electrode was placed behind the ears as grounding electrode. The fNIRS sensor pad was placed on the forehead. The HMD ViewPoint Eye tracker was placed on top of the fNIRS sensor pad as shown in Figure 22. The sensor pad and the eye tracker were held in place by a head band.



*Figure 22.* Subject performing ATC task.

#### **5.4 Tasks**

The experimental protocol was summarized in Figure 23. The participant performed three ATC tasks sessions labeled as ATC1, ATC2, and ATC3, consecutively. The ATC1, ATC2, and ATC3 were the repeated experimental treatments. The experimental treatments were based on the cognitive loading and task difficulty. The cognitive loading was the number of aircrafts on the radar with separation conflicts.

The cognitive loading had two levels labeled as low (3) and high (9) while task difficulty had four levels based on the separation conflicts labeled as vertical, horizontal, combined horizontal and vertical, and none. A high maneuver (ATC3) had a maximum number of nine aircraft with either combined horizontal and vertical or none for separation conflicts, and a low maneuver (ATC1) had 2-3 aircraft conflicts in the airspace.

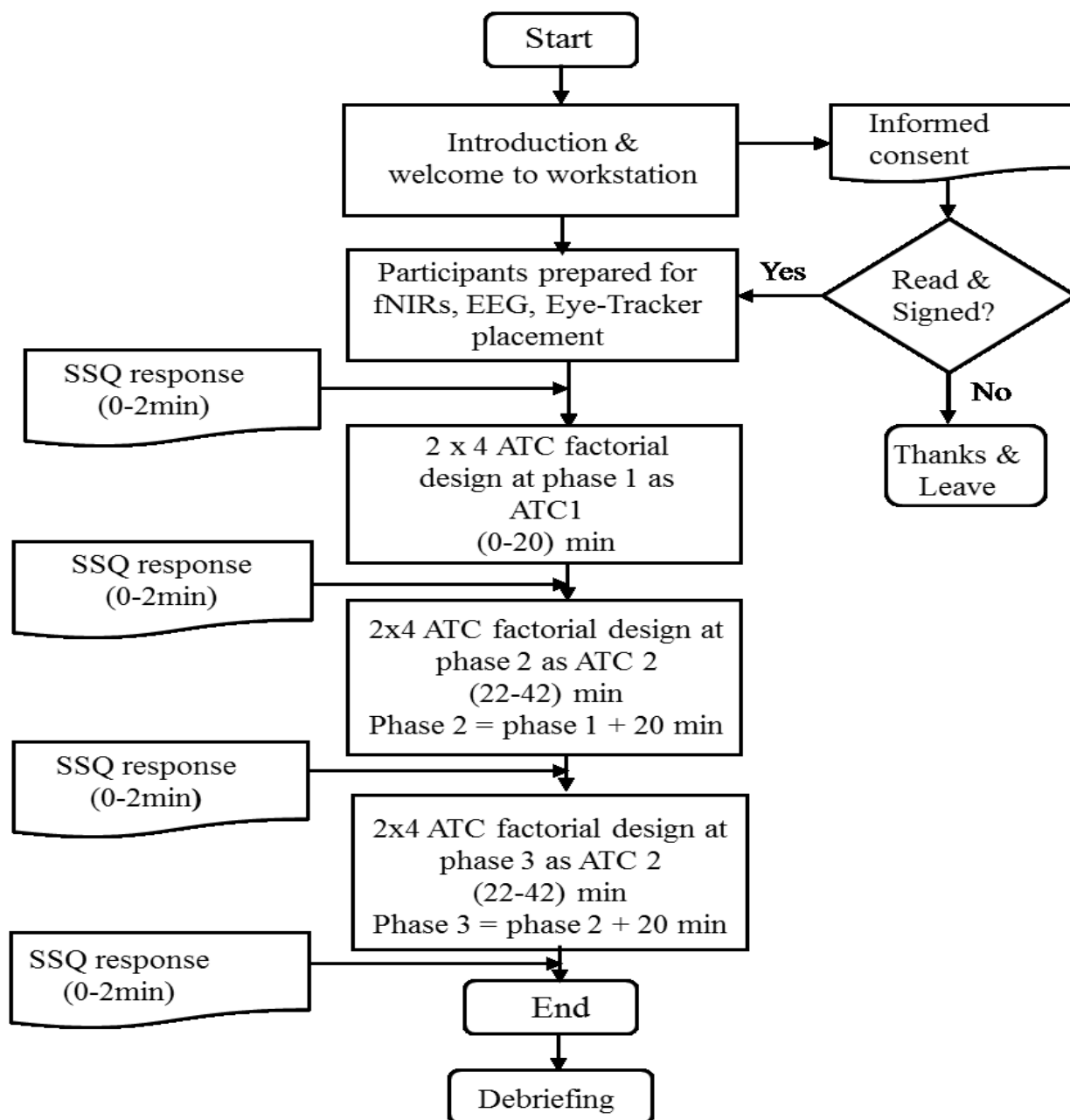


Figure 23. Experimental protocol for simulated air traffic control (ATC) tasks.

Before starting the experiment, each subject rated his/her psychological sense of visual fatigue using SSQ. The tasks involved monitoring; that is, the participant visually scan the display and if two or more self-separation violations were detected, they responded by pressing the “CLICK BUTTON” located at the interface of the ATCIM. However, if they detected no self-separation violations, no response was issued, and after 20 seconds, the display refreshed

itself for a new display. After the completion of each session, subjects were required to rate their perceptions of visual fatigue. The subjects were required to perform the experimental tasks as quickly and accurately as possible. The average time for the experimental section was about two hours per participant; which was inclusive of subject preparation, briefing, and debriefing times.

## 5.5 Analysis, Results and Discussion

The acronyms ATC1, ATC2, and ATC3 denote the first, second, and third experimental sections, respectively. Data for each of the participants' was retrieved from a compiled database generated for each experimental section. One participant could not finish the last section for both experimental treatment and SSQ. The missing values were replaced by the mean of that variable for the SSQ (Pang-Ning et al., 2006). The dependent measures were SSQ, Response Time, hemodynamic responses, and visual responses. The response datasets were pre-processed and analyzed as described in Chapter 4.

**5.5.1 Experimental hypotheses testing.** Four hypotheses were investigated in this study. A model adequacy check was performed to test the three ANOVA assumptions of normality, independence, and homogeneity of variance. Tests for normality showed that all the dependent variables in the dataset were normally distributed. For response time, the Shapiro-Wilk ( $W$ ) = 0.83,  $p > 0.05$  and visual response variables,  $W = 0.841$ ,  $p > 0.05$ .

The hypotheses tested were as follows:

Hypothesis 2.1: A prolonged use of stereoscopic display does not cause visual fatigue.

$$H_0: \mu_{\text{BATC}} = \mu_{\text{ATC 3}}$$

$$H_a: \mu_{\text{BATC}} < \mu_{\text{ATC 3}}$$

That is, the mean SSQ response before task is the same after performing the task and the significant level ( $\alpha$ ) is 0.05.

Cronbach's alpha reliability test was applied to the SSQ responses using SAS. The Cronbach was evaluated based on participants' overall SSQ scores for each ATC tasks sessions. The dataset consisted of 24 observations and 4 attributes representing BATC, ATC1, ATC2, and ATC3. A Cronbach alpha 0.81 was obtained. This shows stable responses considering 0.7 as cut off for acceptable response (Cronbach, 1951; Hatcher, 1994; Nunnaly, 1978; Santos et al., 1998). The descriptive statistics for SSQ responses has been summarized in Figure 24. The box plot results indicated that SSQ response at BATC was low since the box plot for BATC was lower than the median responses.

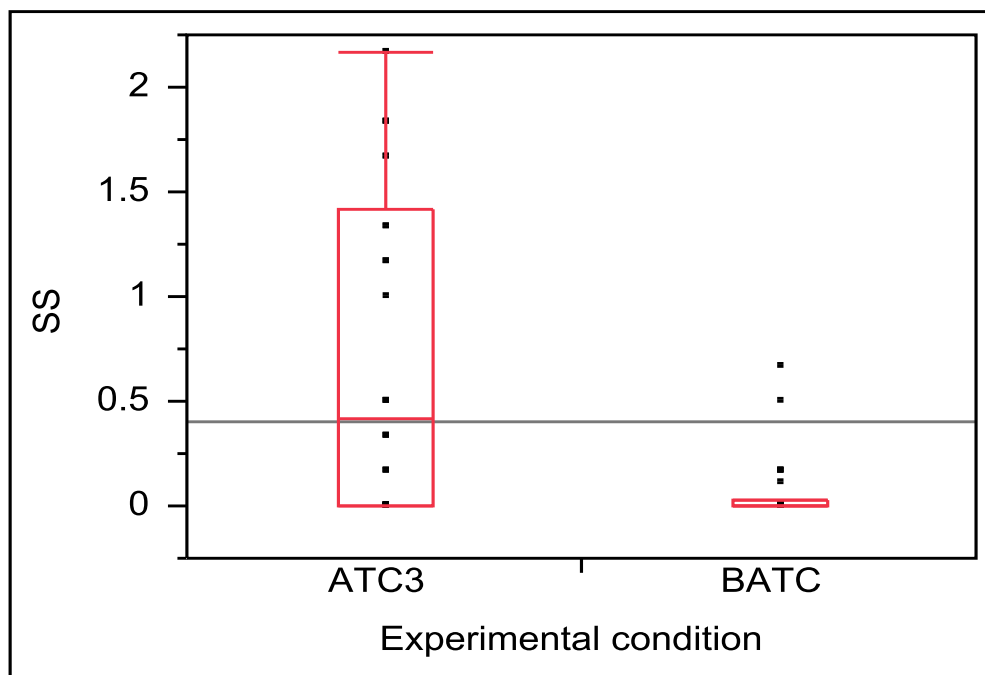


Figure 24. Side-by-side box plot of participants' SSQ ratings for BATC and ATC 3.

Hence, the participants' perception of visual fatigue was almost none at the beginning of the experiments. Further, BATC plot had about four outliers. ATC 3 task appears to have a higher variability than BATC; the ATC 3 box plot was taller than BATC. The highest SSQ ratings for ATC 3 occurred around the time in which the participants felt moderate to severe visual fatigue.

A paired t-test was conducted by using SAS for visual performance and visual fatigue. The null hypothesis was rejected. At the significance level ( $\alpha$ ) = 0.05, there was enough evidence to conclude that a prolonged use of a stereoscopic display was likely to cause visual fatigue as there was significant difference between SSQ responses for before air traffic control task (BATC1) and after air traffic control task (ATC 3),  $t(7) = -11.19, p < 0.05$ .

It was observed that 11 out of the 32 symptoms were more pronounced after ATC 3 as shown in Figure 25.

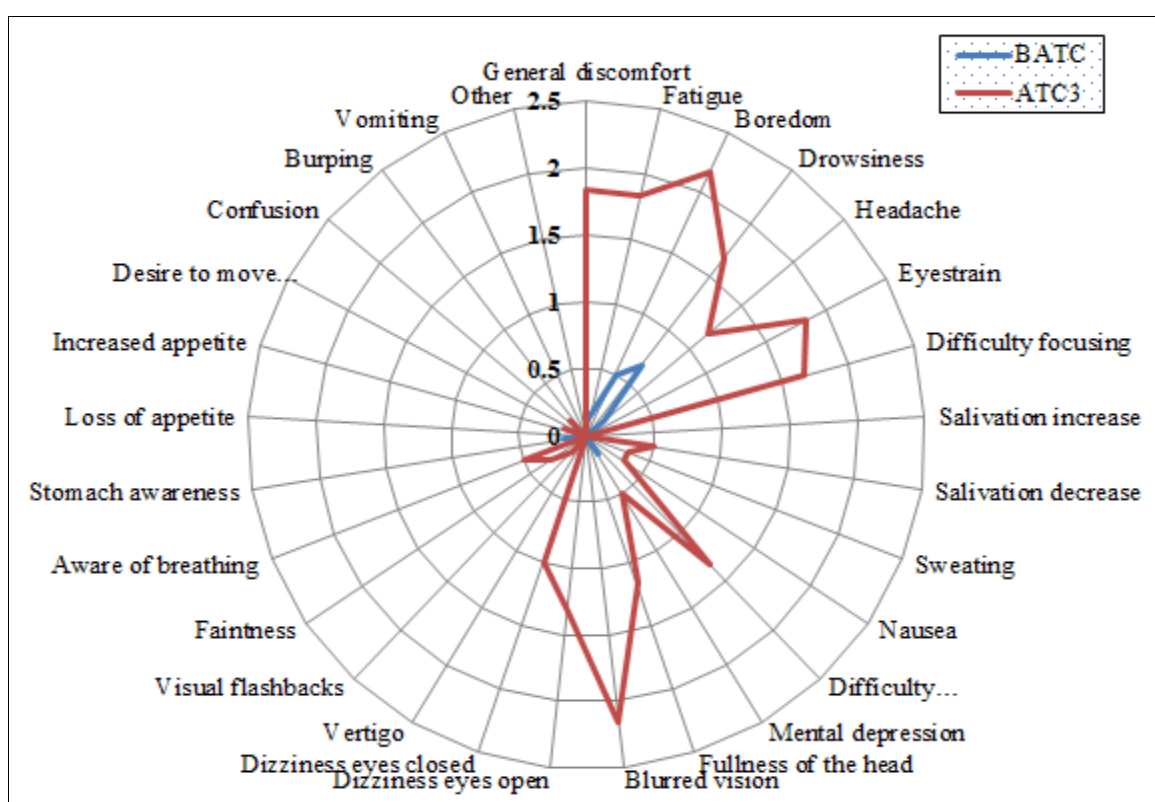


Figure 25. A radial plot of SSQ rated symptoms on ATC task session during BATC and ATC 3.

The SSQ ratings are from 0 to 3 for 34 symptoms, and  $N = 8$  subjects.

These symptoms were discomfort, fatigue, boredom, drowsiness, headache, eyestrain, difficulty in focusing, difficulty in concentrating, blurred vision, and dizziness eye closed. Boredom and blurred vision received moderate to severe ratings after ATC 3. Four symptoms,

namely, discomfort, drowsiness, eyestrain, and difficulty in focusing were rated moderate ratings after ATC 3, while headache and dizziness eye closed symptoms were rated slight after ATC3.

Hypothesis 2.2: A prolonged use of stereoscopic display has no effects on response time.

$$H_0: \mu_{ATC1} = \mu_{ATC3}$$

$$H_a: \mu_{ATC1} < \mu_{ATC3}$$

The mean response time at the beginning of the task is the same after the last task. The significance level ( $\alpha$ ) = 0.05.

The descriptive statistics for SSQ and response time are shown in Figure 26. For response time, the maximum and minimum response time for ATC 3 were higher than ATC1. The upper quartile range in the Box-and-whisker plot for the response time for ATC 1 was equal to the median response time for the two conditions.

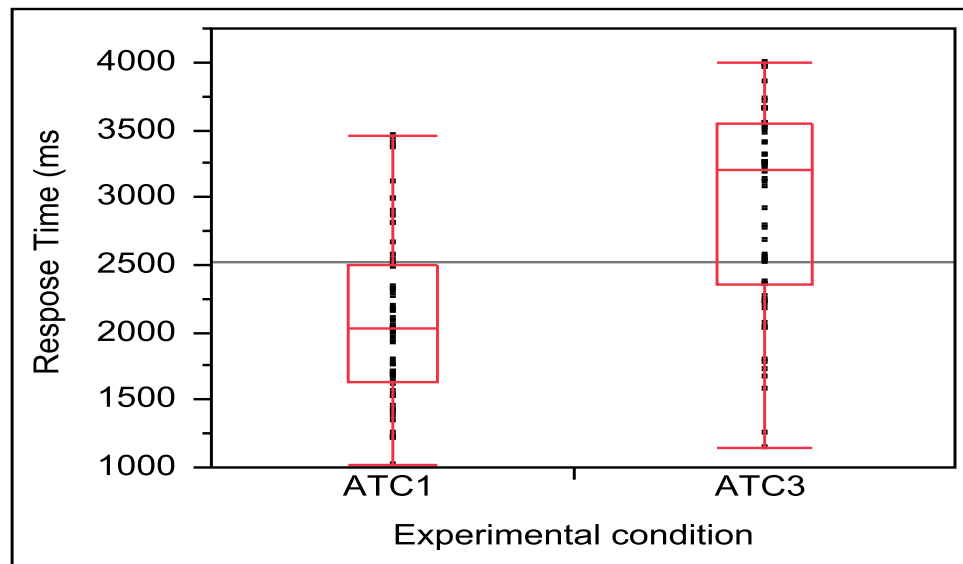


Figure 26. Side-by-side box plot of response time for ATC1 and ATC 3.

Similarly, a paired  $t$ -test was conducted to using SAS for response time. The null hypothesis was rejected for both hypotheses. At 0.05 level of significance, a prolonged use of a stereoscopic display has an effect on response time as there was a significant difference between

after air traffic control task 1(ATC 1) and after air traffic control task (ATC 3),  $t(7) = 3.16$ ,  $p < 0.05$

Three hypotheses investigated the effects of cognitive loading and task difficulty on response time. The hypotheses are as following:

Hypothesis 2.3: Cognitive loadings have no effects on response time.

Hypothesis 2.4: Task difficulty (i.e., aircraft separation types) has no effects on response time.

Hypothesis 2.5: There is no effect of interaction between cognitive workload response variables and task difficulty on response time.

Analysis of response time (RT) data; the descriptive statistics for the RT were summarized in Table 19.

Table 19

*Summary of Descriptive Statistics of Response Time for All ATC Task Sessions*

Cognitive Load	Statistics (ms)	Task Difficulty			
		Vertical	Horizontal	Combined vertical and horizontal	None
Low	RT(Mean)	2435	2802	2781	2812
	RT(St.Dev)	1178	1164	1316	1053
High	RT(Mean)	2949	2658	3001	3151
	RT(St.Dev)	1356	1281	1128	1101

A two-way repeated measure ANOVA statistical technique was used. The independent measures were cognitive loading and task difficulty. The data was analyzed with SAS. For any level of significance, a Tukey analysis was conducted to test for any significant differences.

In a repeated measure experimental design, the sphericity is met when the variations in between the experimental treatments are equal. This indicates that pairs of experimental treatments are

equal. The effect of violating sphericity is loss of power (i.e increased probability of type II error; Field, 2009). The Mauchly test statistics results showed non-significant for the repeated measure variables, hence sphericity assumption was met; for cognitive workload,  $\chi^2(2) = 11.41$ ,  $p = 0.074$ , task difficulty,  $\chi^2(4) = 1.21$ ,  $p = 0.051$ , and interaction effect of cognitive workload and task difficulty,  $\chi^2(8) = 22.761$ ,  $p = 0.086$ .

### Hypothesis 2.3

$H_0$ : Cognitive loading has no effects in response time.

$H_a$ : Cognitive loading has effects in response time.

From the repeated ANOVA results, the null hypothesis was rejected; at 0.05 significance level, there was enough evidence to conclude that no main effect of cognitive load response variable on response time,  $F(1, 58) = 257.44$ ,  $p = 0.083$ .

### Hypothesis 2.4

$H_0$ : The level of task difficulty has no effects on response time.

$H_a$ : The level of task difficulty has effect on response time.

From the ANOVA results, the null hypothesis was rejected. At 0.05 significant level, there was enough evidence to conclude that a significant main effect of task difficulty on response time,  $F(3, 58) = 266.44$ ,  $p < 0.05$ . This indicated that response times were different for task processing of ATC at vertical, horizontal, combined horizontal and vertical, and none, repetitively.

### Hypothesis 2.5

$H_0$ : There is no interaction between cognitive loading and task difficulty on response time.

$H_a$ : There is interaction between cognitive loading and task difficulty on response time.

From the ANOVA results, the null hypothesis was rejected. At 0.05 significant level, there was evidence to conclude that a significant interaction between task difficulty and the cognitive load response variable on response time during visual task of air traffic control task  $F(2.32, 20.84) = 134.91, p < 0.05$ . The interaction plot is shown in Figure 27.

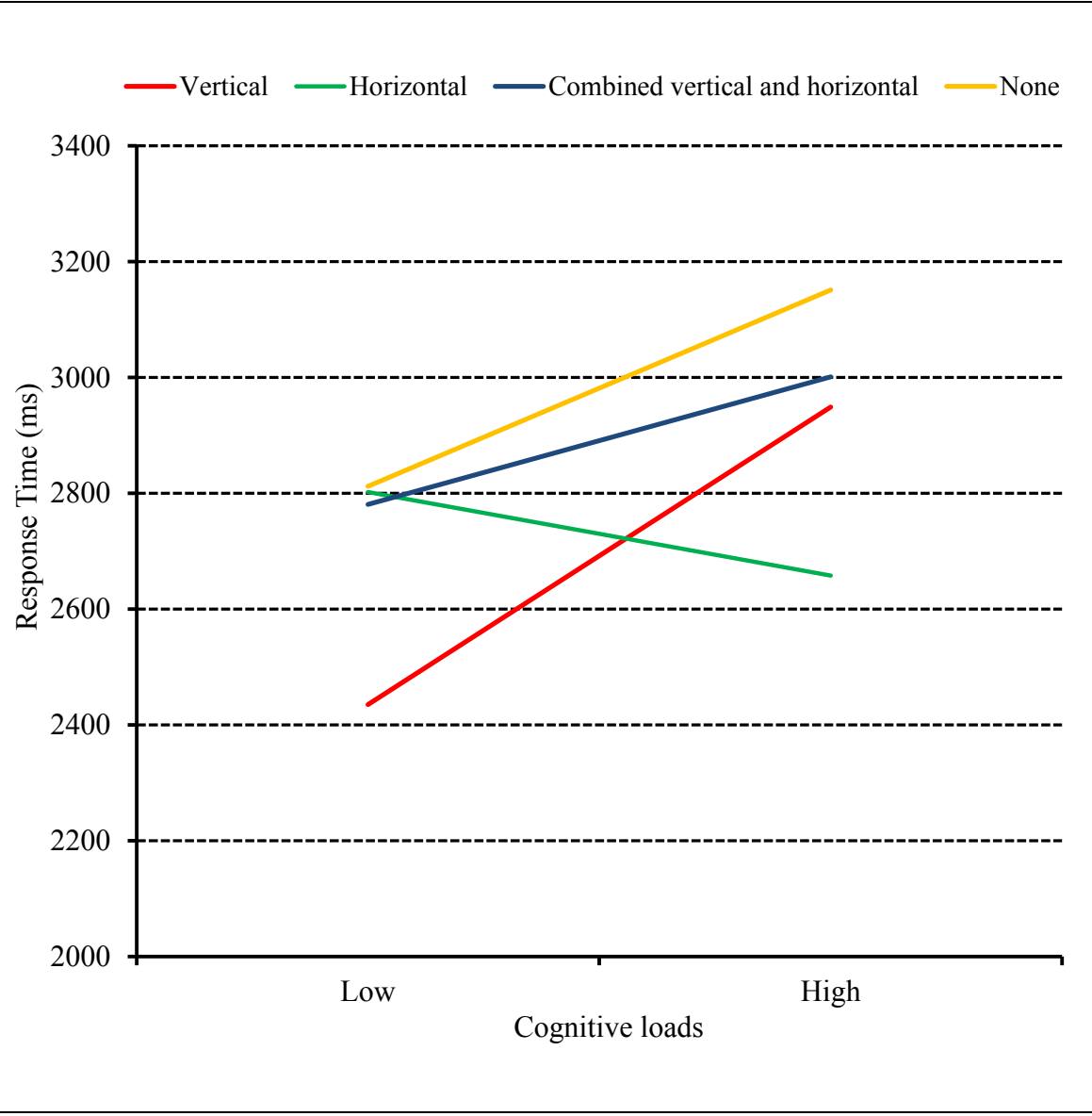


Figure 27. Line graph of the interactive effect plot for cognitive response variables and task difficulty on response time.

This means that response times at different levels of cognitive load response variables were different for task difficulty which process ATC tasks at vertical, horizontal, combined horizontal and vertical, and none, respectively. From Figure 27, the mean response time was different for the levels of the cognitive loads. There was interaction between vertical and horizontal task difficulty levels. With the exception of horizontal separation task difficulty, the response times were generally high at high cognitive load. For the horizontal task difficulty, cognitive load had a big impact on the response time; low cognitive loads had high response time and high cognitive load had a low response time.

For “none”, combined vertical and horizontal, and vertical task difficulty levels, response times were high at the high cognitive load. Hence, tasks processed at none combined vertical and horizontal, and vertical task difficulties were highly affected by cognitive loads.

Since there was a significant interaction effect between cognitive loading and task difficulty, the results about the main effect might not have been true. To explore further, a post-hoc analysis using slicing was used based on the simple main effect of task difficulty and cognitive loading. The hypotheses are as follows:

Hypothesis 2.5.1: Simple main effect on cognitive loading

$H_0$ : there is no simple main effect for task difficulty when separation types are vertical (horizontal, combined vertical and horizontal, none).

$H_a$ : there is simple main effect for task difficulty when separation types are vertical (horizontal, combined vertical and horizontal, none).

The significant level ( $\alpha$ ) = 0.05. At 0.05 level of significance, there was not enough evidence to conclude that there is a significant simple main effect for cognitive loading when task difficulty was at vertical horizontal, combined vertical and horizontal, none.

Hypothesis 2.5.2: Simple main effect on task difficulty

$H_0$ : there is no simple main effect for task difficulty when cognitive loading low (high).

$H_a$ : there is simple main effect for task difficulty when cognitive loading is low (high).

The significant level ( $\alpha$ ) = 0.05.

At 0.05 level of significance, there was not enough evidence to conclude that there is a significant simple main effect for task difficulty when cognitive loading was low. However, there was enough evidence to conclude that there is a significant simple main effect for task difficulty when the cognitive loading was high,  $F(3, 47) = 3.58, p = 0.022$ .

## 5.6 Relationship between Visual Fatigue and other Physiological Signals

To explore the evidence of visual fatigue (measured by SSQ) as results of visual task (ATC) with stereoscopic display, the next response data analyzed were based on the ATC tasks sessions. Recall that the SSQ ratings are 0 (None), 1 (Slight), 2 (Moderate), and 3 (Severe). Using One-way repeated ANOVA, the Mauchly test indicated that the assumption of sphericity has been met,  $\chi^2(5) = 0.136, p = 0.047$ . The ANOVA results showed a significant main effect ATC task session on visual fatigue responses (SSQ),  $F(3, 18) = 3.91, p < 0.05$ . A Tukey post-hoc test revealed that the following pairs had significant differences: (BATC, ATC2) and (BATC, ATC3;  $p < 0.05$ ). This is shown in Figure 28.

As the ATC task progressed in time and higher mental loads, participants continued to report some increased experience of visual fatigue symptoms. Figure 29 shows the radial graph display of the SSQ responses ratings for the four consecutive task sessions. Moderate to severity ratings of SSQ symptoms were more pronounced at the ATC2. These symptoms were discomfort, boredom, drowsiness, headache, and difficult focusing. At ATC 3, the composite weighted SSQ score was 2.46, which indicated severity perception of visual fatigue.

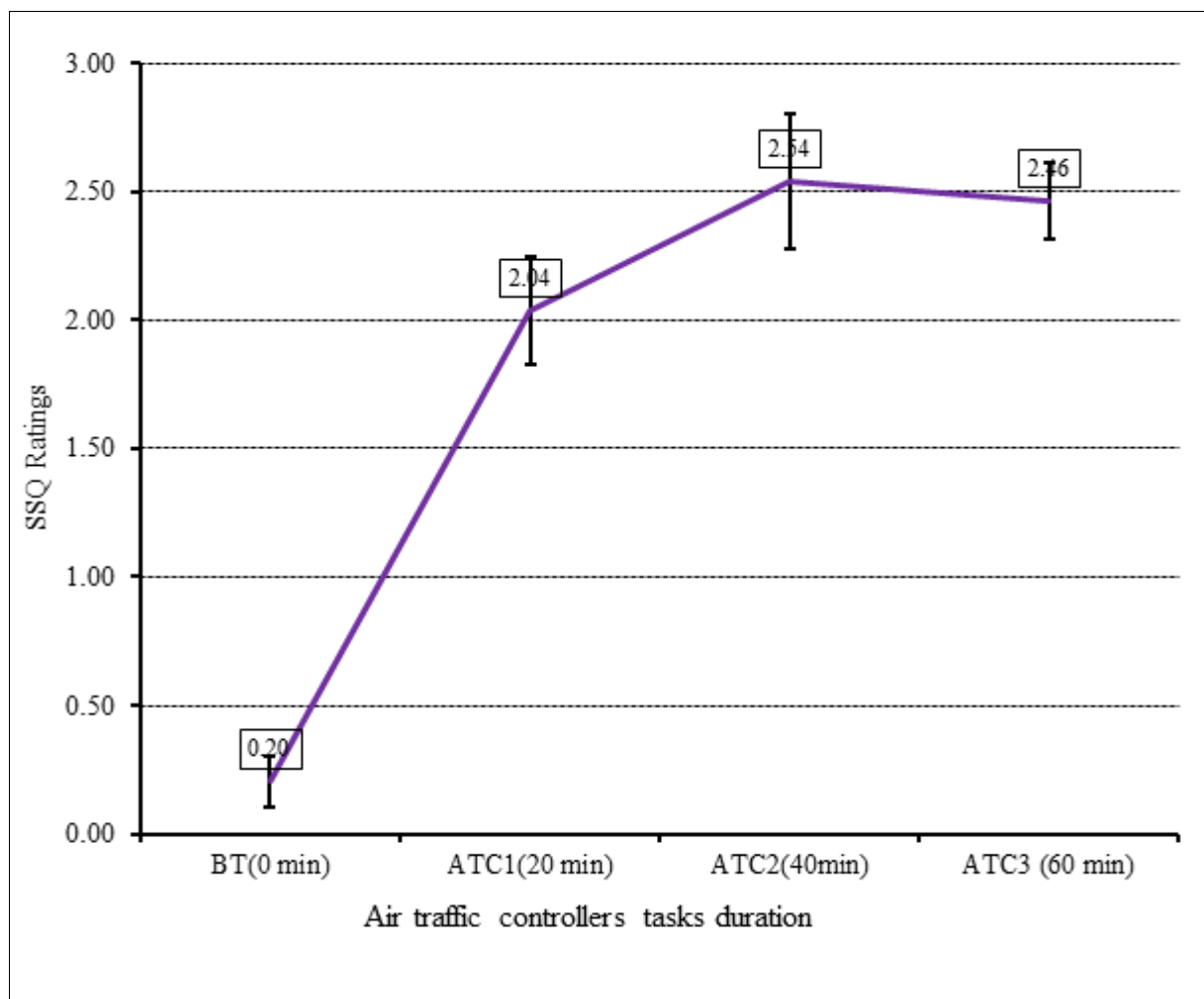


*Figure 28.* Change of mean psychological rating score of visual fatigue with time. The SSQ ratings are from 0 to 3 for 34 symptoms, and  $N = 8$  subjects. SSQ ratings are 0 (None), 1 (Slight), 2 (Moderate), and 3 (Severe).

A correlation technique was used to explore the continual ATC tasks sessions on visual fatigue (SSQ) and other dependent variables: visual response variables (pupil dilation saccades, residence time, and fixation) and hemodynamic response variables (oxygenation and deoxygenation hemoglobin). The correlation model explored here is to determine the linear relationship between SSQ variables and the other variables namely, the visual and hemodynamic responses. A correlation technique was used with SAS.

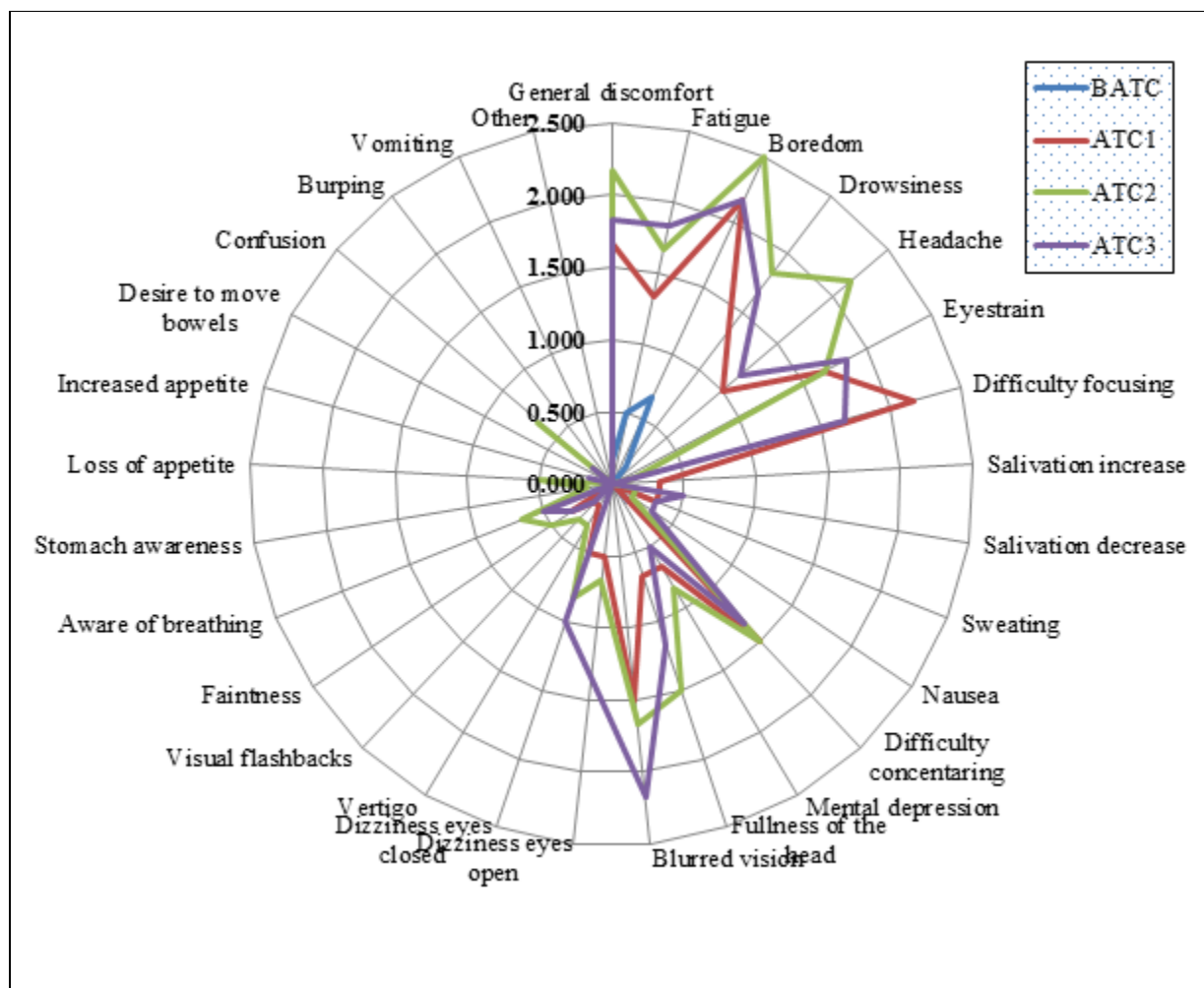


Figure 29. A radial plot of SSQ symptoms ratings on ATC task sessions.

The correlation analysis revealed the SSQ responses were statistically significant. Pearson correlation coefficients statistics ( $r$ ) for the degree of linear association between two variables were: (SSQ and maximum pupil diameter,  $r = 0.9125$ ,  $p < 0.05$ ), (SSQ and minimum pupil diameter,  $r = 0.5826$ ,  $p < 0.05$ ), (SSQ and fixation,  $r = 0.6061$ ,  $p < 0.05$ ), SSQ and saccade,  $r = 0.759$ ,  $p < 0.05$ ), (SSQ and Oxygenation hemoglobin at left dorsolateral prefrontal cortex,  $r = 0.7179$ ,  $p < 0.05$ ), (SSQ and Oxygenation hemoglobin at right dorsolateral prefrontal cortex,  $r = 0.3107$ ,  $p < 0.05$ ), (SSQ and de-oxygenation hemoglobin at left dorsolateral prefrontal cortex,  $r = 0.79442$ ,  $p < 0.05$ ), (SSQ and de-oxygenation hemoglobin at right dorsolateral prefrontal

cortex,  $r = 0.70927$ ,  $p < 0.05$ ). Generally, as SSQ ratings increased, the other variables such as visual response variables and hemodynamic response also increased. The pair with the strongest correlation with visual fatigue was maximum pupil diameter. The descriptive statistics for hemodynamics response are shown in Figure 30, and the visual response is shown in Table 20. Figure 31 shows the relationship between hemodynamic changes and the response times for one subject across all channels. Essentially, the response time measure indicates the time needed to make some judgments on visual task.

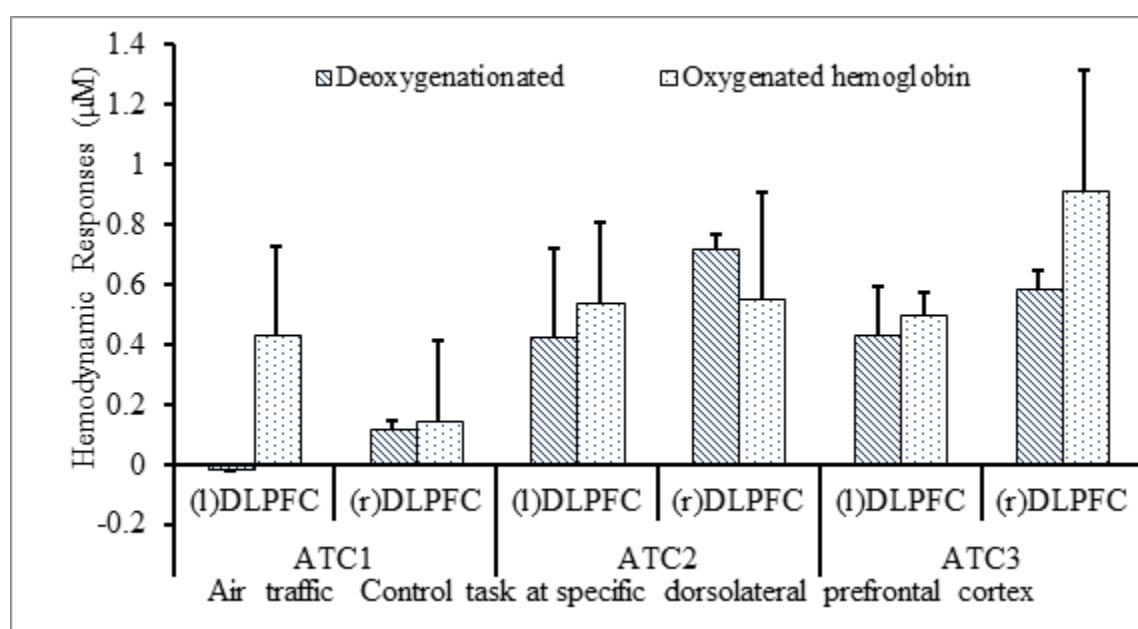


Figure 30. Bar plot of mean changes in oxygenated hemoglobin and deoxygenated hemoglobin.

Table 20

*Descriptive Statistics for the Visual Responses*

ATC task	Pupil diameter (mm)				Residence Time (sec)		Average Saccade (deg/sec)	
	Maximum dilation		Minimum Dilation					
	<i>M</i>	<i>(SD)</i>	<i>M</i>	<i>(SD)</i>	<i>M</i>	<i>(SD)</i>	<i>M</i>	<i>(SD)</i>
ATC 1	0.732	(0.063)	0.032	(0.008)	0.035	(0.009)	0.172	(0.120)
ATC 2	0.916	(0.005)	0.058	(0.015)	0.092	(0.032)	0.603	(0.131)
ATC 3	0.831	(0.119)	0.055	(0.019)	0.624	(0.176)	0.404	(0.206)

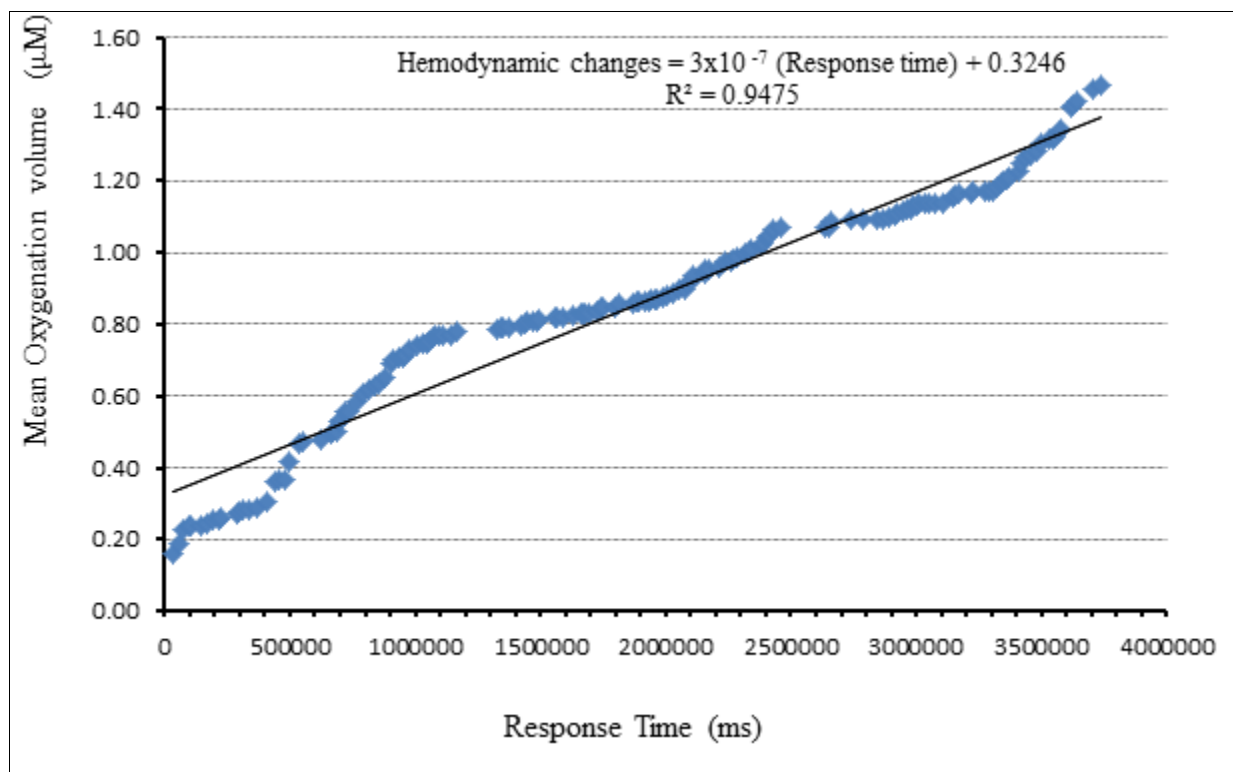


Figure 31. Mean hemodynamic changes with response time for an individual.

As explained by Zelinsky and Sheinberg (1995), the longer the response time, the more difficult the tasks. Deducing from Figure 31, the response time is positively correlated to oxygenation levels. This may be attributed to experimental task difficulty which has the high cognitive workload with (9 planes to monitor) and aircraft separation type (combined vertical and horizontal separation or none).

In the visual response analysis, the visual response variables were maximum and minimum pupil diameters, average saccade and the mean resident time (fixate). The changes of mean maximum and minimum pupil diameters with ATC task periods are shown in Figure 32.

Both measures tended to decrease with the amount of time a subject was engaged in the ATC task. The mean maximum pupil dilation at 20-min (ATC1), 40-min (ATC 2) and 60-min (ATC 3) were 0.932 mm, 0.994 mm, and 0.664 mm, respectively.

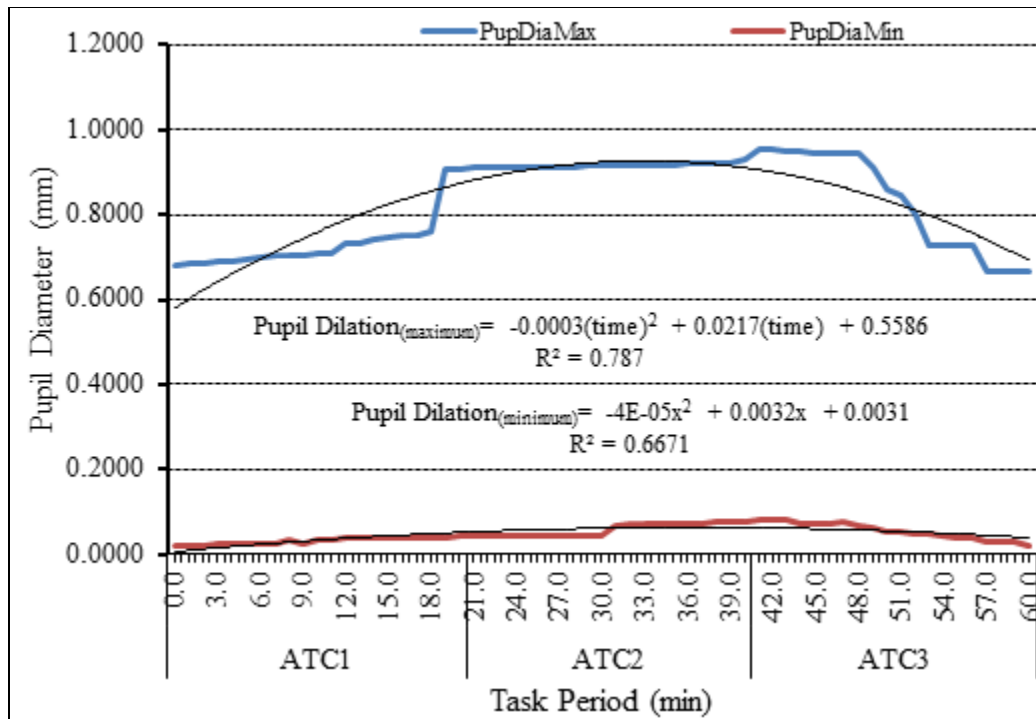


Figure 32. Change of mean maximum and minimum pupil diameters with ATC task sessions.

The corresponding parabolic equation with a correction coefficient of  $R^2$  as 0.787 as follows:

$$\text{Pupil Dilation}_{(\text{maximum})} = -0.0003 * (\text{time})^2 + 0.0217 * (\text{time}) + 0.5586 \quad (11)$$

Similarly, the mean minimum pupil dilation for time stamps of 20-min (ATC1), 40-min (ATC2), and 60-min (ATC3) were 0.022mm, 0.045mm and 0.005mm, respectively. The parabolic equation with  $R^2$  value of 0.6671 as follows:

$$\text{Pupil Dilation}_{(\text{minimum})} = -4 \times 10^{-5} * (\text{time})^2 + 0.0032 * (\text{time}) + 0.0031 \quad (12)$$

By using differential calculus, the inflection point of equations 11 and 12 indicates, theoretically that, the maximum eye pupil dilation occurs at 0.95mm at about 36.2min which is toward the end of ATC 2. The dilation stayed constant for about 11.58 min until the end of 48 min from which the dilation decreases. For example, the maximum dilation from equation 11 was obtained by taking the first derivative and setting to zero and solving to obtain the time as  $0.0217/0.0006 = 36.2\text{min}$ . The on-set of visual fatigue is noted to occur during ACT2 task.

Between 42 to 48 minutes, the eyes tried to adjust for increased workload at ACT3 tasks by over-extensive dilation. After this point, eye dilations decrease to seek for the normal physiologic states. The average saccadic movements are plotted in Figure 33. As shown in the figure, there was noticeable increase in the eye movements from 6-min mark to 0.7513 deg/sec at about 41-min, and then steeply decreases to 0.3005 deg/sec at 51 minutes mark. The predicted parabolic equation for the average saccadic movement with  $R^2 = 0.814$  as follows:

$$\text{Average Eye Saccade} = -0.0007 * (\text{time})^2 + 0.0472 * (\text{time}) - 0.220 \quad (13)$$

From equation 13, it was determined that the theoretical maximum point saccadic rest is 0.575 deg/sec at about 33.71min, which also occurred towards the end of ATC 2. After the average saccade rest time of 33.71min (at eye saccades speed of 0.575deg/sec), saccade speeds tended to decrease as a possible result of fatigue on-set.

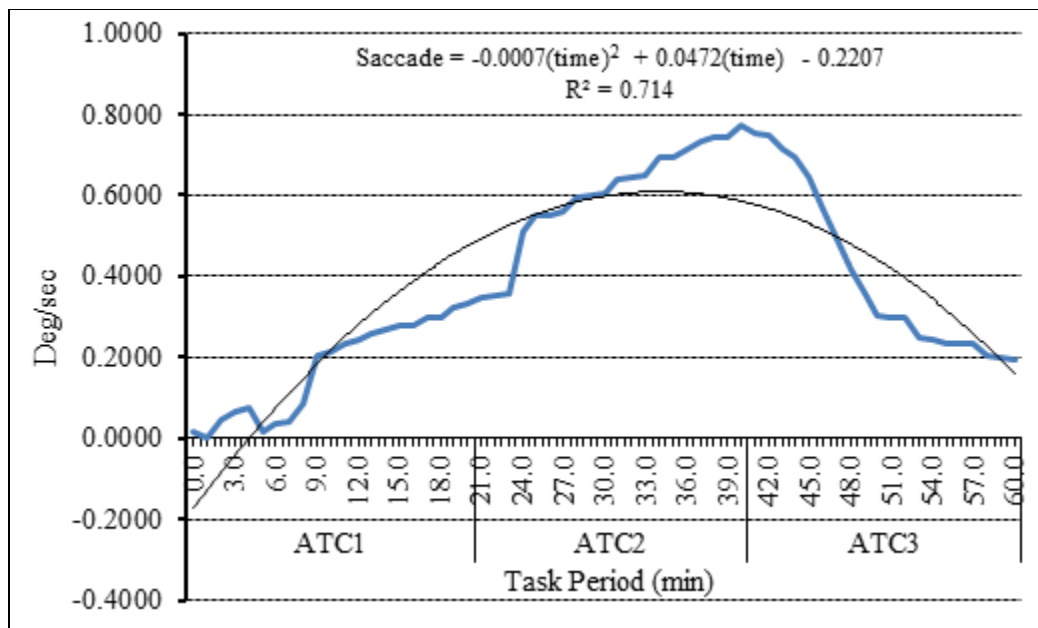


Figure 33. Change of mean saccade with ATC task sessions.

After the 33.71min point, saccadic movements begin to decrease rapidly to a 2.0098 deg/sec in about 16.53min which occurs during ATC 3. To obtain the time for point of inflection,

first derivative was taken in equation 13 and set it to zero, and solving yields  $0.0472/0.0014 = 33.71\text{min}$ . The decrease in saccade activities points to the likelihoods of visual fatigues.

The mean residence time (also known as fixation time) is the time in seconds for the eye to fixate on a particular section of stimuli. The mean fixation time changes are shown in Figure 34. The parabolic equation for the average saccadic movement with  $R^2 = 0.7677$  is:

$$\text{Residence Time} = -0.0005 * (\text{time})^2 + 0.0144 * (\text{time}) - 0.1092 \quad (14)$$

As shown in Figure 34, eye fixation time increases gradually as the workload increases from ACT1 to ACT3. The optimal rise in fixation starts to show evidence at 14.4minutes. The suspected onset of visual fatigue was noticed to occur between 30 to 39 minutes during ACT2 tasks and increased steadily thereafter.

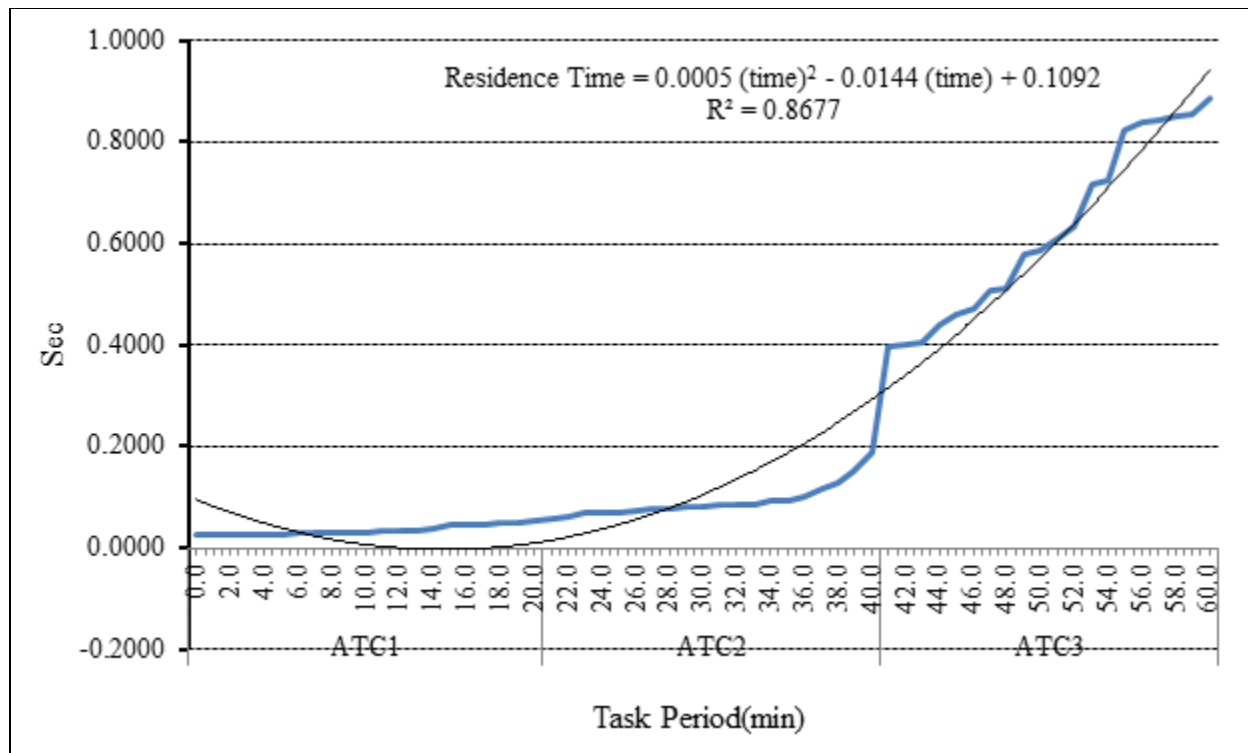


Figure 34. Mean fixation changes with ATC task sessions.

This result simply means that the eyes stayed fixed at particular information for longer time than they did before workload increase, and the subsequent experience of visual fatigue.

Table 21 summarizes the physiological response characteristics related to on-set visual fatigue. A sample eye movement for each ATC task is shown in Figure 35.

Table 21

*Physiological Response Characteristics Related to Onset Visual Fatigue*

Visual responses	Suspected time for onset of visual fatigue	Physiological indicator
Pupil dilation	36.2-40.0 min, Avg = 38.1 min	0.95mm
Mean saccadic speed	33.71 min	0.575°/sec
Mean eye fixation time	30-39 min (experienced workload rise time of 14.4min)	0.005sec

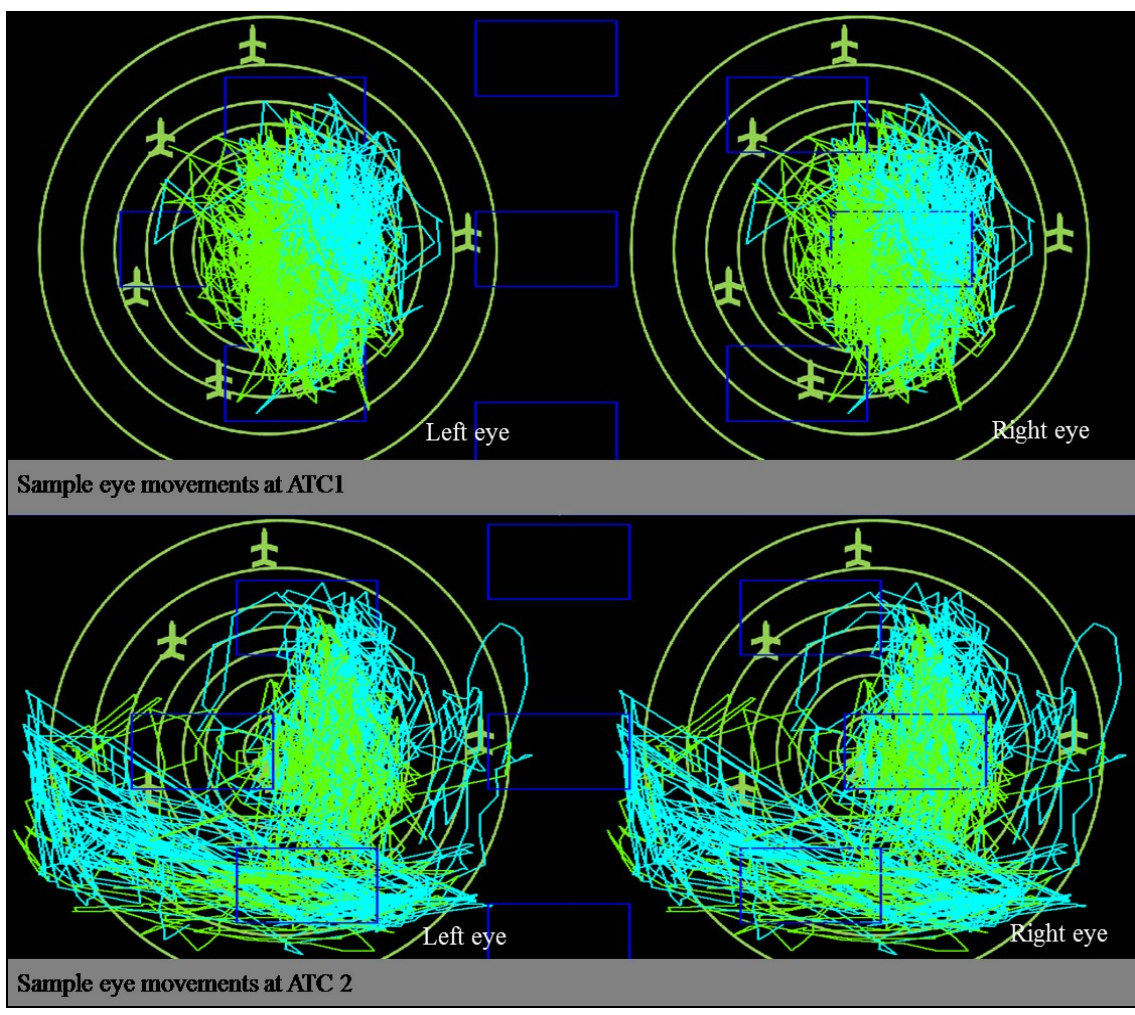


Figure 35. Sample eye movements at ATC task sessions.

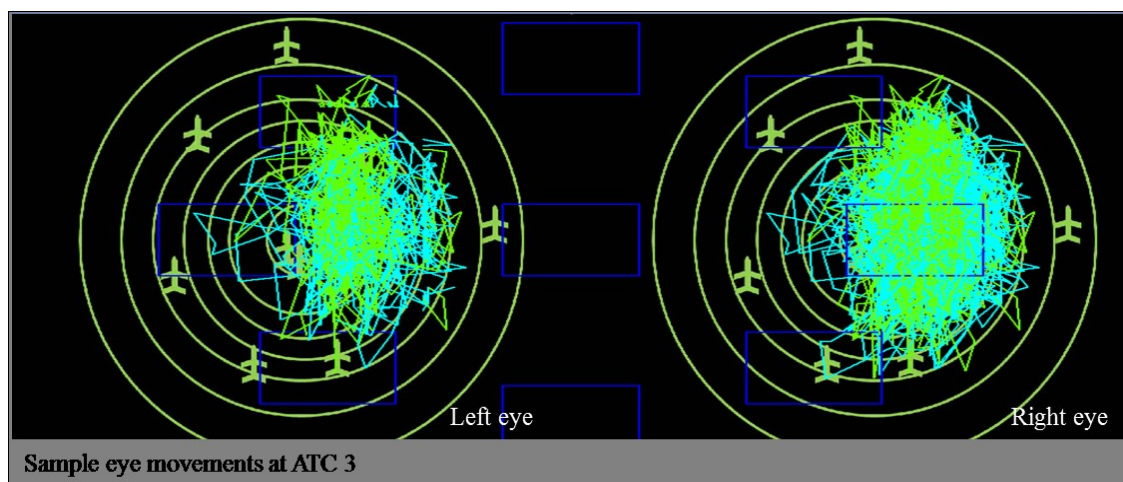


Figure 35. (cont.)

Theoretically, a sluggish period occurs at 14.4 min with 0.005 sec residence time before a rapid jump due to perceived visual fatigue on-set at 30 min. This effect was realized at about 46-52min mark. As asserted by Wolverton and Zola (1983), during high velocity of saccade no useful information is acquired, but rather information is usually acquired during fixation. Thus, during ATC2, where the longest fixation occurred, may have been attributed to two main reasons: (1) participants take time to process the visual tasks and (2) the occurrence of visual fatigue inhibits the information process. These effects are cumulative in the slow response time. Characteristically, the onset of visual fatigue may induce changes in oculomotor variables, such as increase in fixation duration, decrease in saccade length, and larger pupil dilations. Measures of hemodynamic changes were used to study energy expenditures during visual activities. There was energy requirement to perform the cognitive task as a possible compensation for the period on visual fatigue onset. As speculated by Uetake, Murata, Otsuka, and Takasawa (2000), visual fatigue is induced during a visual display task lasting about one hour. Cognitive-induced time compensation changes with corresponding effect in real-time brain activity have been reported during performance of visual activation (Gratton, Corballis, Cho,

Fabiani, & Hood, 1995; Kato, Kamei, Takashima, & Ozaki, 1993; Villringer, Planck, Hock, Schleinkofer, & Dirnagl, 1993), motor activity (Hirth, Obrig, Villringer, Thiel, Bernarding, Muhlnickel, Flor, Dirnagl & Villringer, 1996; Obrig, Hirth, Junge-Hulsing, Doge, Wolf, Dirnagl, & Villringer, 1996), cognitive tasks (Son, Guhe, Gray, Yazici, & Schoelles, 2005). More specifically, there is a positive correlation between the increase of oxygenated blood flow and the increase in cognitive activities (Izzetoglu, 2004). Table 22 is the summary of correlation analyses between Visual Fatigue (SSQ) and other response variables and Table 23 22 is the summary of hypotheses.

Table 22

*Summary of Correlation Analyses of Visual Fatigue (SSQ) with Visual Responses and Hemodynamic Responses*

	Correlation Analyses
Input variables	SSQ, maximum pupil diameter, minimum pupil diameter, fixation, saccade, Oxygenation hemoglobin, de-oxygenation hemoglobin
Output	<ul style="list-style-type: none"> <li>a. SSQ and maximum pupil diameter, <math>r = 0.9125, p &lt; 0.05</math></li> <li>b. SSQ and minimum pupil diameter, <math>r = 0.5826, p &lt; 0.05</math></li> <li>c. SSQ and fixation, <math>r = 0.6061, p &lt; 0.05</math></li> <li>d. SSQ and saccade, <math>r = 0.759, p &lt; 0.05</math></li> <li>e. SSQ and Oxygenation hemoglobin at left dorsolateral prefrontal cortex, <math>r = 0.7179, p &lt; 0.05</math></li> <li>f. SSQ and Oxygenation hemoglobin at right dorsolateral prefrontal cortex, <math>r = 0.3107, p &lt; 0.05</math></li> <li>g. SSQ and de-oxygenation hemoglobin at left dorsolateral prefrontal cortex, <math>r = 0.79442, p &lt; 0.05</math></li> <li>h. SSQ and de-oxygenation hemoglobin at right dorsolateral prefrontal cortex, <math>r = 0.70927, p &lt; 0.05</math></li> </ul>

Table 23

*Summary of Major Findings from Hypotheses in Study II*

<p>Hypothesis 2.1: A prolonged use of stereoscopic display does not cause visual fatigue.</p>	
Dependent variable:	SSQ
Independent variable	BATC and ATC 3
Outcome	Yes, at 0.05 level of significance a prolonged use of stereoscopic display is likely to cause visual fatigue, $t(7) = -11.19, p < 0.05$ .
<p>Hypothesis 2.2: A prolonged use of stereoscopic display has no effects on response time.</p>	
Dependent Variable	Response time
Independent variable	ATC1 and ATC 3
Outcome	Yes, at 0.05 level of significance a prolonged use of a stereoscopic display to cause visual fatigue, $t(7) = 3.16, p < 0.05$
<p>Hypothesis 2.4: H<sub>0</sub>: The level of task difficulty has no effects on response time. H<sub>a</sub>: The level of task difficulty has effect on response time.</p>	
Dependent variable:	Response time
Independent variable	Task difficulty
Outcome	Yes, at 0.05 significant level, there was enough evidence to conclude that a significant main effect for task difficulty on response time, $F(3, 58) = 266.44, p < 0.05$ .
<p>Hypothesis 2.3 H<sub>0</sub>: There is no interaction between cognitive loading and task difficulty on response time. H<sub>a</sub>: There is interaction between cognitive loading and task difficulty on response time.</p>	
Dependent Variable	Response time
Independent variable	Cognitive loading and task difficulty

Table 23

*(cont.)*

Outcome	Yes, at 0.05 significant level, there was evidence to conclude that a significant interaction between task difficulty and the cognitive load response variable on response time during visual task of air traffic control task $F(2.32, 20.84) = 134.91, p < 0.05$ .
<p>Hypothesis 2.5.2: Simple main effect on task difficulty</p> <p><math>H_0</math>: there is no simple main effect for task difficulty when cognitive loading low (high).</p> <p><math>H_a</math>: there is simple main effect for task difficulty when cognitive loading is low (high).</p>	
Dependent variable:	Response time
Independent variable	Task difficulty
Outcome	Yes, at 0.05 level of significance, there is not enough evidence to conclude that there is a significant simple main effect for task difficulty when cognitive loading was low. However, there was enough evidence to conclude that there is a significant simple main effect for task difficulty when the cognitive loading was high, $F(3, 47) = 3.58, p < 0.05$

## CHAPTER 6

### Visual Fatigue Classification with a Neural Network Algorithm

In this chapter, a neural network classifier is used to analyze both the neurophysiological data and subjective rating of visual fatigue. Bartlett (1953) noted that visual fatigue arises from; (i) the attempt to inhibit certain inclinations inherent in the visual mechanism, or (ii) visual attempts on contradictory actions. Methods for measuring either cause have been subject to debate. For example, the existing approaches do not include all the neurophysiological signals and objective classification of visual fatigue factors. The data is analyzed with a feed forward neural network (FF-ANN) so as to combine the objective metrics from neurophysiology signals and subjective perceptual data from simulated sickness questionnaires (SSQ) measures. The purpose is to conduct a meta-analysis using the cognitive loading variables.

#### 6.1 Neurophysiological Basis of Visual Fatigue

Neurophysiological signals have been used to measure mental workload (Ayaz et al., 2012; Kramer et al., 1996; Wilson & Russell, 2003). This is because the measured event related potentials can capture biological signals that have high correlation with sensory muscles (Baldwin & Coyne, 2005; Baldwin & Penaranda, 2012). Electroencephalogram (EEG) is the most common technique for obtaining information on neurophysiological signals that relate the brain to other skeleton-muscular activities. Event-Related Potential (ERP) is a method that measures electrical activity that is specifically related to an event (for example, a sensory stimulus or a cognitive task). High frequency bands such as beta frequencies (i.e. frequencies between 12Hz and 30 Hz) from ERPs are known to measure stressful conditions while low band frequencies are observed to capture attention during task processing. Under stress, attention focus is known to degrade. This situation is best captured by a P300 component, an ERP

component reflecting neuronal resources for paying attention and delays (Li et al., 2008). Li et al. (2008) used the ERP to examine whether the analysis of background EEG (specifically high frequency bands, such as beta band) and P300 ERP component could reveal 3D visual fatigue.

The visual system is a well-developed sensory organ that involves effortless complex interaction between the visual organ and the brain. It involves physiological and a series of hierarchical neural processes from the photoreceptors, retinal ganglion cells, the lateral geniculate nuclei (LGN) of the thalamus, and the visual cortices (DeAngelis, 2000). Malmivuo and Plonsey (1995) estimated that about 50% of the cerebral cortex is involved in visual processing.

The physiological changes of visual fatigue are well established. For example, increased eye blink rates have long been seen as evidence of visual fatigue (Veltman, 1996; Zhu & Ji, 2004a), as have been fixation covary with changes in performance because of drowsiness, loss of vigilance, increasing time-on-task, and visual discomfort (McGregor & Stern, 1996; Van Orden et al., 2000), decrease in eye pupillary aperture to stimuli (Granholm & Steinhauer, 2004), decreased saccade as an indication of alertness during visual task (Kornylo et al., 2003; Pavlas et al., 2012).

The neural bases of eye response to stress, with exception of electrophysiology, have not been investigated thoroughly. Carandini (2000) asserted that visual fatigue in the cerebral cortex encompasses more complex features. According to Carandini (2000), a prolong visual response to stimulation can lead to fatigue of the neurons that respond most strongly and frequently. Established physiological evidence in primates show that after a few seconds of stimulation to a high-contrast stimulus, neurons in the primary visual cortex (V1) give a weaker response than they would to a low-contrast stimulus (Pollen, 1999).

Sanchez-Vives, Nowak, and McCormick (2000) made a strong case that the cortical form of visual fatigue is partly cellular. They observed that visual fatigue involves the hyperpolarization of cortical neurons. The cause of this hyperpolarization could potentially involve changes in the activity of other neurons in the network or in the efficacy of synapses, or the action of some intrinsic cellular mechanism. Beyond the cortical neuronal fatigue, visual fatigue can also prompt a neurological state in the central nervous system (CNS) which is controlled by a myriad of neurons between the brain and spinal cord when an external stimulus is present (Murata, Araki, Kawakami, Saito, & Hino, 1991). For example, ocular motor responses such as accommodation and convergences are triggered by pupillary mechanisms which are controlled by the brain and autonomic nervous system (Ukai & Howarth, 2008; Ukai & Kato, 2002). Murata et al. (1991) observed that VDT work is associated with impairment of the visual nervous system function, that VEP latencies appear to be a sensitive indicator of visual fatigue, at least transiently, and that critical flicker fusion (CFF) appears to be a good parameter for estimations of severe visual fatigue. Li et al. (2008) used “3D oddball paradigm” with background EEG signals to study visual fatigue. The result revealed the effect of binocular parallax and presentation duration on 3D visual fatigue.

## **6.2 A Neural Network Approach**

A classification procedure seeks a functional relationship between the group membership and the features of the objects of interest (Zhang, 2000). Trejo et al. (2005b) classified single EEG epochs using kernel partial least squares decomposition (KPLS) of multichannel EEG spectra coupled with a discrete-output linear regression (DLR) classifier. There are also a group of nonlinear classifiers used to model neural networks for classification tasks. Usually, nonlinear classifiers assign feature vectors to a normative class based on high likelihood scores or the

highest probability (Duda, Hart, & Stork, 2001). Many statistical-based classifiers are accurate for single treatments, but fail to handle multidimensional data which depend on the power of concurrency and robustness in speed processing. Neural networks can provide nonlinear models, which make them flexible in modeling real world complex situations (Ge & Wang, 2004; Huang & Lewis, 2003) - specifically, applications of artificial neural networks to analyze EEG studies for workload classification (Baldwin & Penaranda, 2012; Wilson, Esteppe, & Davis, 2009; Wilson, Russell, Monnin, Esteppe, & Christensen, 2010; Wilson & Russell, 2003).

Classification is one of the most frequently encountered decision making tasks of human activity. A classification problem occurs when an object needs a predefined group or class based on attributes related to that object (Zhang, 2000). The advantage of neural networks for classification tasks lies in the following theoretical aspects: First, neural networks are data driven self-adaptive methods in that they can adjust themselves to the data without any explicit specification of functional or distributional form for the underlying model. Second, neural networks can approximate any function with arbitrary accuracy (Cybenko, 1989; Hornik, 1991; Hornik, Stinchcombe, & White, 1989). Finally, neural networks are able to estimate the posterior probabilities, which provide the basis for establishing classification rules and performing statistical analysis. A neural network model with SSQ can provide a robust classification approach for identifying time periods for on-sets of visual fatigue. The purpose of the study is to classify visual fatigue symptoms based on a set of neurophysiological signals and SSQ data.

### **6.3 Selection of the Classification Neural Network Model**

The database is multidimensional consisting of pupil dilation, eye fixate, saccade, blood volume, oxygenation, delta, theta, alpha, beta, gamma. SSQ data represent the subjective measures. These multi-attribute, multidimensional data obviously pose some problems for

multivariate statistical analysis. Artificial neural networks are computational and mathematical systems whose architecture and operation are inspired from the knowledge about biological neural cells (neurons) in the brain. EEG and hemodynamics data collected for our analyses fit the use of a neural network for the classification. A back-propagation feed forward artificial neural network (FF-ANN) was used for the analysis. A back-propagation network simply calculates the gradient of the network; that is the first derivative of the weights in the network and the error signals are propagated backward through the network on a layer-by-layer basis (Kuschewski, Hui, & Zak, 1993).

A three-layer neural network was created with thirteen nodes in the first (input) layer, seven in the hidden layer, and four nodes as the output layer (representing SSQ). To determine the optimal hidden neurons, the lower and upper bounds were determined to be between the number neurons for input and output layers as formulated by (Heaton, 2008; Masters, 1993). To avoid possible over fitting or under fitting the data, the number of nodes in the hidden layer was varied between five and ten during treatment runs to determine the optimal number of hidden nodes as depicted in Figure 36. Due to hardware limitations, seven nodes in the hidden layer were selected to run the final simulation.

As shown in Figure 36, the mean square error plot shows the achieved error value with the best performance at 26 epochs. Further, as revealed in Figure 37, the lowest value of mean square error occurred when seven hidden neurons were used. This indicates that lower mean values have a less probability of false prediction (Ayub & Saini, 2010). For most applications of FF-ANNs, one hidden layer is enough (Boeree, 2006). However, for naturally occurring events such as human behaviors with nonlinear physical relationships, neural network models are very successful.

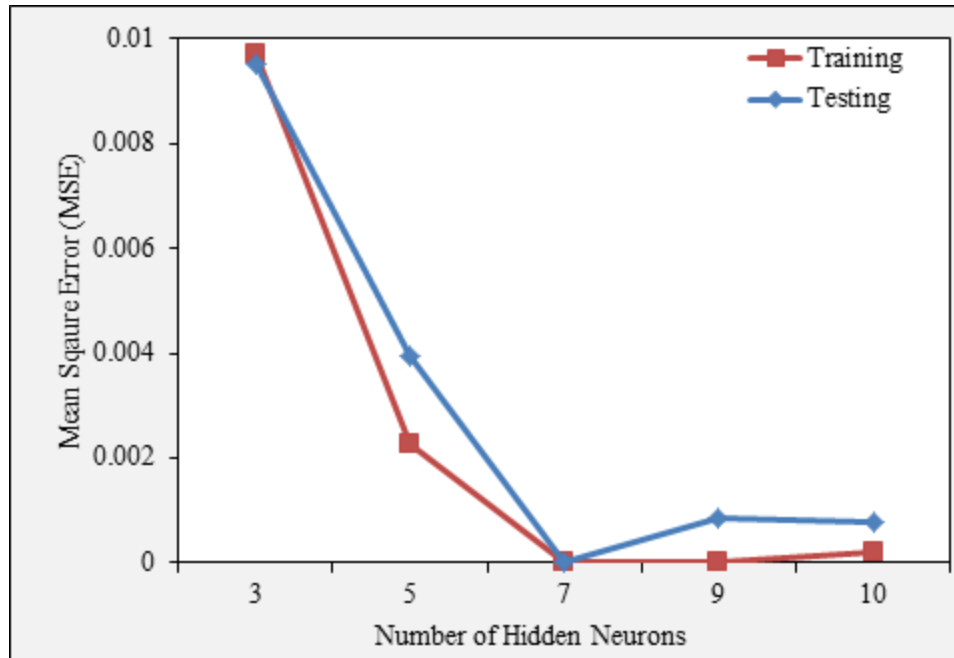


Figure 36. Effects of hidden neuron counts on mean square error with testing and training sets of size 108.

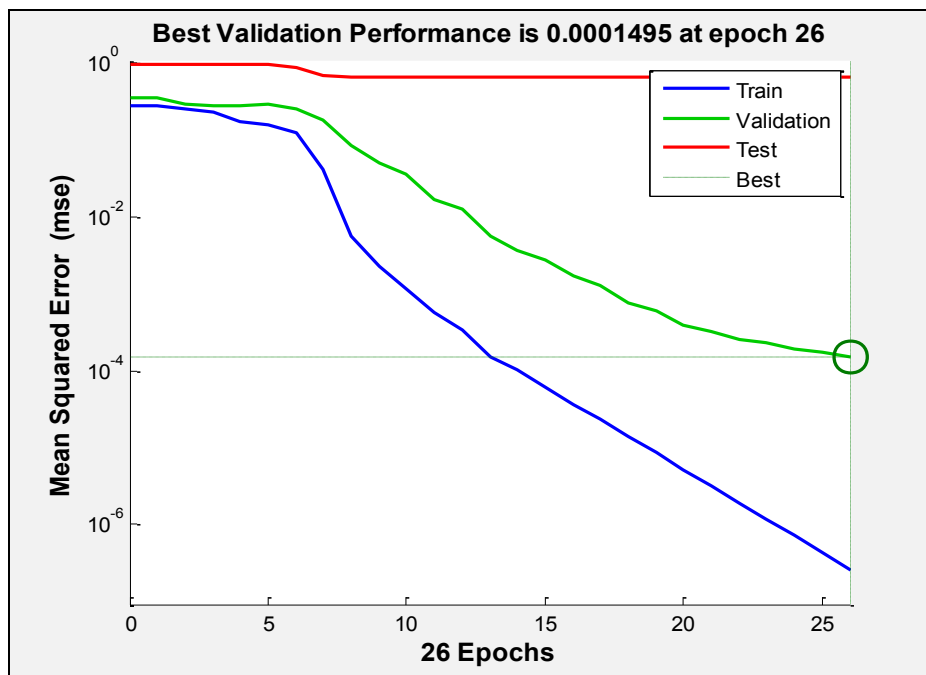


Figure 37. Mean square error verse number of epoch plot for feed forward neural network with piecewise linear function.

Thus, FF-ANN model variants have been used to model a variety of biological and environmental processes (Angelucci & Bullier, 2003; Bullier, Hupé, James, & Girard, 2001; Lamme, Supèr, Landman, Roelfsema, & Spekreijse, 2000; Lee et al., 2010; Levitt & Lund, 2002; López-Aranda et al., 2009; Qiu & Von Der Heydt, 2005; Saksida, 2009). As shown in Figure 38 the connections (synapses)  $w_{ij}$  transfer each neurophysiologic signal (stimulus)  $X_i$  into the neuron.  $W_i$  can be interpreted as a weight representing the “importance” of that specific input  $X_i$ . Inside the neuron, the sum of the weighted inputs  $w_i X_i$  is taken. Given that this sum is greater than an externally applied threshold  $\Psi(x)$ , the neuron emits an output - say  $Z$  - for visual fatigue classifications.

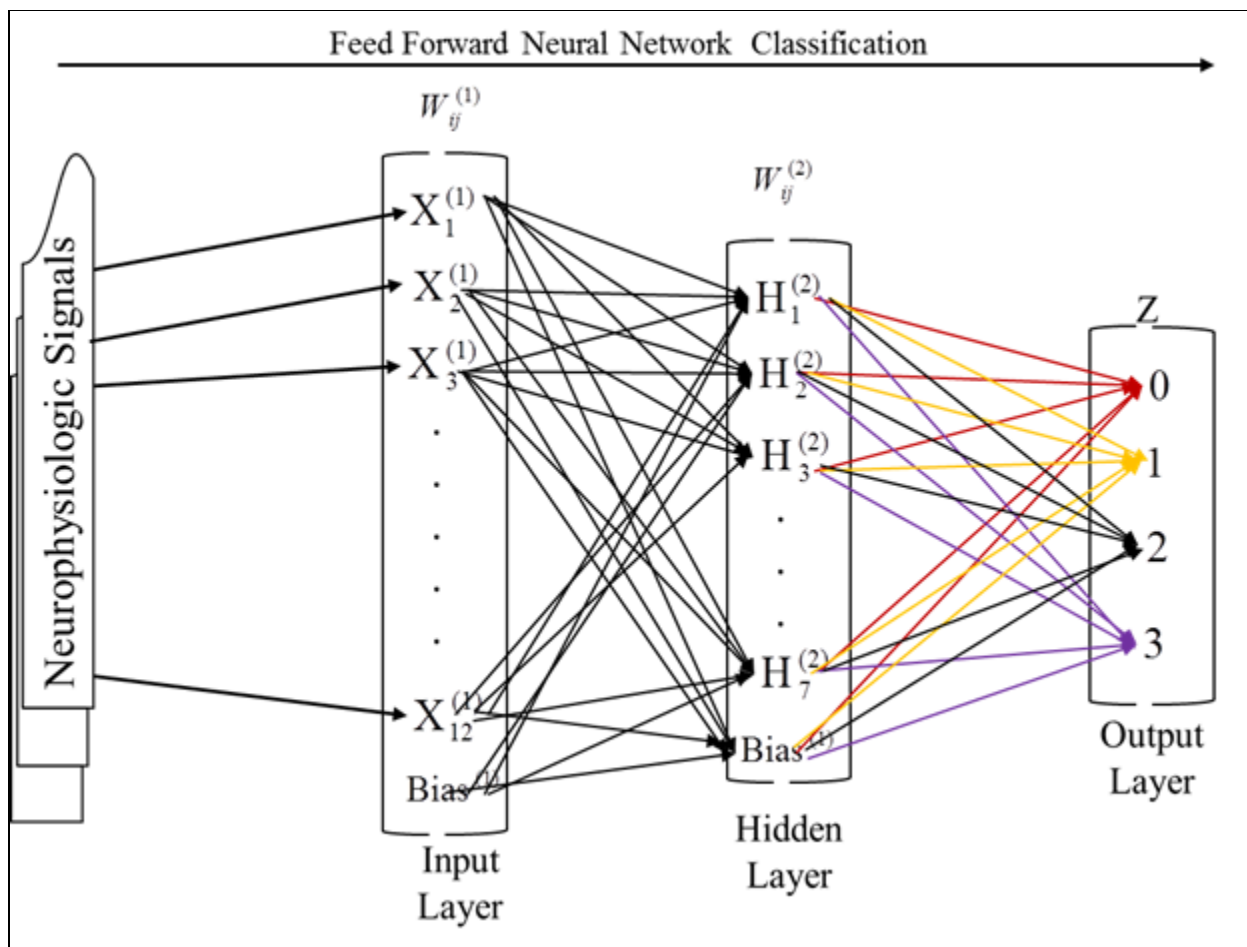


Figure 38. Feed forward neural network with piecewise linear function.

**6.3.1 Preparing data for analysis.** The input and output dataset were partitioned by assigning 70% for training, 15% for validating, and 15% for testing. The training/validation approach was randomly sampled using a greedy scaled conjugate gradient (SCG) algorithm (Orozco & Garcia, 2003). The SCG uses a quadratic approximation to the error in the neighborhood of a point (target; Møller, 1993; Orozco & Garcia, 2003).

It also has the advantage of avoiding a time consuming line-search per learning iteration, which makes the algorithm faster than other second order algorithms (Orozco & Garcia, 2003). The software Network Toolbox in MATLAB (R2011a version 7.12.0.635) was used for implementation. An optimal trained neural network is obtained when the minimum gradient is reached. Table 24 below shows the various signal types, origin, and the organs involved in the study. The role of each variable for the model formulation is described in Table 25. There are twelve inputs as independent variables (IV) and one variable as dependent variable (DV). The FF-ANN is used to classify the data on a scale between 0 and 3 as specified by SSQ using the piecewise linear activation functions in equation 15.

$$Z = \begin{cases} 3 & 2 < x \leq 3 \\ 2 & 1 < x \leq 2 \\ 1 & 0 < x \leq 1 \\ 0 & x \leq 0 \end{cases} \quad (15)$$

Table 24

*Dataset Descriptions for the Model*

Neurophysiological Signal type	Signal Origin	Physiological Organ	Units
Saccade	Z800 <sup>®</sup> Eye tracker	Eye	Deg/sec
Fixate	Z800 <sup>®</sup> Eye tracker	Eye	Sec
Dilation	Z800 <sup>®</sup> Eye tracker	Eye	mm

Table 24

*(cont.)*

Neurophysiological Signal type	Signal Origin	Physiological Organ	Units
Delta	Biopac MP 150 EEG	Cerebral cortex	Hz
Theta	Biopac MP 150 EEG	Cerebral cortex	Hz
Alpha	Biopac MP 150 EEG	Cerebral cortex	Hz
Beta	Biopac MP 150 EEG	Cerebral cortex	Hz
Gamma	Biopac MP 150 EEG	Cerebral cortex	Hz
HbO <sub>2</sub>	Biopac COBI <sup>®</sup> fNIRS	Dorsolateral prefrontal	μM
Hbb	Biopac COBI <sup>®</sup> fNIRS	Dorsolateral prefrontal	μM
Oxygenation	Biopac COBI <sup>®</sup> fNIRS	Dorsolateral prefrontal	μM
Blood volume	Biopac COBI <sup>®</sup> fNIRS	Dorsolateral prefrontal	μM
SSQ response	SSQ	-	Ratings

Table 25

*Variables in the Model Formulation for the Neural Network. Note IV Means Input Variable and OV is the Output Variable for the Network*

Variables	Role	Unique values	Convert Binary?	Neural units	Neural Inputs	Neural Output
Bias	IV	1	No	1	X <sub>1</sub>	-
Saccade	IV	[0,∞)	No	1	X <sub>2</sub>	-
Fixate	IV	[0,∞)	No	1	X <sub>3</sub>	-
Dilation	IV	[0,∞)	No	1	X <sub>4</sub>	-
Delta	IV	[0-3.5]	No	1	X <sub>5</sub>	-
Theta	IV	[4-7]	No	1	X <sub>6</sub>	-
Alpha	IV	[8-12.5]	No	1	X <sub>7</sub>	-
Beta	IV	[13-35]	No	1	X <sub>8</sub>	-

Table 25

*(cont.)*

Variables	Role	Unique values	Convert Binary?	Neural units	Neural Inputs	Neural Output
Gamma	IV	[35-40]	No	1	X <sub>9</sub>	-
HbO <sub>2</sub>	IV	[0,∞)	No	1	X <sub>10</sub>	-
Hbb	IV	[0,∞)	No	1	X <sub>11</sub>	-
Oxygenation	IV	[0,∞)	No	1	X <sub>12</sub>	-
Blood volume	IV	[0,∞)	No	1	X <sub>13</sub>	-
SSQ response	OV	[0-3]	No	1	-	0,1,2,3

#### 6.4 Results and Discussions for Model-Based Visual Fatigue Classification

The FF-ANN used has a structure thirteen neurons at the input layer, seven at the hidden layer and four at the output layers for the classification. With large values of the learning coefficient and momentum, a network may go through large oscillations during training and may never converge. Smaller learning coefficient and momentum tend to create a more stable network but require a long training time. For a good compromise between training speed and network stability, the learning coefficient and momentum were selected in such a way that their values decreased with the increase of the training epoch. In the present work, the normalized root-mean-square (RMS) error of the output layer was used as a criterion to select these parameters. The selected learning coefficients and momenta correspond to the deepest slope of the normalized RMS error. Figure 38 shows the change in the RMS error during a training process. In order to enhance the generalization capability of the neural network, the training and the test sets are formed by data obtained from different signals. It was observed that for some EEG and fNIRS types, there were waveform variations among the vectors belonging to the same class.

The FF-ANN was trained to classify visual fatigue into none, slight, moderate, and severe classes for the combined experimental sessions. The first classification was done with all the physiological signals, and the second classification was done with EEG, fNIRS and eye tracking data separately. The classification accuracy was calculated by taking the number of correctly classified samples by the network divided by the total number of samples into the test dataset. The classification accuracy results from each FF-ANN for every visual fatigue ratings are presented in Table 26. Tables 27 to 33 provide the confusion matrix of the visual fatigue classifications for visual display task using the various data sources. The data in Table 24 suggest that, individually, eye movements (saccade and fixation data) are better predictors of visual fatigue classification and EEG data had the lowest score of 66.2% . Eye movement data combined with EEG and hemodynamics data can predict visual fatigue 86.8% and 84.9%, respectively.

Table 26

*Data Sources and FF-ANN Model Classification Accuracy for Visual Fatigue Ratings*

Data Sources	Classification accuracy
All data combined	78.40%
EEG data	66.20%
Hemodynamic data	68.30%
Eye movement (saccade & fixation data)	90.42%
EEG & Hemodynamic data	70.72%
EEG & Eye movement (saccade & Fixation data)	86.78%
Hemodynamic & Eye movement (saccade & Fixation data)	84.93%

Collectively, all the models performed well. The best and worst model accuracy performance for visual fatigue classification was visual response data and EEG, respectively. The model accuracy for all the dataset was between these two extremities. Thus, for one to

correctly classify visual fatigue, eye movements data is recommended. The multi-signal approached is worth adopting in classifying visual fatigue since it considers all the organs that are affected by the manifestations of visual fatigue.

Table 27

*Classification of Visual Fatigue Ratings Using All Data Combined*

SSQ Ratings Responses		Predicted Class				Accuracy
		None	Slight	Moderate	Severe	
Actual Class	None	<b>4.30%</b>	2.41%	2.02%	1.60%	
	Slight	1.04%	<b>28.30%</b>	1.90%	0.80%	
	Moderate	1.70%	1.96%	<b>35.20%</b>	2.90%	
	Severe	3.30%	2.14%	0.03%	<b>10.50%</b>	
Total						<b>78.40%</b>

Table 28

*Classification of Visual Fatigue Ratings Using Electroencephalogram (EEG) Data*

SSQ Ratings Responses		Predicted Class				Accuracy
		None	Slight	Moderate	Severe	
Actual Class	None	<b>1.90%</b>	2.41%	3.11%	4.10%	
	Slight	3.40%	<b>32.40%</b>	1.90%	2.96%	
	Moderate	3.63%	2.76%	<b>19.00%</b>	2.81%	
	Severe	2.10%	2.32%	2.30%	<b>12.90%</b>	
Total						<b>66.20%</b>

Table 29

*Classification of Visual Fatigue Ratings Using Saccade and Fixation Data*

SSQ Ratings Responses		Predicted Class				Accuracy
		None	Slight	Moderate	Severe	
Actual Class	None	<b>0.00%</b>	0.0%	0.0%	0.0%	
	Slight	0.00%	<b>27.90%</b>	1.06%	1.06%	
	Moderate	0.00%	1.96%	<b>51.09%</b>	2.54%	
	Severe	1.87%	0.0%	1.09%	<b>11.43%</b>	
Total						<b>90.42%</b>

Table 30

*Classification of Visual Fatigue Ratings Using Hemodynamic Response Variables*

SSQ Ratings Responses		Predicted Class				Accuracy
		None	Slight	Moderate	Severe	
Actual Class	None	<b>2.90%</b>	3.41%	2.98%	2.65%	
	Slight	3.54%	<b>26.70%</b>	1.96%	1.25%	
	Moderate	2.90%	2.93%	<b>21.90%</b>	2.74%	
	Severe	2.27%	2.98%	2.09%	<b>16.80%</b>	
Total						<b>68.30%</b>

Table 31

*Classification of Visual Fatigue Ratings Using Hemodynamic Response Variables and EEG*

*Data*

SSQ Ratings Responses		Predicted Class				Accuracy
		None	Slight	Moderate	Severe	
Actual Class	None	<b>5.90%</b>	3.23%	2.69%	0.93%	
	Slight	1.21%	<b>36.70%</b>	2.78%	2.61%	
	Moderate	2.13%	2.06%	<b>21.00%</b>	3.56%	
	Severe	1.16%	2.59%	4.33%	<b>7.12%</b>	
Total						<b>70.72%</b>

Table 32

*Classification of Visual Fatigue Ratings Using EEG Data and Eye Movements (Saccade and Fixation)*

SSQ Ratings Responses		Predicted Class				Accuracy
		None	Slight	Moderate	Severe	
Actual Class	None	<b>19.03%</b>	0.12%	0.87%	0.09%	
	Slight	1.63%	<b>35.30%</b>	1.09%	0.52%	
	Moderate	2.03%	1.60%	<b>24.78%</b>	1.05%	
	Severe	2.36%	0.62%	1.24%	<b>7.67%</b>	
Total						<b>86.78%</b>

Table 33

*Classification of Visual Fatigue Ratings Using Hemodynamic Response Variables and Eye Movements (Saccade and Fixation)*

SSQ Ratings Responses		Predicted Class				Accuracy
		None	Slight	Moderate	Severe	
Actual Class	None	<b>6.14%</b>	1.01%	1.24%	2.01%	
	Slight	0.15%	<b>29.50%</b>	2.61%	1.33%	
	Moderate	1.22%	0.00%	<b>37.59%</b>	1.00%	
	Severe	0.09%	1.86%	2.55%	<b>11.70%</b>	
Total						<b>84.93%</b>

**6.4.1 Sensitivity and specificity.** The plots of the Receiver Operator Characteristics (ROC) curves are shown in Figures 39 to 45. The plots are based on the overall a sensitivity of the model. Sensitivity as used here indicates the probability of the model correctly classifying a true occurrence of visual fatigue. Specificity is the probability that the true classification is correct—that is, the probability of true positive. The curve is a plot of true positive rate (sensitivity) versus false positive rate (1-specificity). A test with perfect discrimination (no overlap in the two distributions) has a ROC curve that passes through the upper left corner (100% sensitivity, 100% specificity; Zweig & Campbell, 1993). As shown in the plots, none of the model had 100% sensitivity and 100% specificity; however, the classification model performs well above average of sensitivity and specificity.

The diagonal line represents the strategy of random guessing of a class, and it indicates that the model has no information about the class to be classified (Fawcett, 2006). The neural network classifier randomly guessed the occurrence of visual fatigue rating class half of the time, and expected to get half of occurrence of visual fatigue ratings correct and half of the occurrence of visual fatigue ratings wrong. For the ROC curves below the diagonal line, the model has useful information, but it is applying the information incorrectly (Flach & Wu, 2003).

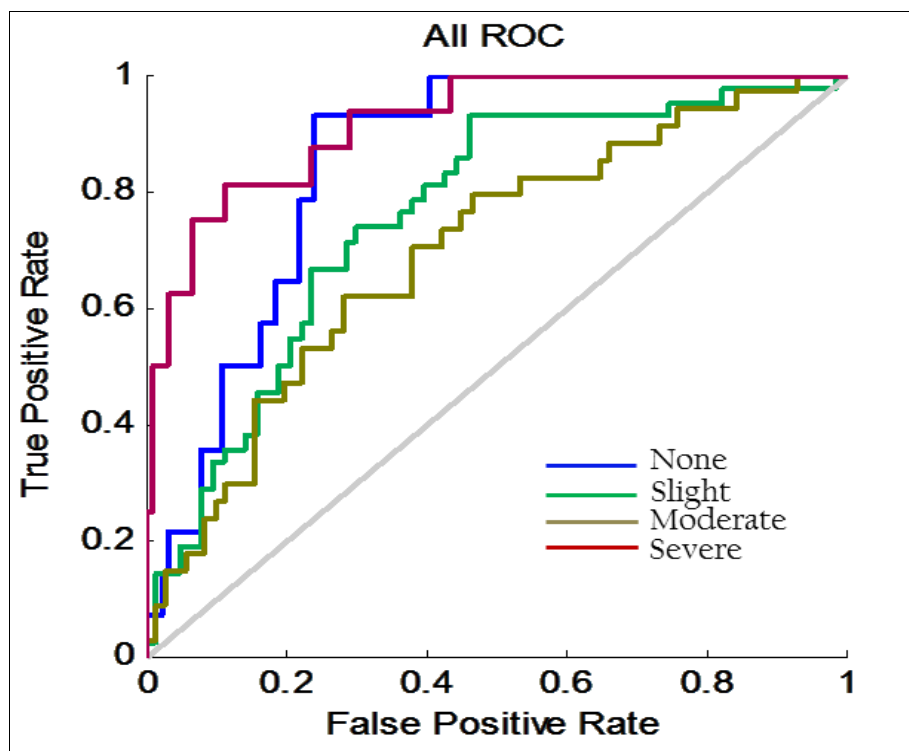


Figure 39. ROC curve for all data combined.

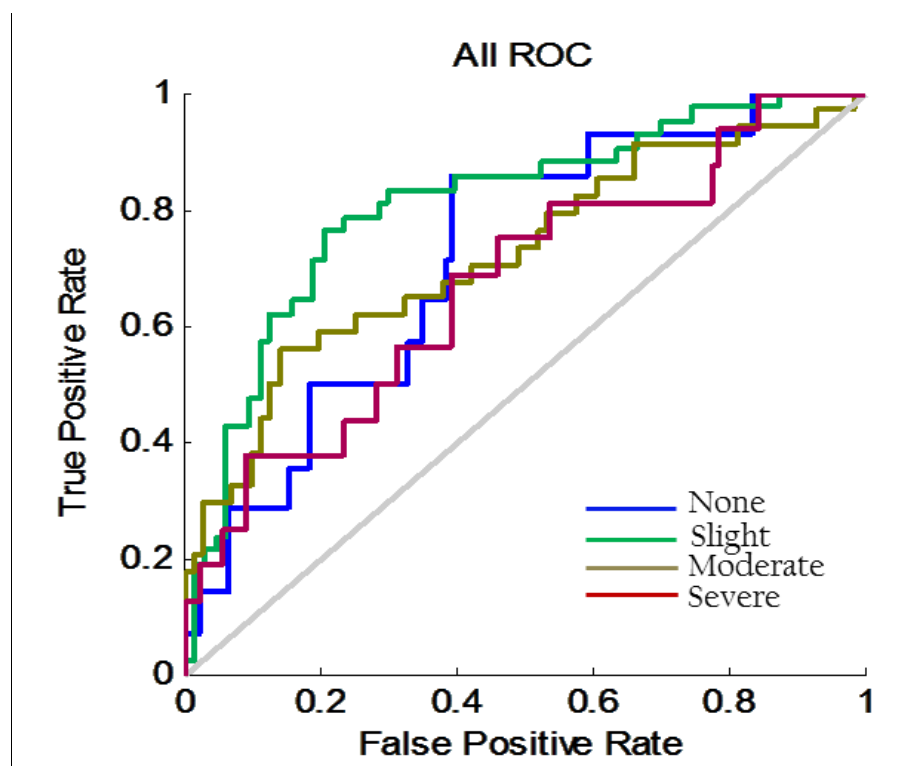


Figure 40. ROC curve for electroencephalogram (EEG) signals.

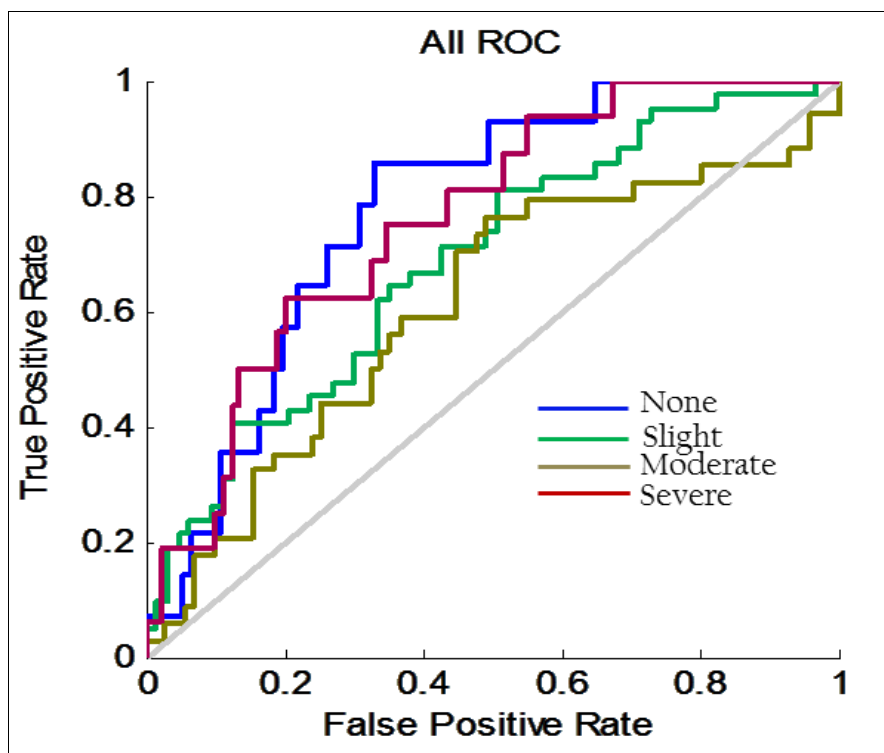


Figure 41. ROC curve for eye movement (saccade and fixation).

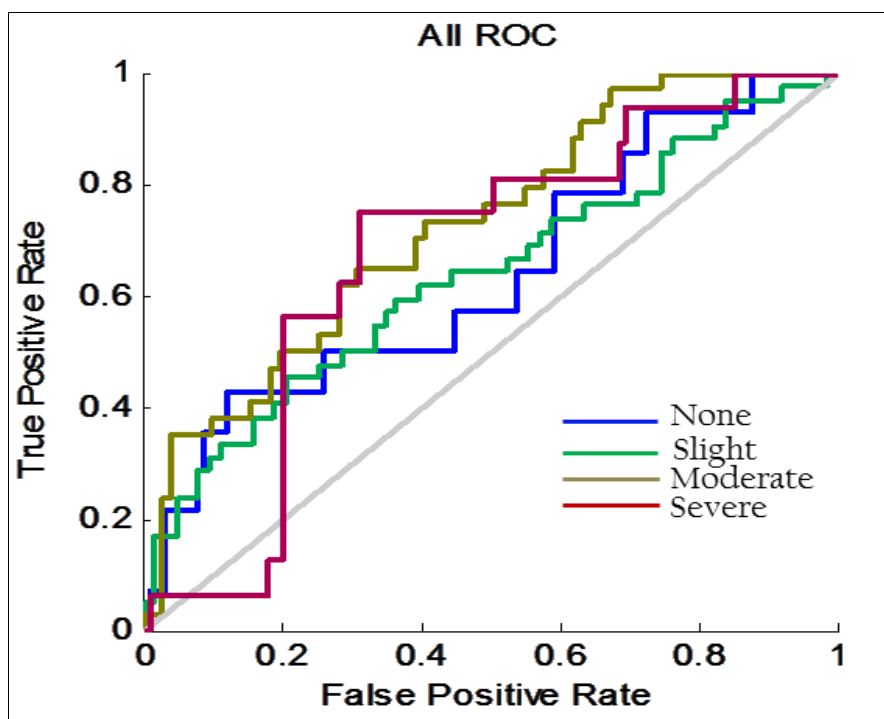


Figure 42. ROC curve for oxygenated and deoxygenated hemoglobin from the dorsolateral prefrontal cortex.

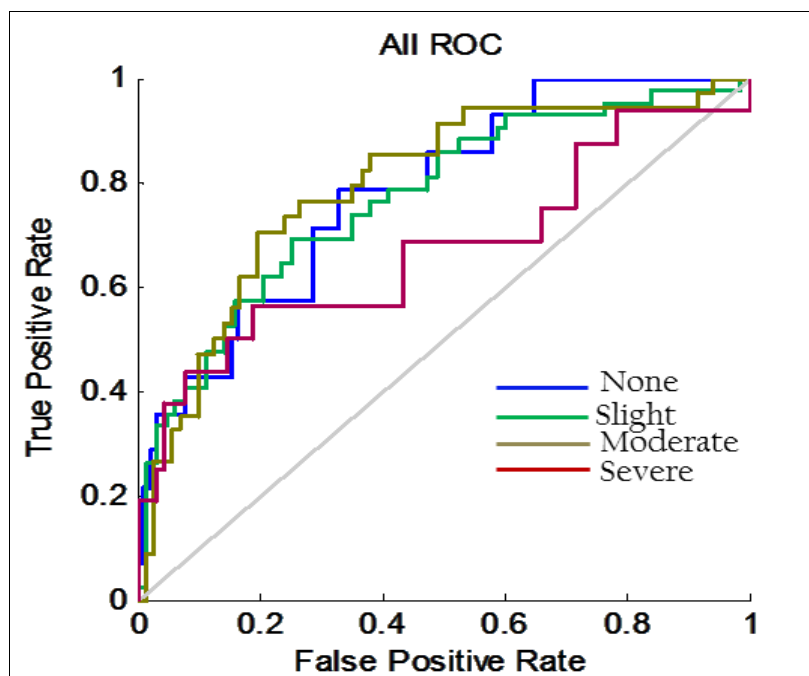


Figure 43. ROC curve for oxygenated and deoxygenated hemoglobin from the dorsolateral prefrontal cortex and electroencephalogram (EEG) signals.

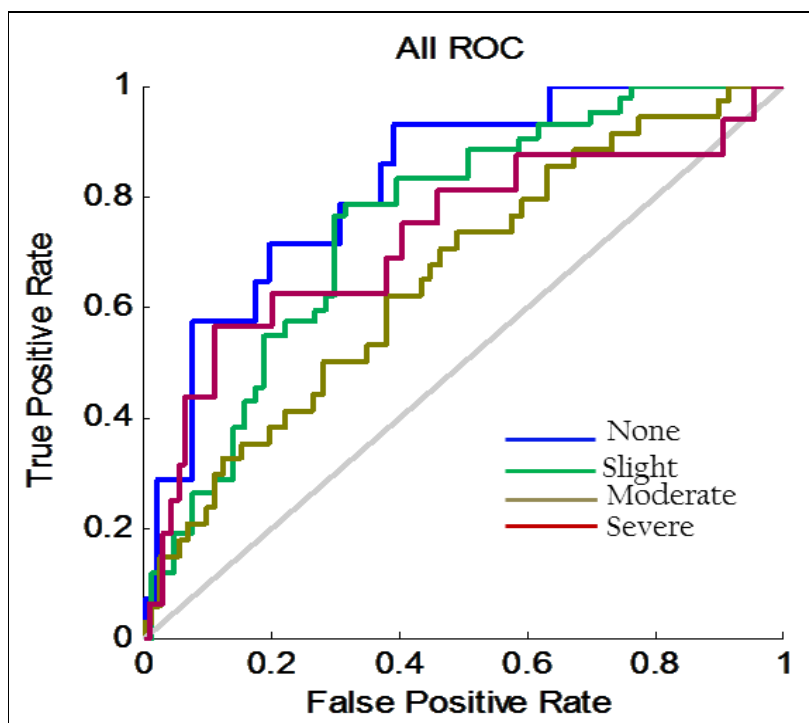


Figure 44. ROC curve for eye movement (saccade and fixation) and electroencephalogram (EEG) signals.

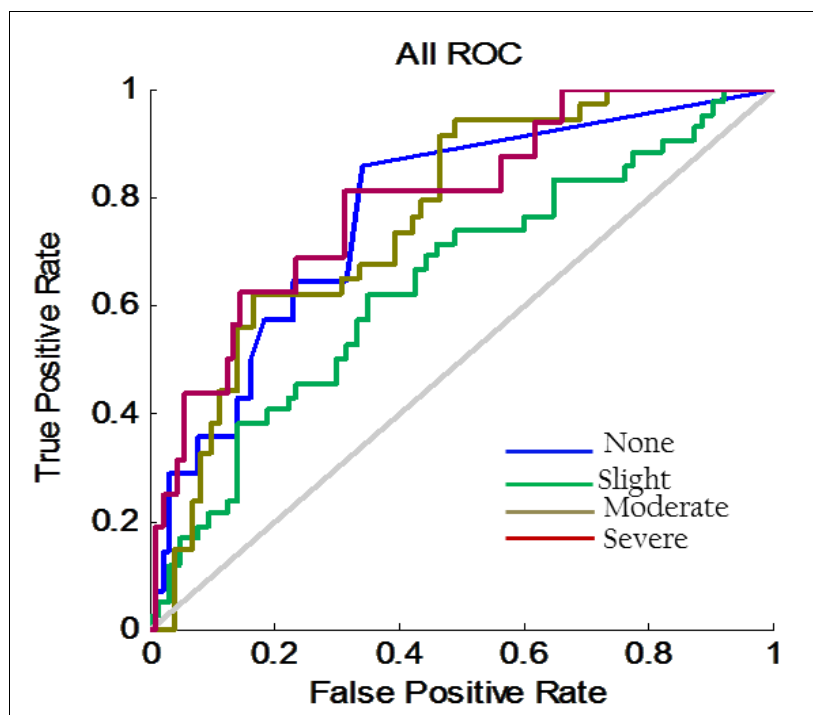


Figure 45. ROC curve for eye movement (saccade and fixation) and oxygenated and deoxygenated hemoglobin from the dorsolateral prefrontal cortex.

## CHAPTER 7

### Summary, Discussions, And Suggestions for Future Research

#### 7.1. Summary

Chapter 1 introduced the problem with literature review. It was noted that factors that cause visual fatigue are varied from physical, cognitive, psychological, and device design factors. It is observed that the existing studies have not explicitly addressed the issue of image alignment between the two eyes and whether visual fatigue is increased by misalignments that may occur inadvertently with HMDs. The objectives are organized into types of experimental investigations to :

- (a) Study the impact of vertical and rotational stereo pair alignment as well as stereo pair magnification differences on visual fatigue. Two hypotheses were investigated for Experiment 1:
  - (i) A prolonged use of stereoscopic display does not induce visual performance and (ii). Alignment errors in stereoscopic displays do not increase the prevalence of visual fatigue
- (b) Study cognitive neuroscience techniques to predict the on-sets of visual fatigue during situation awareness tasks. Three hypotheses were studied in this Experiment 2: (i) A prolonged use of stereoscopic display does not affect performance; (ii) Cognitive workload response variables have no effects on response time; (iii) Task difficulty (Aircraft separation types) has no effects on response time and (iv) There is no effect of interaction between cognitive workload response variables and task difficulty on response time.

Chapter 2 summarized all the equipment and resources used for the experiments. fNIRS was used to measure oxygenated hemoglobin (HbO<sub>2</sub>) and de-oxygenated hemoglobin ( Hbb) levels in the dorsolateral prefrontal cortex (DLPFC) of the brain. The Biopac MP 150 measured the neuronal electrical potential current of the pyramidal cells in the cerebral cortex as

continuous graphical distribution of spatiotemporal of voltage over time. The HMD-ViewPoint Eye Tracker provided oculomotor responses such as pupil dilation, fixation, and saccade of the eye to the stimuli. SSQ measured the subjective ratings of visual fatigue symptoms. The NASA Task Load index is a multi-dimensional rating procedure that provided an overall workload score. The ATCIM provided the experimental testbed for SA task environment.

Chapter 3 presented the experimental methodology, protocols, and experimental design for Experiment 1 which investigates the impact of alignment errors on visual fatigue. Three types of alignment errors studies were: (a) vertical alignment errors caused by an upward or downward tilt in the optical axis of one image that results in a difference in the vertical position of an image; (b) rotational alignment error which is a tilt in one of the images resulting in vertical and horizontal alignment errors with the degree of alignment errors increasing from the center; and (c) magnification difference due to an error in the size difference between the left and right stereo pairs resulting in vertical and horizontal alignment errors over the field view. The results of the study were analyzed in Chapter 4.

Chapter 4 presented the results of Experiment I experiments. The results show the following:

1. There is enough evidence to conclude that a prolong use of stereoscopic display is likely to induce visual fatigue as there was a significant difference between the SSQ responses between before air traffic control task (BATC) and after air traffic control task (ATC 3),  $t(23) = -15.27, p < 0.05$ .
2. For simulator sickness questionnaire (SSQ) rating, a Tukey post ad hoc analyses revealed that there was a significant difference between magnification difference and vertical shift

( $p < 0.05$ ), magnification difference and rotational error ( $p < 0.05$ ), and there was no significant difference between vertical shift and rotational error.

3. There was also a significant difference between the main effect for power band hemisphere and the magnification difference due to ATC task sessions,  $F(2,47) = 0.87$ ,  $p < 0.05$ .
4. The analysis showed that there was significant differences between the dorsal frontal lobes in task processing  $F(1, 47) = 0.034$ ,  $p < 0.05$ , and interaction effects between the processing lobes and tasks  $F(8, 47) = 3.306$ ,  $p < 0.05$ .
5. There is enough evidence to conclude that the transformed hemodynamic response as composite score was significant, Wilk's Lambda = 0.924,  $F(8, 132) = 0.66$ ,  $p < 0.05$ .  
There is enough evidence to conclude that at least one of the stereoscopic alignment errors is different on the following transformed hemodynamic dataset, *l* DLPFC- Hbb  $F(2, 69) = 0.10$ ,  $p < 0.05$ ; *l* DLPFC-HbO<sub>2</sub>  $F(2, 69) = 0.15$ ,  $p < 0.05$ ; *r* DLPFC-Hbb,  $F(2, 69) = 1.09$ ,  $p < 0.05$ .
6. There is enough evidence to conclude that the cerebral cortex relative power as composite score was significant, Wilk's Lambda = 0.0349,  $F(30, 110) = 15.96$ ,  $p < 0.05$ .  
There is enough evidence to conclude that at least one of the stereoscopic alignment errors is different on the following relative power bands *m* OCCH (O<sub>2</sub>): Delta,  $F(2, 96) = 18.8$   $p < 0.05$ , *r* OCCH (O<sub>2</sub>): Alpha,  $F(2, 69) = 139.26$ ,  $p < 0.05$ , *r* OCCH (O<sub>2</sub>): Theta,  $F(2, 69) = 18.98$ ,  $p < 0.05$ , *r* OCCH (O<sub>2</sub>): Delta,  $F(2, 69) = 0.5$ ,  $p < 0.05$ .
7. For the vertical shift, the overall model was statistically significant,  $F(9, 14) = 3.33$ ,  $p < 0.05$ , and model accounts for 81% of the variability observed in the SSQ perception of visual fatigue. For magnification differences, the model was significant  $F(9, 14) = 0.80$ ,  $p$

< 0.05 with the model accounting for 79% of the variability observed in the SSQ perception of visual fatigue. As the ATC task sessions progressed toward a higher workload (NASA-TLX), the weighted ratings for SSQ and overall mental workload increases ( $r = 0.89, p < 0.05$ ). Magnification difference display error is likely to have the most impact on participants' visual loadings.

8. Post ad hoc analyses of EEG data for alignment errors on cerebral cortex hemisphere revealed the relationships between hemodynamics and hemispheric differences between the alignment errors. The results are shown in Table 34.

Table 34

*Post Ad Hoc Analyses of EEG Data for Alignment Errors on Cerebral Cortex Hemisphere*

Location	Hemodynamic responses	Tukey post ad hoc analyses for alignment display errors ( $p < 0.05$ )
<i>r</i> DLPFC	Deoxygenated hemoglobin (Hbb)	(Magnification difference and Rotation error) and (Magnification difference and Vertical Shift)
<i>l</i> DLPFC	Oxygenated Hemoglobin (HbO <sub>2</sub> )	(Magnification difference and Rotation error) and (Magnification difference and Vertical Shift)
	Oxygenation (Hbb)	(Magnification difference and Rotation error) and (Magnification difference and Vertical Shift)

Chapter 5 used cognitive neuroscience techniques to investigate the occurrence of visual fatigue.

Four hypotheses were studied as follows: (i) A prolonged use of stereoscopic display does not affect visual performance ; (ii) Cognitive loading has no effects on response time; (iii) Task difficulty (aircraft separation types) have no effects on response time; and (iv) There is no interaction between cognitive load and Task difficulty (aircraft separation types) on response time. The following results were obtained:

1. There was a significant main effect of task difficulty on response time,  $F(3, 58) = 266.44, p < 0.05$ . This indicated that response times were different for vertical, horizontal, combined horizontal and vertical, and none as results of task difficulty.

2. There was a significant interaction between task difficulty and the cognitive load response variable on response time during visual task of air traffic control.
3. There was effect of task sessions on visual fatigue as measured by SSQ  $F(F(3, 18) = 3.91, p < 0.05)$ .
4. Correlation analyses revealed positive relations as follows: (SSQ and maximum pupil diameter,  $r = 0.9125, p = 0.0091$ ), (SSQ and minimum pupil diameter,  $r = 0.5826, p < 0.05$ ), (SSQ and fixation,  $r = 0.6061, p < 0.05$ ), (SSQ and saccade,  $r = 0.759, p < 0.05$ ), (SSQ and Oxygenation hemoglobin at left dorsolateral prefrontal cortex,  $r = 0.7179, p < 0.05$ ), (SSQ and Oxygenation hemoglobin at right dorsolateral prefrontal cortex,  $r = 0.3107, p < 0.05$ ), (SSQ and de-oxygenation hemoglobin at left dorsolateral prefrontal cortex,  $r = 0.79442, p < 0.05$ ), (SSQ and de-oxygenation hemoglobin at left dorsolateral prefrontal cortex,  $r = 0.70927, p < 0.05$ ). Thus, an increase in cognitive response variable is likely to result in an increase of visual fatigue experience.
5. Physiological response characteristics using eye movement revealed the predictions of onset of visual fatigue as shown in Table 35.
6. The results showed that a prolonged use of stereoscopic displays is likely to induce visual fatigue, as analyzed with SSQ,  $t(7) = -11.19, p < 0.05$  and response time  $t(7) = 3.16, p < 0.05$ . Task difficulty had an impact on response time,  $F(3, 58) = 266.44, p < 0.05$ . Information load and task difficulty in stereoscopic display had an impact on response time during visual task of air traffic control task  $F(2.32, 20.84) = 134.91, p < 0.05$ . Thus, increase in cognitive workload and task difficulty can greatly impact users' response time with the task.

Table 35

*Predictions of Onset of Visual Fatigue*

Visual Responses	Suspected time for onset of visual fatigue	Physiological indicator
Pupil dilation	36.2-40.0 min Avg = 38.1 min	0.95mm
Mean saccadic speed	33.71 min	0.575deg/sec
Mean eye fixation time	30-39 min (experienced workload rise time of 14.4 min)	0.005sec

Chapter 6 used a feed forward neural network (FF-ANN) to combine the objective data (SSQ) and objective data obtained from multi-dimensional measures from EEG, hemodynamics, and eye movements. The FF-ANN used was a three-layered network with thirteen neurons at the input layer, seven at the middle, and four as output layer. The output layer corresponded to the SSQ classes. The results of the classification experiments reveal classification accuracies, as shown in Table 36. The results of the experiment revealed that, individually, eye movement (saccade and fixation data) are better predictors of visual fatigue with 90.42 % accuracy. Also, eye movement data combined with EEG and hemodynamics data can predict visual fatigue with accuracies of 86.8% and 84.93% , respectively.

Table 36

*Classification Accuracies*

Data Sources	Classification Accuracy
All data combined	78.40%
EEG data	66.20%
Hemodynamic data	68.30%
Eye movement (saccade & Fixation data)	90.42%
EEG & Hemodynamic data	70.72%
EEG & Eye movement (saccade & Fixation data)	86.78%
Hemodynamic & Eye movement (saccade & Fixation data)	84.93%

## 7.2. Discussions and Observations

From alignment errors display experiments (Experiment I), the followings are the major take away:

1. EEG data suggest that there is a possibility of cognitively-induced time compensation changes due to a corresponding effect in real-time brain activity by the eyes trying to compensate for the alignment. The magnification difference error shows more significant effects on all EEG band waves which are indications of likely visual fatigue as shown by the prevalence of SSQ increase across all task levels. Vertical shift errors were observed to be prevalence in theta and beta bands of EEG which are likely to induce alertness (in theta band) as a result of likely stress. Rotation errors were significant in the gamma band which implies the likelihood of cognitive decline because of theta band influence. A post ad hoc analysis revealed that there were significant differences between magnification error and rotational error, and magnification error and vertical shift error.
2. The hemodynamic responses revealed that significant differences exist between the left and right dorsolateral prefrontal due to alignment errors in displays that affect visual attention. Generally, oxygenation levels were increased in both left and right dorsolateral prefrontal; however, it was more pronounced in the left dorsolateral prefrontal due to the corresponding increased oxygenated hemoglobin and blood volume. There is enough evidence to suggest some interaction between left, middle, and right sides of the brain and the ATC task session used as a result of magnification difference display error. There was also a significant difference between the main effect for power band hemisphere and the ATC task sessions. The analyses reveal that there was significant differences between

the dorsal frontal lobes in task processing ( $F = 0.034$ ,  $p < 0.05$ ) and interaction effects between the processing lobes and tasks ( $F = 3.306$ ,  $p < 0.05$ ).

3. The mean oxygenated hemoglobin and the oxygenated levels were significant at the left dorsolateral prefrontal cortex. The 3-D scatter plots for neuroimaging datasets comprising of the de-oxygenated hemoglobin, oxygenated hemoglobin and oxygenation level revealed increase in the oxygenated levels. The same pattern was exhibited in the right dorsolateral prefrontal cortex. However, for the right dorsolateral prefrontal cortex, the distribution is narrower than the left dorsolateral prefrontal cortex.

From the cognitive neuroscience study (Experiment II), the result show that

4. The behavioral and physical performance can be used to predict on-set times for visual fatigue. Pupil dilation becomes more and more outstanding with time as an important variable for use in predicting on-sets of visual fatigue. The physiologic indicator of pupil dilation was 0.95mm which occurred at a mean time of 38.1 min, after which the pupil dilation begins to decrease. After the average saccade rest time of 33.71 min (at eye saccades speed of 0.575deg/sec), saccade speeds tend to decrease as a possible result of fatigue on-set. Theoretically, a sluggish period occurs at 14.4 min with 0.005 sec residence time before a rapid jump due to perceived visual fatigue on-set at 30 min. With fatigue muscles, longer fixations and decreased saccadic effects set in as changes of the eye respond to time with increased workload. This effect was realized at about 46-52 min mark. Previous studies noted that a decrease in pupil diameter indicates the dominance of the parasympathetic nervous system and the deceleration in activity of the autonomic nervous system (Uetake et al., 2000). Granholm and Steinhauer (2002).

For example, changes in resting pupil diameter over time have been used to index tonic

arousal state or fatigue.

6. The model-based classification by neural network classifier validates the finding of both experimental tasks: Visual response data from eye movement was identified to be the best predictor of visual fatigue with a classification accuracy of 90.42%. Experimental data actually confirmed that 11.43% of the participants actually experienced visual fatigue symptoms after the prolonged task under ATC3.

### **7.3. Suggestions for Future Research**

The following are suggested for future research in this area:

1. Expand the study to include display depth perception, especially with augmented and virtual reality displays with varying accommodation distances.
2. Extend the study to investigate sleep deprivation so as to validate the anecdotal scientific claims that visual and mental fatigues are related. This will lead to a robust composite measure of stress.
3. Extend the study to personalize individual performance through a multifactorial study that includes inter-pupil distance, visual acuity, age, gender, task complexity, and display screen size.
4. Extend the study to analyze the differences between experienced and novice users of HMD-related device in battle field information management.

## References

- Aarås, A., Horgen, G., Bjørset, H.-H., Ro, O., & Thoresen, M. (1998). Musculoskeletal, visual and psychosocial stress in VDU operators before and after multidisciplinary ergonomic interventions. *Applied Ergonomics*, 29(5), 335-354.
- Abd-Manan, F. A., Jenkins, T. C. A., & Collinge, A. J. (2001). THE EFFECT OF CLINICAL VISUAL STRESS ON STEREOACUITY MEASURED WITH THE TNO TEST. *Malaysian Journal of Medical Sciences*, 8(2), 25-31.
- Abdi, S. (2007). *Asthenopia in Schoolchildren*. (Doctor of Philosophy), Karolinska Institutet, Stockholm, Sweden.
- Adikarapatti, V. K. (2007). *OPTIMAL EEG CHANNELS AND RHYTHM SELECTION FOR TASK CLASSIFICATION*. Wright State University.
- Akgül, C. B. (2004). Analysis of Functional Near Infrared Spectroscopy Signals. *Yüksek Lisans Tezi, Bo aziçi Üniversitesi, İstanbul*.
- American Optometric Association. (1999). Guide to the clinical aspects of computer vision syndrome. In A. O. Association (Ed.). St. Louis, USA.
- Ames III, O. K. (2004). Concerns about the lack of professionalism: Root causes rather than symptoms must be addressed. *Am. J. Trial Advoc.*, 28, 531.
- Anderson, J. (1993). *Rules of the Mind*. Hillsdale, NJ: Lawrence Erlbaum Associates.
- Andreassi, J. L. (2009). *Psychophysiology: Human Behavior & Physiological Response* (Vol. 5). New Jersey, USA: Taylor & Francis.
- Angelucci, A., & Bullier, J. (2003). Reaching beyond the classical receptive field of V1 neurons: horizontal or feedback axons? *Journal of Physiology-Paris*, 97(2-3), 141-154.

- Anshel, J. (2006). Visual Ergonomics in the Workplace Improving eye care and vision can enhance productivity. *Professional Safety*, 51(8), 20-25.
- Arrington Research Inc. (2010). ViewPoint EyeTracker ® Arrington Research, Inc. USA.
- Ayaz, H., Shewokis, P. A., Bunce, S., Izzetoglu, K., Willems, B., & Onaral, B. (2012). Optical brain monitoring for operator training and mental workload assessment. *NeuroImage*, 59(1), 36-47.
- Ayub, S., & Saini, J. (2010). Abnormality Detection in ECG Using Artificial Neural Networks. *Electronic Journal of Biomedicine, Spain, ISSN*, 47-52.
- Backus, B. T., Fleet, D. J., Parker, A. J., & Heeger, D. J. (2001). Human cortical activity correlates with stereoscopic depth perception. *Journal of Neurophysiology*, 86(4), 2054-2068.
- Baddeley, A. D. (2003). Working Memory: Looking back and looking forward. *Nature Reviews Neuroscience*, 4, 829-839.
- Baldwin, C. L., & Coyne, J. T. (2005). Dissociable aspects of mental workload: Examinations of the P300 ERP component and performance assessments. *Psychologia*, 48(2), 102-119.
- Baldwin, C. L., & Penaranda, B. (2012). Adaptive training using an artificial neural network and EEG metrics for within-and cross-task workload classification. *NeuroImage*, 59(1), 48-56.
- Baloh, R. W., Sills, A. W., Kumley, W. E., & Honrubia, V. (1975). Quantitative measurement of saccade amplitude, duration, and velocity. *Neurology*, 25(11), 1065-10679.
- Barlow, J. S. (1993). The electroencephalogram: Its patterns and origin. Cambridge, MA: MIT Press.

- Bartlett, F. C. (1953). Psychological criteria of fatigue. Symposium on Fatigue. In W. F. Floyd & A. T. Welford (Series Eds.), (pp. 1-5). London: Lewis, H. K.
- BIOPAC Systems Inc. (2011). MP System Hardware and Software Guide (Vol. 2). California: BIOPAC Systems, Inc.
- Blehm, C., Vishnu, S., Khattak, A., Mitra, S., & Yee, R. W. (2005). Computer vision syndrome: a review. *Survey of ophthalmology*, 50(3), 253-262.
- Boeree, C. G. (2006). The Lobes Retrieved [webpace.ship.edu/cgboer/lobes.html](http://webpace.ship.edu/cgboer/lobes.html), October, 7, 2012,
- Brookings, J. B., Wilson, G. F., & Swain, C. R. (1996). Psychophysiological responses to changes in workload during simulated air traffic control. *Biological Psychology*, 42(3), 361-377.
- Bullier, J., Hupé, J. M., James, A. C., & Girard, P. (2001). The role of feedback connections in shaping the responses of visual cortical neurons. *Progress in brain research*, 134, 193-204.
- Buxton, R. B., Uludag, K., Dubowitz, D. J., & Liu, T. T. (2004). Modeling the hemodynamic response to brain activation. *Neuroimage*, 23, S220-S233.
- Cabeza, R., & Nyberg, L. (2000). Imaging cognition II: An empirical review of 275 PET and fMRI studies. *Journal Cognitive Neuroscience*, 21(1), 1-47.
- Carandini, M. (2000). Visual cortex: Fatigue and adaptation. *Current Biology*, 10(16), R605-R607.
- Carpenter, R. H. S. (1988). *Movements of the Eyes* (Vol. 2, pp. 593). Pion, London.
- Chance, B., Nioka, S., & Luo, Q. (1998). Optical system and method for non-invasive imaging of biological tissue: Google Patents.

- Cheung, K. M., & Milgram, P. (2000). *Visual detection with hyperstereoscopic video for aerial search*. Paper presented at the Annual Meeting of the Human Factors and Ergonomics Society.
- Chi, C. F., & Lin, F. T. (1998). A comparison of seven visual fatigue assessment techniques in three data-acquisition VDT tasks. *Human Factors: The Journal of the Human Factors and Ergonomics Society*, 40(4), 577-590.
- Chia-Fen, C., & Fang-Tsan, L. (1998). A comparison of seven visual fatigue assessment techniques in three data-acquisition VDT tasks. (visual display terminal). *Human Factors* 40(4), 577-561.
- Chiovenda, P., Pasqualetti, P., Zappasodi, F., Ercolani, M., Milazzo, D., Tomei, G., . . . Tecchio, F. (2007). Environmental noise-exposed workers: Event-related potentials, neuropsychological and mood assessment. *International Journal of Psychophysiology, Elsevier*, 228-237.
- Cohen, J. (1977). *Statistical power analysis for the behavioral sciences*. New York.: Academic Press;.
- Collins, M. J., Brown, B., Bowman, K. J., & Carkeet, A. (1990). Symptoms associated with VDT use. *Clinical and Experimental Optometry*, 73(4), 111-118.
- Costanza, M. A. (1994). Visual and Ocular symptoms: Related to the use of video display terminal. *Journal of Behavioral Optometry*, 5, 2-31.
- Cronbach, L. J. (1951). Coefficient alpha and the internal structure of tests. *Psychometrika*, 16, 297-334.
- Cybenko, G. (1989). Approximation by superpositions of a sigmoidal function. *Mathematics of Control, Signals, and Systems (MCSS)*, 2(4), 303-314.

Damos, D. L., & Wickens, C. D. (1980). The identification and transfer of timesharing skills.

*Acta Psychologica*, 46, 15-39.

Dean, A. M., & Voss, D. (1999). *Design and analysis of experiments*: Springer Verlag.

DeAngelis, G. C. (2000). Seeing in three dimensions: the neurophysiology of stereopsis. *Trends*

*in cognitive sciences*, 4(3), 80-90.

Dell, R. B., Holleran, S., & Ramakrishnan, R. (2002). Sample size determination. *Ilar Journal*,

43(4), 207.

Demos, J. N. (2005). *Getting started with neurofeedback*: WW Norton.

Duda, R. O., Hart, P. E., & Stork, D. G. (2001). *Pattern Recognition (2nd)*: Wiley, New York,

ISBN.

Dussault, C., Jouanin, J.-C., Philippe, M., & Guezennec, C.-Y. (2005). EEG and ECG changes

during selected flight sequences. *Aviation Space and Environmental Medicine*, 75(10),

889-8897.

Emoto, M., Niida, T., & Okano, F. (2005). Repeated vergence adaptation causes the decline of

visual functions in watching stereoscopic television. *Display Technology, Journal of*,

1(2), 328-340.

Emoto, M., Nojiri, Y., & Okano, F. (2004). Changes in fusional vergence limit and its hysteresis

after viewing stereoscopic TV. *Displays*, 25(2-3), 67-76.

Fawcett, T. (2006). An introduction to ROC analysis. *Pattern recognition letters*, 27(8), 861-874.

Flach, P., & Wu, S. (2003). *Repairing concavities in ROC curves*. Paper presented at the

Proceeding of UK Workshop on Computational Intelligence, University of Bristol.

fNIR Devices LLC. (2010). *fNIR Imager & COBI Studio Manual*. 10801 Pleasant Hill Drive,

Potomac, MD 20854 USA.

- Francis, G., Rash, C. E., & Russo, M. B. (2009). Cognitive Factors. In C. E. Rash, M. B. Russo, T. R. Letowski & E. T. Scheimeiser (Eds.), *Helmet-Mounted Displays: Sensation, Perception and Cognition Issues* (Vol. 2, pp. 29-44). Fort Rucker, America: U.S. Army Aeromedical Research Laboratory.
- Fukushima, T., Torii, M., Ukai, K., Wolffsohn, J. S., & Gilmartin, B. (2009). The relationship between CA/C ratio and individual differences in dynamic accommodative responses while viewing stereoscopic images. *Journal of Vision*, 9(13).
- Ge, S. S., & Wang, C. (2004). Adaptive neural control of uncertain MIMO nonlinear systems. *Neural Networks, IEEE Transactions on*, 15(3), 674-692.
- Gobba, F. M., Broglia, A.,
- Sarti, R., Luberto, F., & Cavalleri, A. (1988). Visual fatigue in video display terminal operators: Objective measure and relation to environmental conditions. *International Arch Occupational Environmental Health*, 60(2).
- Going, W. M. (2008). *A visual fatigue in Stereoscopic display*. (MS Human Factors), North Carolina A & T State University.
- Gomarus, H. K., Althaus, M., Wijers, A. A., & Minderaa, R. B. (2006). The effects of memory load and stimulus relevance on the EEG during a visual selective memory search task: An ERP and ERD/ERS study. *Clinical Neurophysiology, Elsevier*, 871-884.
- Goussard, Y., Martin, B., & Stark, L. (1987). A New Quantitative Indicator of Visual Fatigue. *IEEE TRANSACTIONS ON BIOMEDICAL ENGINEERING*, 34(1).
- Granholm, E. E., & Steinhauer, S. R. (2004). Pupillometric measures of cognitive and emotional processes. *International Journal of Psychophysiology*.

GRASS Technologies. (2012). Retrieved October,30, 2012, Astro-Med Industrial Park • 600 East Greenwich Avenue • West Warwick, RI 02893 U.S.A:

<http://www.grasstechnologies.com/>

Gratton, G., Corballis, P. M., Cho, E., Fabiani, M., & Hood, D. C. (1995). Shades of gray matter: Noninvasive optical images of human brain responses during visual stimulation.

*Psychophysiology*, 32(5), 505-509.

Gratton, G., Maier, J. S., Fabiani, M., Mantulin, W. W., & Gratton, E. (1994). Feasibility of intracranial near infrared optical scanning. *Psychophysiology*, 31(2), 211-215.

Gundel, A., & Wilson, G. F. (1992). Topographical changes in the ongoing EEG related to the difficulty of mental tasks. *Brain Topography*, 5, 17-25.

Hancock, P., Meshkati, N., & Robertson, M. (1985). Physiological reflections of mental workload. *Aviation, space, and environmental medicine*.

Hancock, P., Wulf, G., Thom, D., & Fassnacht, P. (1990). Driver workload during differing driving maneuvers. *Accident Analysis & Prevention*, 22(3), 281-290.

Harrison, Y., & Home, J. A. (1999). One night of sleep loss impairs innovative thinking and flexible decision-making. *Organizational Behavior and Human Decision Processes*, 78, 128-145.

Harrison, Y., & Home, J. A. (2000). A review the impact of sleep deprivation on decision making. *Journal of Experimental Psychology: Applied*, 3, 236-249.

Hart, S. G. (2006). *NASA-Task Load Index (NASA-TLX); 20 Years Later*. Paper presented at the Proceedings of the Human Factors and Ergonomics Society 50th Annual Meeting, Santa Monica: HFES.

- Hatcher, L. (1994). *A step-by-step approach to using the SAS(R) system for factor analysis and structural equation modeling.* , Cary, NC: SAS Institute.
- Heaton, J. (2008). The Number of Hidden Layers Retrieved September, 21;<http://www.heatonresearch.com/node/707>, 2012
- Hennessey, D., Iosue, R., & Rouse, M. (1984). Relation of symptoms to accommodative infacility of school-aged children. *American Journal of Optometry and Physiological Optics*, 61(3), 177.
- Hirth, C., Obrig, H., Villringer, K., Thiel, A., Bernarding, J., Mühlnickel, W., . . . Villringer, A. (1996). Non-invasive functional mapping of the human motor cortex using near-infrared spectroscopy. *Neuroreport*, 7(12), 1977.
- Hoffman, D. M., Girshick, A. R., Akeley, K., & Banks, M. S. (2008). Vergence–accommodation conflicts hinder visual performance and cause visual fatigue. *Journal of Vision*, 8(3).
- Hopkins, V. D. (1995). *Human Factors in Air Traffic c Control*. London: Taylor & Francis.
- Hornik, K. (1991). Approximation capabilities of multilayer feedforward networks. *Neural networks*, 4(2), 251-257.
- Hornik, K., Stinchcombe, M., & White, H. (1989). Multilayer feedforward networks are universal approximators. *Neural networks*, 2(5), 359-366.
- Huang, J. Q., & Lewis, F. (2003). Neural-network predictive control for nonlinear dynamic systems with time-delay. *Neural Networks, IEEE Transactions on*, 14(2), 377-389.
- Hušák, M., Tecchia, F., Carrozzino, M., Rossi, F., Bergamasco, M., Vescovi, M., . . . Holliman, N. (2006). Stereoscopic Displays and Virtual Reality Systems XIII (Proceedings Volume).

- Inoue, T., & Ohzu, H. (1997). Accommodative responses to stereoscopic three-dimensional display. *Applied Optics*, 36(19), 4509-4515.
- International Centre for Eyecare Education (ICEE). (2009). Interpupillary Distance: Student Manual. *ICEE Refractive error training package* Retrieved August, 18.  
vm.icee.org/.../A%20Comprehensive%20Refractive%20Error%20Tra... 2012,
- Izzetoglu, K., Bunce, S., Onaral, B., Pourrezaei, K., & Chance, B. (2004). Functional optical brain imaging using near-infrared during cognitive tasks. *International Journal of Human-Computer Interaction*, 17(2), 211-227.
- Izzetoglu, K., Yurtsever, G., Bozkurt, A., Yazici, B., Bunce, S., Pourrezaei, K., & Onaral, B. (2003). *NIR spectroscopy measurements of cognitive load elicited by GKT and target categorization*. Paper presented at the System Sciences, 2003. Proceedings of the 36th Annual Hawaii International Conference on.
- Izzetoglu, M., Bunce, S. C., Izzetoglu, K., Onaral, B., & Pourrezaei, K. (2007). Functional brain imaging using near-infrared technology. *IEEE Engineering in Medicine and Biology Magazine*, 26(4), 38.
- Jacob, R. J. K., & Karn, K. S. (2003). Eye tracking in human-computer interaction and usability research: Ready to deliver the promise[Section complimentary]. In J. Hyona, R. Radach & H. Duebel (Eds.), *The mind's eye: Cognitive and applied aspects of eye movements*. Oxford, UK: Elsevier Science.
- Jaschinski-Kruza, W. (1984). Transient myopia after visual work. *Ergonomics*, 27(11), 1181-1189.

- Jaschinski-Kruza, W. (1991). Eyestrain in VDU users: viewing distance and the resting position of ocular muscles. *Human Factors: The Journal of the Human Factors and Ergonomics Society*, 33(1), 69-83.
- Jaschinski-Kruza, W., & Schweflinghaus, W. (1992). Relations between dark accommodation and psychosomatic symptoms. *Ophthalmic and Physiological Optics*, 12(1), 103-105.
- Jaschinski-Kruza, W. (1993). Fixation disparity at different viewing distances of a visual display unit. *Ophthalmic and Physiological Optics*, 13(1), 27-34.
- Jin, E. W. (2011). System Considerations for Optimizing Stereo Image Quality. © 2009 Aptina Imaging Corporation: Aptina Imaging Corporation.
- Jobsis, F. F. (1977). Noninvasive, infrared monitoring of cerebral and myocardial oxygen sufficiency and circulatory parameters. *Science*, 198(4323), 1264.
- Juliussen, E., & Petska-Juliussen, K. (1994). Paper presented at the he 7th Annual Computer Industry Almanac. Computer Industry, Almanac, Dallas, TX.
- Kaplan, E., & Shapley, R. M. (1986). The primate retina contains two types of ganglion cells, with high and low contrast sensitivity. *Proceedings of the National Academy of Sciences*, 83(8), 2755.
- Kato, T., Kamei, A., Takashima, S., & Ozaki, T. (1993). Human visual cortical function during photic stimulation monitoring by means of near-infrared spectroscopy. *Journal of Cerebral Blood Flow and Metabolism*, 13, 516-516.
- Kennedy, R. S., Lane, N. E., Berbaum, K. S., & Lilienthal, M. G. (1993). Simulator sickness questionnaire: an enhanced method for quantifying simulator sickness. *International Journal of Aviation Psychology*, 3(3), 203-220.

- Kim, D., Jung, Y. J., Kim, E., Man Ro, Y., & Park, H. (2011). HUMAN BRAIN RESPONSE TO VISUAL FATIGUE CAUSED BY STEREOSCOPIIC DEPTH PERCEPTION. *DSP IEEE*, 7(11), 1-5.
- Kim, D., Min, D., Oh, J., Jeon, S., & Sohn, K. (2009). Depth map quality metric for three-dimensional video. *SPIE Stereoscopic Displays and Applications XX*, 7237.
- Knave, B., Wibom, R. I., Vos, M., Hedstrom, L. D., & DBerquist, U. O. V. (1985). Work with video terminals among office employees: A subjective symptoms and discomfort. *Scandanavian Journal of Work Environmental Health*, 11(6), 457-466.
- Koh, D., Ong, C., & Jeyaratnam, J. (1994). The safe use of visual display units. *Singapore medical journal*, 35, 381-381.
- Kooi, K. L., & Toet, A. (2004). Visual comfort of binocular and 3D displays. *Displays*, 25(99-1008).
- Kornylo, K., Dill, N., Saenz, M., & Krauzlis, R. J. (2003). Canceling of pursuit and saccadic eye movements in humans and monkeys. *Journal of Neurophysiology*, 89(6), 2984.
- Kramer, A. F., Trejo, L. J., & Humphrey, D. (1996). Psychophysiological measures of workload: Potential applications to adaptively automated systems. In R. Parasuraman & J. Mouloua (Eds.), *Automation and Human Performance: Theory and Applications* (pp. 137-162). Mahwah, NJ: Lawrence Erlbaum Associates, .
- Kupper, L. L., & Hafner, K. B. (1989). How appropriate are popular sample size formulas? *American Statistician*, 101-105.
- Kuschewski, J. G., Hui, S., & Zak, S. H. (1993). Application of feedforward neural networks to dynamical system identification and control. *Control Systems Technology, IEEE Transactions on*, 1(1), 37-49.

- Kuze, J., & Ukai, K. (2008). Subjective evaluation of visual fatigue caused by motion images. *Displays*, 29(2), 159-166.
- Lambooj, M., IJsselsteijn, W., Fortuin, M., & Heynderickx, I. (2009). Visual discomfort and visual fatigue of stereoscopic displays: a review. *Journal of Imaging Science and Technology*, 53, 030201.
- Lamme, V. A. F., Supèr, H., Landman, R., Roelfsema, P. R., & Spekreijse, H. (2000). The role of primary visual cortex (V1) in visual awareness. *Vision research*, 40(10-12), 1507-1521.
- Leavitt, S. (1995 ). Lower your VDT monitors. *Workplace Ergonomics*, 32-35.
- Lee, S. E., Simons, S. B., Heldt, S. A., Zhao, M., Schroeder, J. P., Vellano, C. P., . . . Feng, Y. (2010). RGS14 is a natural suppressor of both synaptic plasticity in CA2 neurons and hippocampal-based learning and memory. *Proceedings of the National Academy of Sciences*, 107(39), 16994-16998.
- Len, C., & Huang, K. (2006). Effects of Ambient Illumination and Screen Luminance Combination on Character Identification Performance of Desktop TFT-LCD Monitors. *International Journal of Industrial Ergonomics*, 36, 211-218.
- Levitt, J. B., & Lund, J. S. (2002). The spatial extent over which neurons in macaque striate cortex pool visual signals. *Visual neuroscience*, 19(4), 439-452.
- Li, H. C. O., Seo, J., Kham, K., & Lee, S. (2008, May, 28-30). *Measurement of 3D visual fatigue using event-related potential (ERP): 3D oddball paradigm*. Paper presented at the 3DTV-CON'08, Istanbul, Turkey.

- Lin, J. T., Liang, G. F., Hwang, S. L., & Wang, E. M. (2010). Predicting visual fatigue in integrated circuit packaging plants. *Human Factors and Ergonomics in Manufacturing & Service Industries*, 20(5), 461-469.
- Liu, Y., Wang, F., & Wang, C. (2009). The research on visual fatigue factor in stereoscopic image observation. *Computer-Aided Industrial Design & Conceptual Design. IEEE 10th International Conference on*.
- Liu, Y., Wang, F., & Wang, C. (2009a). The research on visual fatigue factor in stereoscopic image observation. *IEEE*, 1882-1887.
- López-Aranda, M. F., López-Téllez, J. F., Navarro-Lobato, I., Masmudi-Martín, M., Gutiérrez, A., & Khan, Z. U. (2009). Role of layer 6 of V2 visual cortex in object-recognition memory. *Science*, 325(5936), 87-89.
- Maki, A., Yamashita, Y., Ito, Y., Watanabe, E., Mayanagi, Y., & Koizumi, H. (1995). Spatial and temporal analysis of human motor activity using noninvasive NIR topography. *Medical Physics*, 22, 1997.
- Malmivuo, J., & Plonsey, R. (1995 ). *The Electric Signals Originating in the Eye*. New York Oxford: OXFORD UNIVERSITY PRESS.
- Mansfield, J. S., & Legge, G. E. (1996). The binocular computation of visual direction. *Vision Research*, 36(1), 27-41.
- Martínez, R. M. R., de la O Escápita, R., de la Riva, J., & Rodríguez, A. C. F. B. (2009). Categorization of Factors Causing Athenopia in Reserach Center Professors at the ITCJ by reading with VDT: A Shared Experience. . In I. T. d. C. Juárez (Ed.), *XV Congreso International de Ergonomia Ciudad Juárez, Chih., México*.
- Masters, T. (1993). *Practical neural network recipe in C++*. New York: Academic Press.

- McGregor, D. K., & Stern, J. A. (1996). Time on task and blink effects on saccade duration. *Ergonomics*, *39*, 649-660.
- Merzagora, A. C., Maria, T. S., Onaral, B., & Izzetoglu, M. (2011). FUNCTIONAL NEAR-INFRARED SPECTROSCOPY–BASED ASSESSMENT OF ATTENTION IMPAIRMENTS AFTER TRAUMATIC BRAIN INJURY. *Journal of Innovative Optical Health Sciences*, *4*(03), 251-260.
- Millodot, M., & Newton, I. (1981). VEP measurement of the amplitude of accommodation. *British Journal of Ophthalmology*, *65*(4), 294.
- Morris, T. L., & Miller, J. C. (1996). Electrooculographic and performance indices of fatigue during simulated flight. *Biological Psychology*, *42*, 343-360.
- Mourant, R. R., Lakshmanan, R., & Chantadisaï, R. (1981). Visual fatigue and cathode ray tube display terminals. *Human Factors: The Journal of the Human Factors and Ergonomics Society*, *23*(5), 529-540.
- Murata, K., Araki, S., Kawakami, N., Saito, Y., & Hino, E. (1991). Central nervous system effects and visual fatigue in VDT workers. *International Archives of Occupational and Environmental Health*, *63*(2), 109-113.
- Mutti, D., & Zadnik, K. (1996). Is computer use a risk factor for myopia? . *Journal of American Optometry Association*, *67*, 521-530.
- Nahar, K. N., Sheedy, J. E., Hayes, J., & Tai, Y., C. (2007). Objective Measurements of Lower-Level Visual Stress. *OPTOMETRY AND VISION SCIENCE*, *84*(7), 620-629.
- National Eye Institute. (2002). *Why fund the National Eye Institute? Eye Diseases Health and Research Information*. Bethesda, MD: National Alliance for Eye and Vision Research (NAEVR).

- Neugebauer, A., Fricke, J., & Rüssmann, W. (1992). Asthenopia: frequency and objective findings *German Journal of Ophthalmology* (Vol. 1, pp. 122-124). Federal Republic of Germany: Abteilung für Schielbehandlung und Neuroophthalmologie, Universität, Köln,.
- Nolan, M. S. (1994). *Fundamentals of Air Traffic Control*. Wadsworth Publishing Company, Belmont, CA.
- Nunnally, J. (1978). *Psychometric theory*. New York: McGraw-Hill. .
- O'Sullivan, S. B., & Schmitz, T. J. (2007). *Physical Rehabilitation*. Philadelphia, PA: Davis. ISBN 978-0-8036-1247-1.
- Obrig, H., Hirth, C., Junge-Hulsing, J., Doge, C., Wolf, T., Dirnagl, U., & Villringer, A. (1996). Cerebral oxygenation changes in response to motor stimulation. *Journal of Applied Physiology*, *81*(3), 1174.
- Okada, Y., Ukai, K., Wolffsohn, J. S., Gilmartin, B., Iijima, A., & Bando, T. (2006). Target spatial frequency determines the response to conflicting defocus-and convergence-driven accommodative stimuli. *Vision research*, *46*(4), 475-484.
- Ong, C. N. (1984). VDT workplace design and physical fatigue: a case study in Singapore *Ergonomics and health in modern offices*, . London: Francis and Taylor.
- Orozco, J., & Garcia, C. A. R. (2003). *Detecting pathologies from infant cry applying scaled conjugate gradient neural networks*. Paper presented at the ESANN'2003 proceedings - European Symposium on Artificial Neural Networks, 23-25 April, Bruges (Belgium).
- Ousler, G. W., Wilcox, K. A., Gupta, G., Abelson, M. B., & Fink, K. (2004). An evaluation of the ocular drying effects of 2 systemic antihistamines: loratadine and cetirizine hydrochloride. *Annals of Allergy, Asthma & Immunology*, *93*(5), 460-464.

- Ousler III, G. W., Hagberg, K. W., Schindelar, M., Welch, D., & Abelson, M. B. (2008). The ocular protection index. *Cornea*, 27(5), 509.
- Palaniappan, R., & Jayant, N. (2006). SUBJECTIVE QUALITY IN 3DTV: EFFECTS OF UNEQUAL BIT ALLOCATION TO LEFT AND RIGHT VIEWS. *IEEE Trans. Circuits Syst. Video Technol.*, 13(11), 1092-1106.
- Pang-Ning, T., Steinbach, M., & Kumar, V. (2006). *Introduction to data mining*: Pearson Addison Wesley Boston.
- Pastoor, S., & Wöpking, M. (1997). 3-D displays: A review of current technologies. *Displays*, 17(2), 100-110.
- Pavlas, D., Lum, H., & Salas, E. (2012). How to Build a Low-Cost Eye-Tracking System. *Ergonomics in Design*, 20(1).
- Petsche, H., & Rappelsberger, P. (1992). Is there any message hidden in the human EEG? . In E. Basar & T. H. Bullock (Eds.), *Induced Rhythms in the Brain* (pp. 103-116). Boston: Birkhuser.
- Pollen, D. A. (1999). On the neural correlates of visual perception. *Cerebral Cortex*, 9(1), 4-19.
- Psychological Software Tools Inc. (2010). Sharpsburg, PA, USA
- Qin, D., Takamatsu, M., & Nakashima, Y. (2004). Measurement for the Panum's Fusional Area in Retinal Fovea Using a Three- Dimension Display Device. *Journal of Light & Visual Environment*, 28(3), 126-131.
- Qiu, F. T., & Von Der Heydt, R. (2005). Figure and ground in the visual cortex: V2 combines stereoscopic cues with Gestalt rules. *Neuron*, 47(1), 155-166.
- Rabbetts, R. B. (2000). Clinical Visual Optics (Oxford: Butterworth-Heinemann) ray tube display terminals. *Human Factors*, 23(5), 529-540.

- Rolfe, R. D. (2000). The role of probiotic cultures in the control of gastrointestinal health. *The Journal of nutrition*, 130(2), 396S-402S.
- Saksida, L. M. (2009). Remembering outside the box. *Science*, 325(5936), 40-41.
- Salibello, C., & Nilsen, E. (1995). Is there a typical VDT patient? A demographic analysis. *Journal of American Optometry Association*, 66, 475-483.
- Sallamander, C. (2010). Astaxanthin and eye fatigue. [www.anyvitamins.com/astaxanthin-eye-health.htm](http://www.anyvitamins.com/astaxanthin-eye-health.htm) Retrieved September,15, 2011
- Sanchez-Vives, M. V., Nowak, L. G., & McCormick, D. A. (2000). Cellular mechanisms of long-lasting adaptation in visual cortical neurons in vitro. *J Neurosci* 20, 4286 - 4299.
- Santos, J. R. A., Lippke, L., & Pope, P. (1998). *PROC FACTOR: A tool for extracting hidden gems from a mountain of variables*. . Paper presented at the Proceedings of the 23rd Annual SAS Users Group International Conference., Cary, NC: SAS Institute Inc. .
- SAS Institute Inc. (2008). 100 SAS Campus Drive, Cary, North Carolina ,USA. .
- Sauter, S. L. (1985). *Improving VDT work: causes and control of health concerns in VDT use*. . State of Winsconsin Department of Administration.
- Sauter, S. L., Schleifer, L. M., & Knutson, S. J. (1991). Work posture, workstation design, and musculoskeletal discomfort in a VDT data entry task. *Human Factors: The Journal of the Human Factors and Ergonomics Society*, 33(2), 151-167.
- Self, H. C. (1986). Optical tolerances for alignment and image differences for binocular helmet-mounted displays. (Report No. AAMRL-TR-86-019).
- Seuntiëns, P., Meesters, L., & IJsselsteijn, W. (2005). Perceptual attributes of crosstalk in 3D images. *Displays*, 26(4-5), 177-183.

- Sheedy, J. E., & Hayes, J. (2003). Is all asthenopia the same? *Optometry & Vision Science*, 80(11), 732.
- Sheedy, J. E., Kang, J. M., & Ota, W. T. (2002). Vertical eye gaze position: effect on task performance and visual comfort. In S. J. E. & P. Shaw-McMinn (Eds.), *Diagnosing and Treating Computer-Related Vision Problems* (pp. 190-191). Boston: Butterworth-Heinemann.
- Shimmura, S., Shimazaki, J., & Tsubota, K. (1999). Results of a population-based questionnaire on the symptoms and lifestyles associated with dry eye. *Cornea*, 18, 408-411.
- Simons, D. J., & Levin, D. T. (1997). Change blindness. *Trends in cognitive sciences*, 1(7), 261-267.
- So, P. (2010). NASA LTX: Task load Index Retrieved October, 14th, [humansystems.arc.nasa.gov/groups/TLX/](http://humansystems.arc.nasa.gov/groups/TLX/), 2012
- Sommerich, C. M., Starr, H., Smith, C. A., & Shivers, C. (2002). Effects of notebook computer configuration and task on user biomechanics, productivity, and comfort. *International journal of industrial ergonomics*, 30(1), 7-31.
- Son, I. Y., Guhe, M., Gray, W., Yazici, B., & Schoelles, M. J. (2005). *Human performance assessment using fNIR*.
- Springer, S., & Deutsch, G. (1989). *Left brain, right brain* (3rd Edition ed.). New York:: W.H. Freeman.
- Stein, H. A., & Stein, R. M. (1994). *The ophthalmic assistant: a guide for ophthalmic medical personnel* (Vol. 6): Mosby (St. Louis).
- Sterman, M., & Mann, C. (1995). Concepts and applications of EEG analysis in aviation performance evaluation. *Biological Psychology*, 40(1), 115-130.

- Strangman, G., Boas, D. A., & Sutton, J. P. (2002). Non-invasive neuroimaging using near-infrared light. *Biological Psychiatry*, 52(7), 679-693.
- Sullivan, J. M. (2008). Visual Fatigue and the Driver (Vol. 1, pp. 1-27). Ann Arbor, MI: The University of Michigan, Transportation Research Institute: 302753, UMTRI-2008-50.
- Svensson, P. (2011, January 21, 2011). A HEADACHE IN 3-D, Companies push technology despite illnesses, *News & Record*, Greensboro, NC:USA, p. B5.
- Tamez, G. S., Ortiz, H. L., & Martínez, A. S. (2003). Riesgos y daños a la salud derivados del uso de Video terminal. *Salud Pública de México*. Universidad Autónoma Metropolitana (UAM). Unidad Xochimilco. México, DF, México. (pp. 45 (43)).
- Tarutta, E., Chua, W.-h., Young, T., Goldschmidt, E., Saw, S.-M., Rose, K. A., . . . Stone, R. A. (2011). Myopia: Why Study the Mechanisms of Myopia? Novel Approaches to Risk Factors Signaling Eye Growth-How Could Basic Biology Be Translated into Clinical Insights? Where Are Genetic and Proteomic Approaches Leading? How Does Visual Function Contribute to and Interact with Ametropia? Does Eye Shape Matter? Why Ametropia at All? *Optometry & Vision Science*, 88(3), 404.
- TCO Work Environment Committee. (1986). *VDU work the right way*.
- Thomson, W. D. (1998). Eye problems and visual display terminals—the facts and the fallacies. *Ophthalmic and Physiological Optics*, 18(2), 111-119.
- Travis, J., & Kring, J. (2002). *LabVIEW for everyone*: prentice Hall.
- Trejo, L. J., Kochavi, R., Kubitz, K., Montgomery, L., Rosipal, R., & Matthews, B. (2005a). *EEG-based estimation of cognitive fatigue*.
- Trejo, L. J., Kochavi, R., Kubitz, K., Montgomery, L. D., Rosipal, R., & Matthews, B. (2005b). *EEG-based estimation of cognitive fatigue* (Vol. 5797): NASA Ames Research Center.

- Tsao, D. Y., Vanduffel, W., Sasaki, Y., Fize, D., Knutsen, T. A., Mandeville, J. B., . . . Tootell, R. B. H. (2003). Stereopsis activates V3A and caudal intraparietal areas in macaques and humans. *Neurology*, *36*(3), 555-568.
- Turville, K. L., Psihogios, J. P., Ulmer, T. R., & Mirka, G. A. (1998). The effects of video display terminal height on the operator: a comparison of the 15 and 40 recommendations. *Applied Ergonomics*, *29*(4), 239-246.
- Uetake, A., Murata, A., Matsumoto, S., & Takasawa, Y. (2000). *A method to measure muscular fatigue in VDT tasks*.
- Uetake, A., Murata, A., Otsuka, M., & Takasawa, Y. (2000). *Evaluation of visual fatigue during VDT tasks*. Paper presented at the Systems, Man, and Cybernetics, 2000 IEEE International Conference on, Nashville, TN.
- Ukai, K., & Howarth, P. A. (2008). Visual fatigue caused by viewing stereoscopic motion images: Background, theories, and observations. *Displays*, *29*(2), 106-116.
- Ukai, K., & Kato, Y. (2002). The use of video refraction to measure the dynamic properties of the near triad in observers of a 3 D display. *Ophthalmic and Physiological Optics*, *22*(5), 385-388.
- Ukai, K., & Kibe, A. (2003). Counterroll torsional eye movement in users of head-mounted displays. *Displays*, *24*(2), 59-63.
- van der Linden, D., Frese, M., & Meijman, T. F. (2003). Mental fatigue and the control of cognitive processes: effects on perseveration and planning. *Acta Psychologica*, *113*(1), 45-65.

- Van Orden, K. F., Jung, T. P., & Makeig, S. (2000). Combined eye activity measures accurately estimate changes in sustained visual task performance. [Article]. *Biological Psychology*, 52(3), 221-240. doi: 10.1016/s0301-0511(99)00043-5
- Veltman, J. (1996). Physiological workload reactions to increasing levels of task difficulty: DTIC Document.
- Villringer, A., & Chance, B. (1997). Non-invasive optical spectroscopy and imaging of human brain function. *Trends in Neurosciences*, 20(10), 435-442.
- Villringer, A., Planck, J., Hock, C., Schleinkofer, L., & Dirnagl, U. (1993). Near infrared spectroscopy (NIRS): a new tool to study hemodynamic changes during activation of brain function in human adults. *Neuroscience letters*, 154(1-2), 101-104.
- Wang, P. C., Hwang, S. L., Chen, K. Y., Chen, J. S., Yang, J. C., & Chang, H. L. (2011). The Effects of Stereoscopic Display Luminance and Ambient Illumination on Visual Comfort. *HCI International 2011-Posters' Extended Abstracts*, 369-373.
- Wiggins, N., & Daum, K. (1991). Visual discomfort and astigmatic refractive errors in VDT use. *Journal of the American Optometric Association*, 62(9), 680.
- Wiggins, N., Daum, K., & Snyder, C. (1992). Effects of residual astigmatism in contact lens wear on visual discomfort in VDT use. *Journal of the American Optometric Association*, 63(3), 177.
- Wilkins, A. (1995). *Visual Stress*. Oxford, UK: Oxford University Press.
- Wilkins, A., & Neary, C. (1991). Some visual, optometric and perceptual effects of coloured glasses. *Ophthalmic and Physiological Optics*, 11(2), 163-171.

- Wilson, G. F., Estepp, J., & Davis, I. (2009). *A comparison of performance and psychophysiological classification of complex task performance*. Paper presented at the Proceedings of the Human Factors and Ergonomics Society Annual Meeting.
- Wilson, G. F., Russell, C., Monnin, J., Estepp, J., & Christensen, J. (2010). *How Does Day-to-Day Variability in Psychophysiological Data Affect Classifier Accuracy?* Paper presented at the Proceedings of the Human Factors and Ergonomics Society Annual Meeting.
- Wilson, G. F., & Russell, C. A. (2003). Operator functional state classification using multiple psychophysiological features in an air traffic control task. *Human Factors: The Journal of the Human Factors and Ergonomics Society*, 45(3), 381-389.
- Wimalasundera, S. (2009). Computer vision syndrome. *Galle Medical Journal*, 11(1), 25-29.
- Wiyor, H. D. (2009). *A MODEL OF DYNAMIC SITUATION AWARENESS*. (MS), North Carolina Agriculture and Technical State University, Greensboro, NC-USA. (W57525 2009 )
- Wolverton, G. S., & Zola, D. (1983). The temporal characteristics of visual information extraction during reading. *Eye movements in reading: Perceptual and language processes*, 41-51.
- Wong, D. F., Maini, A., Rousset, O. G., & Brasic, J. R. (2003). Positron emission tomography-a tool for identifying the effects of alcohol dependence on the brain. *Alcohol Research and Health*, 27(2), 161-173.
- Woods, A., Docherty, T., & Koch, R. (1999). *Image Distortions in Stereoscopic Video Systems*. Paper presented at the Proceedings of the SPIE Volume Stereoscopic Displays and Applications IV, San Jose, California.

- Wyczesany, M., Kaiser, J., & Coenen, A. M. L. (2008). Subjective mood estimation co-varies with spectral power EEG characteristics. *Acta neurobiologiae experimentalis*, 68(2), 180.
- Xu, X., Bosking, W., Sáry, G., Stefansic, J., Shima, D., & Casagrande, V. (2004). Functional organization of visual cortex in the owl monkey. *The Journal of neuroscience*, 24(28), 6237.
- Yano, S., Emoto, M., & Mitsuhashi, T. (2004). Two factors in visual fatigue caused by stereoscopic HDTV images. *Displays*, 25(4), 141-150.
- Yano, S., Ide, S., Mitsuhashi, T., & Thwaites, H. (2002). A study of visual fatigue and visual comfort for 3D HDTV/HDTV images. *Displays*, 23(4), 191-201.
- Zelinsky, G., & Sheinberg, D. (1995). WHY SOME SEARCH TASK TAKE LONGER THAN OTHERS: USING EYE MOVEMENTS TO REDEFINE REACTION TIME. In J. M. Findlay, R. Walker & R. W. Kentridge (Eds.), *EYE MOVEMENTS RESEARCH: Mechanisms, Processes and Applications* (pp. 325-366). North-Holland: ELSEVIER.
- Zhang, A., Zhao, Z., & Wang, Y. (2009a). *Estimating VDT Visual Fatigue Based on the Features of ECG Waveform*. Paper presented at the International Workshop on Information Security and Application, Qingdao, China.
- Zhang, A., Zhao, Z., & Wang, Y. (2009b). *Estimating VDT Visual Fatigue Based on the Features of ECG Waveform*. Paper presented at the proceedings of the International Workshop on Information Security and Application (IWISA 2009), Qingdao, China.
- Zhang, G. P. (2000). Neural networks for classification: a survey. *Systems, Man, and Cybernetics, Part C: Applications and Reviews, IEEE Transactions on*, 30(4), 451-462.
- Zhu, Z., & Ji, Q. (2004a). *Real time and non-intrusive driver fatigue monitoring*. Paper presented at the 7th International IEEE Conference Washington DC.

Zhu, Z., & Ji, Q. (2004b). Real time and non-intrusive driver fatigue monitoring. *IEEE*, 53(14), 1052 - 1068

*Appendix A*

*Summary of Visual Fatigue Measurements from Medical Perspective*

Authors(s)	Experimental Stimuli and Conditions	Measurement Techniques	Findings	Research Gap
Abd-Manan, Jenkins, and Collinge, (2001)	25 subjects without fixation disparity (FD) and second group of 25 subjects with FD related visual stress.	Stereo performance with TNO test (Stereo grams).	Visual stress increases as fixation disparity (FD) decreases.	The study lacks the exact point for measuring the onset of visual fatigue.
Sheedy, Hayes and Engels (2003)	Subjects performed reading tasks in random order of eight conditions: astigmatism, close viewing distance, upward gaze, dry eyes, lens flipper, and small font.	Subjective ratings of burning, ache, strain, irritation, tearing, blurred vision, double vision, dryness, and headache.	Classified symptoms of visual fatigue based on internal symptoms factors (ISF) and external symptoms factors (ESF).	The subjective responses are flawed with individualistic responses.
Nahar, Sheedy, Hayes, and Tai, (2007)	Subjects read on a computer display for 27 trials of low-level asthenopic conditions: font size, font type, contrast, refractive error, and glare.	Oculi activity and blink rates were recorded using surface EMG. Subjects rated the severity of visual discomfort experienced.	Increased EMG power results in the increased Orbicularis and Blink Rate (BR). All conditions showed significant visual discomfort.	Longer EMG recordings were required due to sensitivity of blinks.

Authors(s)	Experimental Stimuli and Conditions	Measurement Techniques	Findings	Research Gap
Gowrisankaran, Sheedy, and Hayes. (2007)	20 subjects read passages under different asthenopia-inducing condition: glare, low contrast, small font size, refractive error, up gaze, accommodative stress and convergence stress.	Surface electromyography (EMG) was used to study the orbicularis oculi response from the right eye and rate the severity and type of visual discomfort experienced.	Refractive error, glares, low contrast, small font, and up gaze resulted in a significant increase in EMG power. Conditions induced significant visual discomfort.	No quantitative model for estimating the onset of visual fatigue.
Neugebauer, Fricke, and Rüssmann, (1992)	Fifty young adults were interviewed about the asthenopic symptoms experienced in the preceding 6 months by means of a questionnaire; they then underwent ophthalmic investigation.	Frequency of occurrence of single asthenopic symptoms.	Frequencies of single complaints were: headache (84%), ocular pain (34%), foreign body sensation (50%), red eyes (44%), photophobia (48%), double vision (10%), and difficulties when changing fixation distance (42%).	There was no preference for any one of the symptoms in any of the subgroups mentioned. Study conclusion is based on the subjective ratings.

*Appendix B*

*Summary of Visual Fatigue Measurements from Human Factor Perspective*

Authors (s)	Experimental Stimuli and Conditions	Measurement Techniques	Findings	Research Gap
Yano et al. (2002)	Comparison of image quality characteristics using two technologies: HDTV and stereoscopic HDTV. The experiment started with 20 subjects but 7 failed to complete their experiment.	Subjective ratings of visual fatigue. Estimation of accommodation changes before and after viewing HDTV and stereoscopic HDTV.	Visual fatigue may occur due to the conflict between convergence, and accommodation eye movement, and depth of focus.	The designs of HDTV and stereoscopic HDTV technologies lack user-centered design.
Ukiah & Heath, (2008)	Playing TV games using a HMDTV with a stereoscopic movie.	Subjective questionnaire to assess symptoms caused by viewing motion images.	The severity of visual fatigue depends on time, detail of visual task, convergence, and accommodation.	Lack of empirical studies to assess individual susceptibilities to stereoscopic visual fatigue.
Zhang, Zhao, and Wang, (2009a)	Comparison of image quality characteristics using two technologies HDTV and stereoscopic HDTV.	Physiological measurement based on Average Heart Rate (AHR) and Standard Deviation of Heart Rate (SDHR).	Increase in visual fatigue resulted in the increase in SDHR and AHR.	Using SDHR and AHR as indexes for indirectly measuring visual fatigue are misleading and can lead to misinformed conclusion.

Authors (s)	Experimental Stimuli and Conditions	Measurement Techniques	Findings	Research Gap
Inoue and Ohzu (1997)	Varying the depth of stereoscopic images.	Using the pupillimeter to estimate accommodation and convergence response to stereoscopic images.	Accommodation response to 3D images and real objects are driven by convergence effort. However, perception of 3D images required other psychological cues.	Lack of a quantitative estimation of the amount of depth that causes visual fatigue.
Goussard, Martin, and Stark, (1987)	5 subjects performed a read aloud tasks for 2hr on Cathode Ray Tube (CRT) screen.	Fixation, saccadic, and subjective questionnaire.	Sensation of visual fatigue. Small variations of impulse response before and after task for saccade and fixation.	Violates the central limit theorem due to small sample for the study.
Mocci, Serra, and Corrias (2000)	Queried subjects on a ten-point subjective scale after 8-10 hours usage of VDT from banking institutions. The independent factors were psychological, environmental, and physiological. 212 subjects were used and had qualified for nonexistence of ophthalmological diseases.	Evaluate correlation between the variables for each independent factors and asthenopia (dependent factor).	31.9% of the subjects reported symptoms of asthenopia during, or soon after work. 13.6% met the criterion of strong asthenopia every day. Notably, there was a positive correlation between asthenopia and environmental discomfort factors.	The authors explored multiple regression (statistical) analysis on the various variables as predictors for asthenopia. Subjective reports can be very misleading since subjects may know the intent of the experimenter.

Authors (s)	Experimental Stimuli and Conditions	Measurement Techniques	Findings	Research Gap
Gobba, Broglia, Sarti, Luberto, and Cavalleri, (1988)	53 female subjects of VDT data-acquisition clerks were used for the study. The stimuli were lighting conditions, luminance, contrast, and design of the workplace. VDT-induced symptoms were assessed by means of subject answers to a questionnaire.	Refraction power was determined before and at the end of work shift by an infrared autorefractometer.	Significant correlation between eye discomfort, ocular asthenopia, and myopization base on stimuli.	The independent variables (stimuli) were not varied to see which stimuli provided the indicator of visual fatigue.
Uetaka, Murata, Otsuka and Takasawa (2000)	14 participants performed 20 min 3 blocks VDT task using CRT screen and pupillary change, focal accommodation and eye movement simultaneously measured.	Subjective ratings of psychological sense of visual fatigue.	Sensation of visual fatigue increased with time along changes in pupil diameter, focal accommodation and saccadic eye movement.	Failed to predict the onset of visual fatigue from psychological factors.
Liu, Wang, and Wang, (2009)	Four 25-years old with the normal corrected visual acuity wear red and green 3D stereosco-glasses and watched 3D film	Questionnaires on sense of immersion and the feeling of fatigue divided into five grades; score of 0-4; with 4 indicating severe fatigue.	Visual fatigue are caused by negative horizontal position disparity are stronger than that caused by positive horizontal position disparity.	Small sample size and generalization of visual fatigue to the population is flawed.

Appendix C

Summary of Neurophysiological Studies of Visual Fatigue

Authors (s)	Experimental Stimuli and Conditions	Measurement Techniques	Findings	Research Gap
Morris and Miller (1996)	Partially induced sleep deprivation on pilots were tasked to undertake two flight conditions: Flight Maneuvered Task (FMT) and Straight Flying Task (SLT). Each task lasted 1.5 hours and it involves 12 subjects.	Measurement of error scores based on altitude, airspeed, heading, and vertical velocity in relation to physiological measures such as Blink Rate (BR), Blink Duration (BD), Long Closure (LCR) Blink Amplitude (BA), Saccade Velocity (SV), Saccadic Rate (SR), and Peak Saccadic Velocity (PSV).	Subjective reports indicated visual fatigue. Errors increased with time. Flying performance decreased due to visual fatigue as reflected on the physiological recordings.	Lack of statistical analysis such as paired <i>t</i> -test within subjects. Gaze fixation and gaze duration were not considered as one of the physiological measurements.
Li, Seo, Kham, and Lee (2008 )	Subjects played two consecutive video games with 2D and 3D stimuli.	Subjective questionnaire and Electroencephalograph (EEG) measurement based on the readings of P700 components.	EEG measurements revealed high correlation with 3D visual fatigue which was consistent with subjective questionnaires.	Using a subjective technique to measure 3D visual fatigue can be misleading since subjects were aware of the intent of the experiment.

Authors (s)	Experimental Stimuli and Conditions	Measurement Techniques	Findings	Research Gap
Goings (2008)	Alternate stimuli of reversed checkerboard pattern with an individual check size of 30' of arc. The pattern reversed at a rate of 1/sec with 64 reversals and with a video game. The independent variables were monoscopic and four variants of stereoscopic alignment error(zero misalignment, vertical, rotation, magnification differences).	The dependent variables were Visual Evoked Potentials, eyeblinks, and Simulator Sickness Survey (SSQ).	The participant's score on SSQ indicate a possible onset of visual fatigue and more driving errors were noticed. 54% of the top 15 oculomotor fatigue ratings had medium to high prism diopters of heterophoria, and stereopair misalignments.	There was no objective method to predict the onset of visual fatigue.
Zhang, Zhao, and Wang, (2009b)	Subjects played 3D video games. Each experiment lasted 1.5 hours and 34 subjects were involved.	Physiological measurement based on Average Heart Rate (AHR) and Standard Deviation of Heart Rate (SDHR).	Increase in visual fatigue resulted in the increase in SDHR and AHR.	Using SDHR and AHR as indexes of indirectly measurement of visual fatigue are misleading approaches and hence misinformed conclusion.

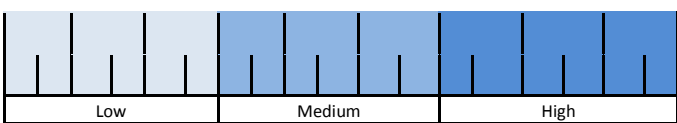
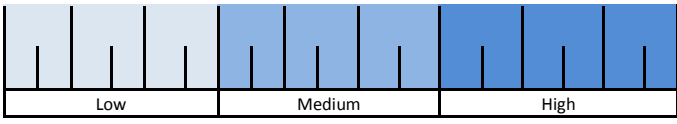
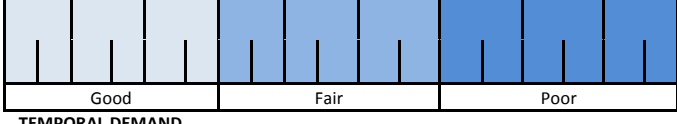
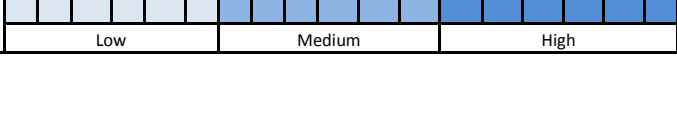
## Appendix D

*Simulator Sickness Questionnaire Symptoms*

No.	Symptoms	0 = None	1= Slight	2 = Moderate	3 = Severe
1	Ache				
2	Aware of breathing				
3	Blurred vision				
4	Boredom				
5	burning				
6	Burping				
7	Confusion				
8	Desire to move bowels				
9	Difficulty concentrating				
10	Difficulty focusing				
11	Dizziness eyes closed				
12	Dizziness eyes open				
13	double vision				
14	Drowsiness				
15	Eyestrain				
16	Faintness				
17	Fatigue				
18	Fullness of the head				
19	General discomfort				
20	Headache				
21	Increased appetite				
22	Loss of appetite				
23	Mental depression				
24	Salivation decrease				
25	Salivation increase				
26	Stomach awareness				
27	strain				
28	Sweating				
29	tearing				
30	Vertigo				
31	Visual flashbacks				
32	Vomiting				

Appendix E

NASA TLX Workload Assessment Sheet

<b>A neurophysiologic study of visual fatigue using a stereoscopic related display</b> <b>Center of Human-Machine Studies</b> <b>Department of Industreatment &amp; systems Engineering</b> <b>North Carolina A&amp;T State University</b>			
RATINGS SCALE DEFINITIONS			ID No. _____ Date: ____/____/____ <b>Instructions:</b> Please kindly read the in scale title, endpoints, and descriptions before checking off the appropriate point
Scale Title	Endpoints	Descriptions	
<b>MENTAL DEMAND</b>	Low/High	How much mental and perceptual activity was required (E.g., thinking, deciding, calculations, remembering, looking, and searching). Was the task easy or demanding, simple or complex, exacting or forgiving?	<b>MENTAL DEMAND</b> 
<b>PHYSICAL DEMAND</b>	Low/High	How much physical activity was required (E.g., pushing, turning, controlling)? Was the task easy or demanding, slow or brisk, slack or strenuous, restful or laborious?	<b>PHYSICAL DEMAND</b> 
<b>PERFORMANCE</b>	Good/Poor	How successful do you think you were in accomplishing the goals of the task set by the experimenter? How much satisfied were you with your performance in accomplishing these goals	<b>PERFORMANCE</b> 
<b>TEMPORAL DEMAND</b>	Low/High	How much time pressure did you feel due to the rate or pace at which the tasks or task elements occurred? Was the pace slow and leisurely or rapid and frantic?	<b>TEMPORAL DEMAND</b> 
<b>EFFORT</b>	Low/High	How hard did you have to work(mental and physically) to accomplish your level of performance?	<b>EFFORT</b> 
<b>FRUSTRATION LEVEL</b>	Low/High	How insecure, discourage, irritated, stressed, and annoyed versus secure gratified, content, relaxed, and complacent did you feel during the task?	<b>FRUSTRATION LEVEL</b> 

## Appendix F

## Neurophysiological Questionnaire

<b>A neurophysiologic study of visual fatigue using a stereoscopic related display</b> <b>Center of Human-Machine Studies</b> <b>Department of Industreatment &amp; systems Engineering</b> <b>North Carolina A &amp; T State University</b>		
<b>Your answers to these questions do not exclude you from the study. The answers are confidential and for statistical control purposes only</b>		
	Yes	No
Are you taking medication at the present time that might have some effects on your behavior and/or cognitive functioning?		
If yes, describe:		
Have you ever had your EEG (electric brain activity) recorded before?		
If yes, explain (include how long ago your EEG was recorded)		
Have you been to a doctor for any neurological problems?		
If yes, explain.		
<u>Only if you are 21 years of age or older.</u> Alcohol alters brainwave activity in specific ways: therefore it is important if you have had any alcohol beverages over the last 24 hours		
If yes, describe:		
Dominate/ Preferred hand(s)    Check both if you can use both hands	Right	Left

## Appendix G

## Ophthalmological and Optometric Questionnaire

Gender	M	F
Age	under 40	over 40
<b>1. Eye History</b>		
History of eye problem(s)?	Yes	No
If you answered <u>YES</u> , check all that applies to you	Yes	No
Myopia (nearsightedness)		
Hyperopia(farsightedness)		
Astigmatism		
Lazy eye		
Presbyopia(near reading glasses)		
Color vision		
Cataract		
Ocular degeneration		
Night blindness		
Congenital		
Excessive blinking		
Contact lenses discomfort		
<b>2. Eye symptoms</b>		
	Yes	No
Redness		
itching		
Burning		
Blurred vision		
Mucous discharge		
Eye watering		
Interpupillary Distance (IPD)	mm	
Date	Sign (Investigator)	
Date	Sign (Participant)	

*Appendix H*

*Summary of Experimental Randomization Outcomes Using Alignment Errors with ATC Sessions*

ID	Gender	ATC1	ATC2	ATC3
S01	Male	Rotational Error	Magnification Difference	Vertical Shift
S02	Male	Rotational Error	Vertical Shift	Magnification Difference
S03	Male	Vertical Shift	Magnification Difference	Rotational Error
S04	Male	Rotational Error	Magnification Difference	Vertical Shift
S05	Female	Magnification Difference	Rotational Error	Vertical Shift
S06	Male	Rotational Error	Magnification Difference	Vertical Shift
S07	Male	Magnification Difference	Vertical Shift	Rotational Error
S08	Male	Rotational Error	Magnification Difference	Vertical Shift
S09	Male	Rotational Error	Vertical Shift	Magnification Difference
S10	Male	Magnification Difference	Rotational Error	Vertical Shift
S11	Male	Rotational Error	Magnification Difference	Vertical Shift
S12	Male	Magnification Difference	Rotational Error	Vertical Shift
S13	Female	Rotational Error	Vertical Shift	Magnification Difference
S14	Male	Magnification Difference	Rotational Error	Vertical Shift
S15	Male	Vertical Shift	Magnification Difference	Rotational Error
S16	Male	Rotational Error	Vertical Shift	Magnification Difference
S17	Male	Magnification Difference	Rotational Error	Vertical Shift
S18	Male	Magnification Difference	Rotational Error	Vertical Shift
S19	Male	Rotational Error	Magnification Difference	Vertical Shift
S20	Male	Magnification Difference	Rotational Error	Vertical Shift
S21	Female	Vertical Shift	Magnification Difference	Rotational Error
S22	Male	Vertical Shift	Rotational Error	Magnification Difference
S23	Male	Magnification Difference	Rotational Error	Vertical Shift
S24	Male	Vertical Shift	Rotational Error	Magnification Difference

*Appendix I*

*Descriptive EEG for Each Relative Band for Each Display Alignment Error (Mean)*

Subjects	Display	Left Hemisphere					Mid-section					Right Hemisphere				
	Misalignment	Alpha	Beta	Theta	Delta	Gamma	Alpha	Beta	Theta	Delta	Gamma	Alpha	Beta	Theta	Delta	Gamma
S01	Magnification differences	0.034	0.047	0.068	0.842	0.010	0.116	0.178	0.137	0.534	0.035	0.033	0.047	0.065	0.845	0.010
S01	Rotational error	0.045	0.066	0.078	0.797	0.014	0.116	0.169	0.134	0.551	0.030	0.046	0.066	0.077	0.799	0.013
S01	Vertical Shift	0.074	0.121	0.094	0.686	0.025	0.096	0.131	0.122	0.628	0.023	0.077	0.125	0.093	0.679	0.026
S02	Magnification differences	0.017	0.026	0.032	0.919	0.005	0.103	0.125	0.167	0.585	0.020	0.033	0.051	0.044	0.862	0.010
S02	Rotational error	0.019	0.028	0.036	0.910	0.006	0.160	0.215	0.175	0.417	0.033	0.041	0.068	0.053	0.824	0.014
S02	Vertical Shift	0.054	0.090	0.068	0.769	0.019	0.115	0.159	0.138	0.564	0.024	0.061	0.100	0.076	0.743	0.021
S03	Magnification differences	0.034	0.051	0.055	0.849	0.010	0.070	0.167	0.090	0.641	0.031	0.037	0.056	0.059	0.837	0.011
S03	Rotational error	0.040	0.057	0.072	0.820	0.011	0.083	0.120	0.094	0.684	0.020	0.041	0.057	0.073	0.818	0.011
S03	Vertical Shift	0.025	0.034	0.044	0.889	0.007	0.140	0.284	0.094	0.424	0.058	0.077	0.123	0.097	0.679	0.025
S04	Magnification differences	0.027	0.038	0.058	0.869	0.008	0.076	0.095	0.096	0.718	0.015	0.028	0.040	0.058	0.866	0.008
S04	Rotational error	0.019	0.025	0.050	0.902	0.005	0.022	0.021	0.054	0.900	0.003	0.013	0.030	0.047	0.905	0.005
S04	Vertical Shift	0.022	0.027	0.059	0.887	0.006	0.018	0.019	0.037	0.922	0.003	0.022	0.029	0.058	0.885	0.006
S05	Magnification differences	0.037	0.023	0.098	0.840	0.003	0.057	0.065	0.083	0.786	0.008	0.036	0.022	0.096	0.844	0.003
S05	Rotational error	0.039	0.017	0.166	0.776	0.001	0.107	0.146	0.109	0.614	0.023	0.039	0.017	0.168	0.775	0.001
S05	Vertical Shift	0.036	0.050	0.060	0.844	0.010	0.124	0.131	0.145	0.587	0.013	0.036	0.050	0.059	0.846	0.010
S06	Magnification differences	0.036	0.054	0.060	0.838	0.011	0.182	0.222	0.204	0.364	0.028	0.033	0.049	0.054	0.854	0.010
S06	Rotational error	0.039	0.061	0.059	0.829	0.012	0.110	0.125	0.142	0.608	0.015	0.040	0.061	0.059	0.828	0.012
S06	Vertical Shift	0.034	0.027	0.124	0.810	0.005	0.141	0.162	0.170	0.507	0.019	0.034	0.027	0.121	0.813	0.005